Numerical Prediction of Expansive Soil Behavior in Changing Climate

Sahand Seyfi

A THESIS SUBMITTED TO THE FACULTY OF GRADUATE STUDIES IN PARTIAL FULFILLMENT OF THE REQUIREMENTS FOR THE DEGREE OF MASTER OF APPLIED SCIENCE

GRADUATE PROGRAM IN CIVIL ENGINEERING

YORK UNIVERSITY

TORONTO, ONTARIO

DECEMBER 2022

Abstract

Expansive soils are relatively high plastic clays that experience considerable volume change due to moisture variations in soil. The wetting/drying of expansive soils, which typically occurs in response to climate cycles, is associated with cycles of soil swelling/shrinkage over the time. The induced ground movements can cause severe structural damage, especially to lightweight structures such as roads, pavements, and residential buildings and therefore, the prediction of expansive soil deformation behavior is of great importance for geotechnical engineers in particular where lightly loaded structures and underground utilities are supported by expansive clays.

It has been shown that the climate has been continuously changing over the last century and there is considerable scientific evidence that climate is changing over next decades. The climate change is anticipated to cause significant changes in the hydrological cycles (e.g., increasing frequency of extreme rainfall events) that consequently results in higher risk of structural damage to the structures constructed on expansive soils.

The generalized consolidation theory based on two-stress state variable framework has been utilized in many previous studies to predict the volume change behavior of unsaturated soils under mechanical stress and matric suction change. This approach requires a constitutive surface that relates the soil void ratio to net stress and soil matric suction. The constants of void ratio surface function for a given soil are normally determined by fitting the equation to the laboratory test data. High number of fitting parameters is typically used to obtain a two-variable void ratio surface function with sufficient degree of approximation. In this study, a single stress state variable framework was adopted to describe the void ratio as a function of effective stress for soils in unsaturated state. A two-dimensional finite element model that couples variably-saturated flow and stress-strain analysis was developed to simulate the volume change behavior of expansive clay subject change in soil moisture content. This hydro-mechanical model is equipped with a soil-atmosphere boundary that has been developed to simulate the moisture dynamics in the near-surface zone of the expansive clay deposit. The finite element model utilizes suction stress-based effective stress to calculate the effective stress field. In the numerical model, a power law equation was considered to incorporate the dependency of soil modulus on volumetric water content of soil. The parameters of the power law equation were obtained from the best-fit curve matched to the calculated soil modulus and corresponding volumetric water content data.

The developed numerical model was validated against a benchmark problem in which a layer of Regina expansive clay is subjected to a constant infiltration rate. The obtained results indicate the capability of the proposed model in simulation of expansive soil deformations under varying moisture conditions over time. The developed numerical model then was used to assess the impact of climate change on the behaviour of Regina Clay in the city of Regina, Saskatchewan.

In this study, a three-staged approach was used to select critical future climate for the city of Regina with respect to expansive soil volume change behavior. The ground movements due to soil moisture fluctuations were simulated for historical climate as well as a selected climate scenario for future climate. The results of numerical model were statistically analyzed to quantify the impact of climate change, and to capture the relationship between ground movement and climatic variable data. The obtained results show that the ground deformation response is not necessarily correlated with climate classification or the maximum daily precipitation events, but the sequence of extreme precipitation events and their concurrency with colder months with minimal evaporation also play a key role influencing the expansive ground response to long term climate. The comparison study indicated that the frequency of large expansive ground heaving events is considerably higher under future Regina climate.

Acknowledgments

I am extremely grateful to Professor Bashir for his supervision, invaluable advice, continuous support during this study. His immense knowledge and experience have assisted me throughout the completion of this research.

I would like to express my sincere gratitude to Professor Lal Samarasekera for his constructive comments and suggestions during this research.

I wish to show my special appreciation to Dr. Ghassemi for his invaluable help and knowledge with the completion of this thesis.

I also must thank to Mr. Moamenbellah Moustafa and Mr. Aneeq Khan for all their assistances during this study.

Thank you to Ms. Sindy Mahal for her precious help and support during my graduate study.

Lastly, I am truly thankful in the constant support of my family for their understanding and support to accomplish this research specially during unprecedented pandemic.

Table of Contents

List of Tables

List of Figures

Chapter 1 Introduction

Expansive soil, also called shrink-swell soil or reactive soil, is a type of clay soil that experience considerable volume change in response to changes in soil moisture content. An increase in moisture content in expansive soils can cause swelling which presents as vertical heave, while decreasing moisture content leads to soil shrinking and cracking. Wetting and drying of expansive soils in response to climate cycles result in cycles of shrinkage and swelling of soils. The excessive shrinkage/swelling causes severe structural damage, especially to lightweight structures such as roads, pavements, and residential buildings. It should be noted that although seasonal variations in climate are considered as the dominate factor for soil moisture variations, other factors such as tree root drying, underground pipe leakage, and garden over-watering can also be responsible for change in soil moisture and the resulting volume changes (Sun, 2015).

Expansive soils are widely distributed in arid and semi-arid climatic regions around the world and more than sixty countries including Australia, U.S.A, Canada, India, South Africa and China are highly affected by the excessive shrink-swell behaviour (Shi et al., 2002). The expansive soil swelling/shrinkage behavior is a major concern for geotechnical engineers, particularly, where lightly loaded structures and underground utilities are supported by expansive clays. Many countries in the world, including Australia, United States, Israel, India and South Arica, have been experienced significant infrastructure damage due to the movement of expansive soils (Adem, 2015). Jones and Holtz (1973) estimated that the annual cost of expansive soil damage in the U.S. is $2.2 billion, which exceeds the combined damage caused by earthquakes, hurricanes, and floods in an average year. A more recent study by Puppala and Cerato (2009) reported that the cost of damage due to expansive soils in the U.S has increased to over $13 billion per year. Considerable loss caused by expansive soils highlights the necessity for more studies in the context of expansive soil behavior due to soil-atmosphere interaction.

The climate has been continuously changing over the last century and there is considerable scientific evidence that climate will be changing over next decades. The climate change is anticipated to cause significant changes in the hydrological cycles e.g., increasing frequency and magnitude of the extreme rainfall events and droughts. This can intensify changes in soil moisture and consequently cause more severe volume change (shrinkage/swell) in expansive soils. Therefore, climate change is anticipated to intensify the future structural damage particularly of lightweight constructions (residential buildings, industrial buildings, pavement structures, pipelines, etc.) supported on expansive soils. For instance, the French Insurance Association estimates that by 2040, the insurance cost of droughts would nearly triple and 60% of this increase would be due to climate change based on the worse case future climate change scenario (Assadollahi and Nowamooz, 2020). When areas that soil typically maintain a higher level of moisture experience drought conditions, the resulting shrinkage can have a significant effect on structure foundations. Therefore, there is an urgent need to develop appropriate methodologies to evaluate the long-term deformation response of expansive soils to climatic cycles considering the impact of climate change.

1.1. Thesis Objectives

In this research, a coupled hydro-mechanical numerical model, which takes into consideration the soil-atmosphere interaction, is utilized to investigate the effects of climate change on swelling/shrinkage behavior of expansive soils. The main objectives of the thesis are as follows:

- Develop a numerical model to predict the expansive soil response to long-term climate data using a single stress state unsaturated soil mechanics framework. The effective stress-based approach proposed by Lu et al. (2010) is utilized to calculate the effective stress field and associated deformation characteristics of an expansive soils. Since its introduction, this approach has been used to simulate several engineering applications such as slope stability assessment using local factor of safety field (Lu et al., 2012, Bagheri, 2022);

- Validate the developed numerical model by comparing its results for a benchmark problem with those reported by other studies;
- Propose an appropriate approach to select critical future climate change scenarios with respect to expansive soil volume change behavior: and
- Assess the impact of climate change on the long-term deformation behavior of Regina expansive clay by comparing the numerical results for historical climate and a selected future climate scenario.

1.2. Thesis Outline

This thesis has been organized into six chapters:

- Chapter 1 presents the importance of the research, main objectives and the thesis outline;
- Chapter 2 provides a review of the theoretical background regarding the numerical simulation of expansive soil behavior including an overview of variably-saturated flow analysis and unsaturated soil mechanics using single stress state variable framework;
- Chapter 3 presents a study on the numerical prediction of expansive soil response to soil moisture changes using the single stress state unsaturated soil mechanics framework. In this chapter, the review of void ratio constitutive relations is also presented. The results of the proposed model for a benchmark problem for Regina expansive clay are presented and compared with those obtained by previous studies using different approaches.

- Chapter 4 assesses the response of Regina clay to long term climate data considering climate change. This assessment is carried by conducting a series of numerical simulations using historical as well as a future climate data for the city of Regina. The results of the numerical simulations are analyzed using statistical analyses;
- Chapter 5 presents the summary and conclusions of this research. This chapter also includes the discussion on the contributions of this research and recommendations for future work.

Chapter 2 : Theoretical background

2.1. Introduction

Expansive soils are relatively high plastic clays that swell or shrink significantly due to moisture variations in the soil. The formation of expansive soils originates from gradual weathering or erosion of basic igneous or sedimentary rocks, and decomposition of the parent rock minerals to highly active clay minerals (e.g., montmorillonite) (Donaldson, 1969).

The clay minerals can be made up of basic units or layers comprising of two or three alternating sheets of silica, and either brucite [$Mg_3(OH)_6$] or gibbsite [$Al_2(OH)_6$]. Generally, the bonding between the sheets of silica and gibbsite or brucite within each layer is strong, but the bonding between layers may be weak. The most common clay mineral groups are kaolinite, montmorillonite and illite. Kaolinite has a two-sheet structure, comprising silica and gibbsite. It has few or no exchangeable cations, and the interlayer bonds are reasonably strong. Illite has a three-sheet structure, comprising a sheet of gibbsite sandwiched between two silica sheets. Illite layers are bonded together by potassium ions. Montmorillonite has a similar structure to illite. The difference is that in montmorillonite there is extensive substitution of silicon (by aluminium) in the silica sheets, and of aluminum (by magnesium, iron, zinc, nickel, lithium and other cations) in the gibbsite sheet. The additional negative charges, which result from these substitutions, are balanced by exchangeable cations such as sodium and calcium located between layers and surfaces of the particles. The interlayers bonds in montmorillonite are weak, and layers are easily separated by cleavage or by absorption of water. Therefore, the mineralogical structure of montmorillonite is extremely expansive in nature when compared to other clay minerals such as illite and kaolinite.

The mechanism of soil swelling has been described by several researchers (e.g., Anderson et al. 1973, Chen 1975, Schafer and Singer 1976, Nelson and Miller 1992, Stavridakis 2006). It has been shown that clay mineral montmorillonite plays a key role in swelling/shrinkage behavior of expansive soils. Its molecular structure tends to attract and hold water molecules between the clay crystal sheets. The clay mineral montmorillonite can absorb large amounts of water molecules into gaps between its clay sheets. As more water is absorbed, the sheets are forced further apart, leading to an increase in soil pressure or increase in soil volume (Figure 2-1).

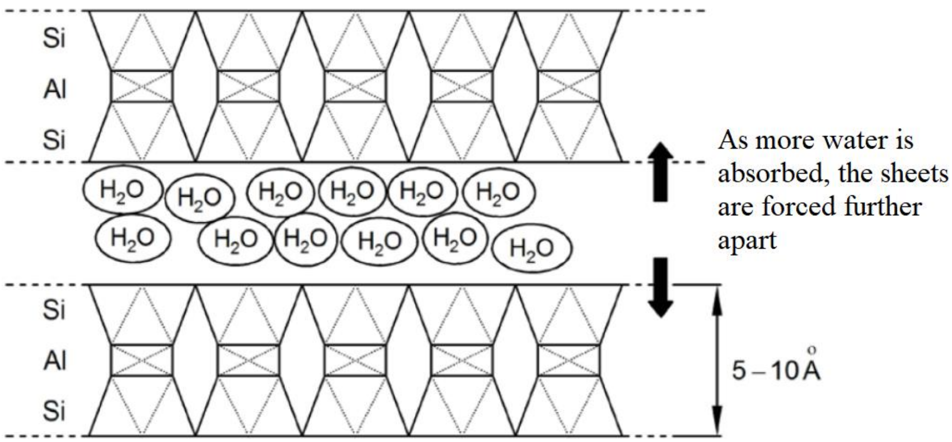

Figure 2-1- The intercalation of water molecules in the inter-plane space of montmorillonite (modified from Taboada (2003))

In addition, orientation of water films around the high charge density clay particles may also play a role in swelling of such soils. In a water molecule, the oxygen atom and hydrogen atoms share electrons in covalent bonds, but the sharing is not equal. In the covalent bond between oxygen and hydrogen, the oxygen atom attracts electrons a bit more strongly than the hydrogen atoms. This unequal sharing of electrons causes bipolar behavior of water molecules: a slight negative charge near its oxygen atom and a slight positive charge near its hydrogen atoms. Since clay particles are mainly flat and electrically charged (usually negative), they can attract bipolar water molecules. Therefore, as negative charges attract water molecules, the clay particles are pushed apart, causing an expansion or swelling of the soil (Figure 2-2).

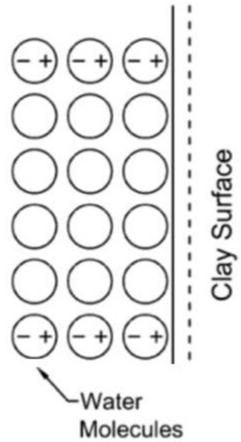

Figure 2-2- The orientation of water films around high density clays (modified from Mitchell and Soga (2005))

Geotechnical engineers often rely on Atterberg limits for the identification of expansive soils. In general, more expansive clay minerals may lead to higher soil plasticity. Peck et al. (1974) suggested a general relationship between soil plasticity index and its expansion potential as presented in Table 2-1. However, the plasticity index alone may not accurately predict the expansion potential of expansive soils. Zapata et al. (2006) suggested that considering soil activity (soil fine content along with plasticity index) can significantly improve the correlation. According to IS 1948 (BIS, 1970), clays with plasticity indices > 25, liquid limits > 40, and natural water content near the plastic limit or less are more likely to swell.

Table 2-1- Expansion potential of soils and plasticity index (Peck et al. 1974)

Plasticity Index	Expansion Potential
0 – 15	Low
0 – 35	Medium
22 – 55	High
> 55	Very High

In addtion to Atterberg limits, several other inedecis have been proposed to assess the soil expansion potential. The free swell index (FSI) and expansion index (EI) are the most common. For example, EI can be determined by expansion index test as per the ASTM D4829-11. The degree of expansion may be very low (EI = 0–20), low (EI = 21–50), medium (EI = 51–90), high (EI = 91–130), and very high (EI > 130) (Patel, 2019).

The International Building Code (2012) adopted EI for identification of expansive soils. According to the code, soils meeting all four of the following provisions shall be considered expansive, except that tests to show compliance with items 1, 2 and 3 shall not be required if the test prescribed in item 4 is conducted:

1) Plasticity index (PI) of 15 or greater, determined in accordance with ASTM D 4318;
2) More than 10 percent of the soil particles pass No. 200 sieve, determined in accordance with ASTM D 422;
3) More than 10 percent of the soil particles are less than 5 micrometers in size, determined in accordance with ASTM D 422; and
4) Expansion index (EI) greater than 20, determined in accordance with ASTM D 4829.

Expansive soils can experience excessive volume changes (heave/shrink) in response to soil moisture content due to soil-atmosphere interaction. Swelling occurs when soil water content increases due to water infiltration into soil because of rainfalls or other activities (e.g., garden watering, or water pipe leaks). On the other hand, shrinking of expansive soils happens as a result of loss of soil moisture due to numerous mechanisms such as evaporation, lowering of groundwater table and high-water demand of mature trees (Chen 1975).

The expansive soil volume change can occur in vertical and lateral directions. When there is no restrain in the field, expansive soils have the potential to expand equally in all direction. However, in most cases, adjacent building or surrounding soil restrains the expansive soil to expand laterally. In these cases, there is only vertical expansion (Figure 2-3).

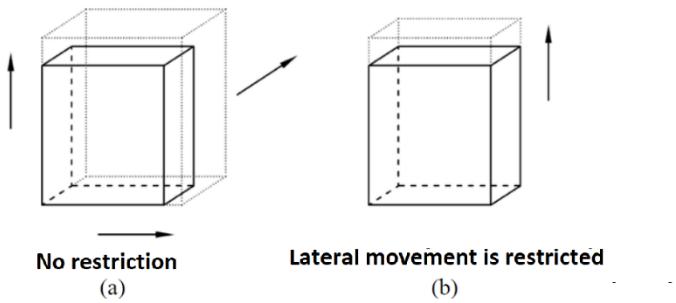

Figure 2-3- Type of expansive soil movements: (a) soil volumetric expansion in three directions when there is no restriction, (b) soil heave when the lateral movement is restricted.

Expansive soils have been commonly classified as problematic soils and are considered critical for geotechnical design engineers (e.g., Coduto, 2001, Tang et al., 2009 and Cui et al., 2013). For example, a common issue for the lightweight structures supported by expansive soils is differential movement across the slab on grade. When a slab on grade is placed on expansive soil, the slab acts a moisture barrier and differential ground movement occurs across the slab. The differential movement along the slab is called mound profile. A mound profile can be in the form of centre heave and edge heave corresponding to two different moisture conditions under the slab. Centre heave would occur in footings where higher soil moisture condition exists under the slab centre while edge heave would occur when higher soil moisture condition exist at the perimeter of the slab. A schematic of these two main types of soil movements and the resulting damage in lightweight structures is presented in Figure 2-4. The first is edge uplift that occurs around the perimeter of the structure (Figure 2-4-a). The second is center heave that occurs beneath the center of the structure, which can cause as an upward long-term dome shaped movement (Figure 2-4-b).

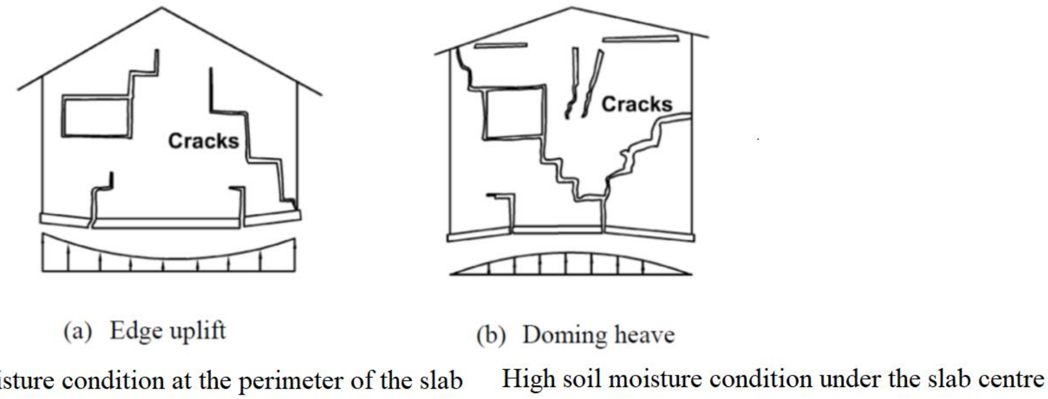

Figure 2-4- Vertical movement of expansive foundation soils: (a) edge uplift, (b) doming heave (modified after Department of the Army USA 1983)

Despite many studies that have been carried out over the past decades, the accurate prediction of volume change movements with respect to environmental factors is still a challenge. Therefore, it is important to develop adequate numerical models to estimate the heave and shrink related volume change of expansive soils considering the long-term climatic conditions. Such a numerical model requires a transient water flow analysis through unsaturated soil as well as a mechanical model to calculate the associated soil movements. The theoretical background for the proposed numerical model in this study is described in the following sections. The details of the numerical model will be discussed in the next chapters of this thesis.

2.2. Variably Saturated Flow Analysis

Unsaturated soils are considered a three-phase medium, consisting of soil as the solid, water as the liquid, and air as the gas phase. The presence of air and water in the unsaturated soils generates negative pore pressure which is also known as matric suction. Total suction within an unsaturated soil consists of a combination of matric suction and osmotic suction (Fredlund et al. 2012). Matric suction describes the difference between air pressure and water pressure, whereas osmotic suction is defined as the negative pressure resulting from the effect of the dissolved salts in the water of the soil matrix. The matric suction plays a key role in estimating the water flow through unsaturated medium. Osmotic suction is commonly disregarded due to its lesser influence on total suction in addition to the difficulty of separating these two variables (López-Acosta and Mendoza-Promotor, 2016).

The two-dimensional isothermal Darcian flow of water in variably saturated porous medium can be given by the following form of Richards' equation (Richards, 1931):

$$\frac{\partial \theta}{\partial t} = \frac{\partial}{\partial x}\left[K(h)(\frac{\partial h}{\partial x})\right] + \frac{\partial}{\partial z}\left[K(h)(\frac{\partial h}{\partial z} + 1)\right] + S_w \qquad [2\text{-}1]$$

where θ is the volumetric water content ($\frac{m^3}{m^3}$), t is time, K(h) is unsaturated hydraulic conductivity (m/s), h is soil water matric head (m), and S_w is source (positive) or sink (negative) term that represents the volume of water added or removed per unit time from a unit volume of soil ($m^3 m^{-3} s^{-1}$).

The equation assumes that the air phase is at atmospheric pressure and plays an insignificant role in the liquid flow process. It is also a highly nonlinear partial differential equation, for which analytical solutions can only be obtained for very simple initial and boundary conditions. The Richards' equation is routinely used and is implemented in different forms in many hydrological software to simulate water flow through unsaturated soils. This equation assumes that the soil is rigid and incompressible (Davies 2011).

The solution of Richards' equation requires the relationship between volumetric water content (θ) and matric suction (h) as well as the relationship between hydraulic conductivity (K) and matric suction (h). The relationship between volumetric water content and matric suction and is called soil water characteristic curve (SWCC) and the relationship between hydraulic conductivity and matric suction is called hydraulic conductivity function (HCF). Figure 2-5 shows typical SWCCs for soils ranging from sand to clay. When soil is in saturation state, the matric suction is zero and the water content is saturated water content, θ_s. If a minimal suction is applied, no water drains out of the soil. With the increase of suction to a critical value, water starts draining. This critical suction is called the air entry value (AEV) or bubbling pressure. After exceeding the AEV, the soil continuously drains with the increase in suction until it reaches the residual water content, θ_r. In the residual condition, the water is tightly held to the soil and flow predominantly occurs as vapor flow.

The grain size of soil has potential effects on the SWCCs. As shown in Figure 2-5, θ_s and AEV are larger for clay, and then decrease for silt and sand. The larger θ_s of clay is related to the larger surface area of the clay particles. Due to smaller particle sizes of clay, largest pore will have a smaller diameter than that for silt and sand. The AEV is affected by the largest pores in a soil matrix, where larger pores empty out first. Figure 2-5 indicates that the typical SWCC curves varies with the soil types. The shape of the draining portion of the SWCC is dependent on the distribution of the pore sizes in the soils. Uniformly graded soils tend to have very steep SWCC curves as most of the pores are of similar size.

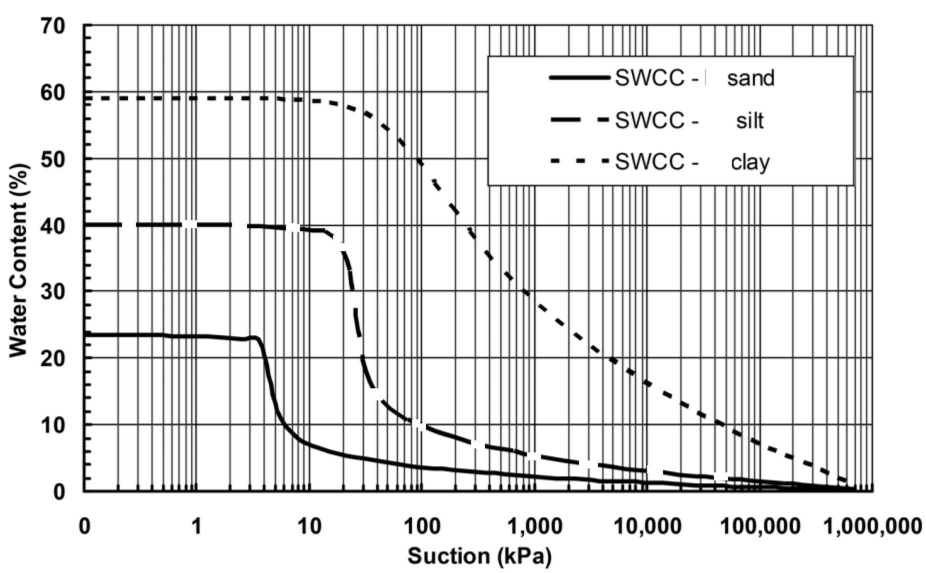

Figure 2-5- Comparative typical SWCCs for sand, silt and clay soils (modified from Tran et al., 2016)

SWCC is the primary soil hydraulic function and most of unsaturated soil behavior can be explained within its context. For SWCCs to be used as the constitutive relationship for unsaturated soils, it is essential to express it as a mathematical relationship. Many mathematical models have been proposed that describe the SWCC with varying degrees of success. The widely used SWCC models are the ones proposed by Brooks and Corey (1964), van Genuchten (1980), and Fredlund and Xing (1994). The most widely used model by van Genuchten (1980) can be expressed as:

$$\theta = \theta r + (\theta s - \theta r) \left[\frac{1}{1+(\alpha|h|)^{n}}\right]^{\left(1-\frac{1}{n}\right)} \qquad [2\text{-}2]$$

This equation describes the relationship between soil volumetric water content and matric suction (h) for given saturated water content (θ_s) and residual water content (θ_r). There are also two empirical coefficients α and n in this function, which are related to the air entry value and pore size distribution of the soil.

Parameters of vG equation (van Genuchten, 1980) can be determined through field or laboratory measurements. The measurement of hydraulic parameters is time-consuming and costly. Therefore, it is usually limited to a small number of tests. In the absence of measurements, vG parameters can also be estimated from available databases. For example, Carsel and Parrish (1988) used an extensive database to obtain the saturated hydraulic conductivity and SWCC parameters for the van Genuchten (1980)'s function using multiple regression techniques for all soil types in the USDA textural triangle. Alternatively, the hydraulic parameters of soils can also be estimated from readily available soil information using correlations, commonly known as pedotransfer functions (PTFs). The main advantage of using PTFs is that the hydraulic parameters of soil can be estimated based on readily available information such as soil gradation, porosity, density and organic content (van Genuchten et al., 1991).

In an unsaturated soil, the hydraulic conductivity is significantly affected by combined changes in the void ratio and the degree of saturation of the soil (Fredlund and Rahardjo, 1993). The degree of saturation can be written as a function of matric suction, and so the hydraulic conductivity of soil can be also written as function of the matric suction and void ratio. The hydraulic conductivity function (HCF) can be directly measured, indirectly computed or estimated by using the soil-water characteristic curve (SWCC) and the saturated hydraulic conductivity. Many hydraulic conductivity functions have been proposed in the literature to describe the HCF of an unsaturated soil (e.g., Gardner, 1958; Phillip, 1986; van Genuchten, 1980; Fredlund and Xing, 1994; Leong and Rahardjo, 1997). van Genuchten (1980) used the statistical pore-size distribution model of Mualem (1976) to obtain a predictive equation for the unsaturated HCF in terms of soil water retention parameters. van Genuchten's model, is written as follows:

$$\frac{K(h)}{K_{sat}} = \Theta^{l} \left[1 - (1 - \Theta^{\frac{1}{m}})^{m}\right]^{2}, \Theta = \frac{\theta - \theta_r}{\theta_s - \theta_r}, m = 1 - \frac{1}{n} \quad [2\text{-}3]$$

where $K(h)$ is hydraulic conductivity (m/s), K_{sat} is saturated hydraulic conductivity (m/s), l is a constant set to 0.5, and n is a fitting parameter of SWCC.

2.3. Effective Stress-based Unsaturated Soil Mechanics

The effective stress is known as a fundamental stress state variable that has been extensively used to calculate the soil strength and simulate the soil deformation behavior within the classical soil mechanics framework. Bishop (1954, 1959) extended the Terzaghi's effective stress to be used for unsaturated conditions:

$$\sigma' = (\sigma - u_a) - \chi(u_w - u_a) \quad [2\text{-}4]$$

where u_a is pore-air pressure, u_w is pore-water pressure, $\sigma - u_a$ is net total stress, and $u_w - u_a$ is matric suction. χ is scaling parameter depending on the soil saturation degree with the constraints of being zero when soil is completely dry and being unity when soil is fully saturated.

The above single-valued effective stress equation was shown to be inadequate for describing both volume change and shear strength behavior (Houston, 2019; Zhang and Lu, 2020). The early efforts to develop a single stress state for unsaturated soil conditions were later followed by two independent stress state variable approaches (Matyas and Radhakrishna, 1968; Fredlund and Morgenstern, 1977).

Despite its popularity, two stress state variable approach is subjected to a major practical limitation: It cannot be utilized within the context of classical mechanics that consider effective stress as the single stress state variable governing the soil behavior (Lu et al. 2010). Moreover, smooth transition from unsaturated to saturated state in elasto-plastic models is another challenge in the use of the two independent stress state approach (Houston, 2019).

Several researchers have proposed modified forms of effective stress for unsaturated soil conditions (e.g., Khalili and Khabbaz 1998; Nuth and Laloui 2008; Lu and Griffiths 2004; Lu and Likos 2006; Lu et al. 2010; Alsherif and McCartney 2014; Manahiloh et al. 2016). In this study, the single stress state approach proposed by Lu et al. (2010) was utilized to calculate the effective stress. The evolution of the effective stress subject to changes in soil moisture was then used to anticipate the volumetric change behavior of the expansive soils.

Lu and Likos (2006) extended the pioneering work by Bishop (1954 and 1959), to define a new stress variable called suction stress (σ^s) within the context of Terzaghi's effective stress equation as following:

$$\sigma' = (\sigma - u_a) - \sigma^s \qquad [2\text{-}5]$$

Lu et al. (2010) proposed a closed-form expression for suction stress for the full range of matric suction:

$$\sigma^s = -(u_a - u_w) \qquad (u_a - u_w) \leq 0 \qquad [2\text{-}6]$$

$$\sigma^s = \frac{(u_a - u_w)}{(1 + [\alpha\,(u_a - u_w)]^n)^{(n-1)/n}} \qquad (u_a - u_w) \geq 0 \qquad [2\text{-}7]$$

where α and n are the parameters used to define the soil water characteristic curve (SWCC) of a soil using van Genuchten's (1980) equation.

2.4. Stress-Strain Analysis

The calculation of effective stress field and soil displacements requires a mechanical model. The mechanical model based on two stress state variables for unsaturated soils is formulated as an extension of the equations used for saturated soil, using two independent stress state i.e., net normal stress and matric suction. However, in the effective stress-based framework which is used in this study, the mechanical model computes the soil stresses and displacements by using the suction stress as a component of the effective stress.

In the elasticity form, strains can be defined by the first derivatives of displacements as follows:

$$\varepsilon_{ij} = \frac{1}{2}\left(u_{i,j} + u_{j,i}\right) \qquad i, j = 1,2,3 \qquad [2\text{-}8]$$

The strain tensor can be written in Cartesian coordinates for the three-dimensional case:

$$[\varepsilon] = \begin{bmatrix} \frac{\partial u_x}{\partial x} & \frac{1}{2}\left(\frac{\partial u_x}{\partial y} + \frac{\partial u_y}{\partial x}\right) & \frac{1}{2}\left(\frac{\partial u_x}{\partial z} + \frac{\partial u_z}{\partial x}\right) \\ \frac{1}{2}\left(\frac{\partial u_x}{\partial y} + \frac{\partial u_y}{\partial x}\right) & \frac{\partial u_y}{\partial y} & \frac{1}{2}\left(\frac{\partial u_z}{\partial y} + \frac{\partial u_y}{\partial z}\right) \\ \frac{1}{2}\left(\frac{\partial u_x}{\partial z} + \frac{\partial u_z}{\partial x}\right) & \frac{1}{2}\left(\frac{\partial u_z}{\partial y} + \frac{\partial u_y}{\partial z}\right) & \frac{\partial u_z}{\partial z} \end{bmatrix} \qquad [2\text{-}9]$$

In linear elasticity, stress and strain can be related by Hook' s law through the introduction of material's elastic properties:

$$\sigma_{ij} = \frac{2G\mu}{1-2\mu}\varepsilon_{kk}\delta_{ij} + 2G\varepsilon_{ij} \qquad i, j, k = 1,2,3 \qquad [2\text{-}10]$$

This equation can be written in three-dimensional in terns of effective stresses as follows:

$$\sigma'_{xx} = \frac{2G\mu}{1-2\mu}\left(\varepsilon_{xx} + \varepsilon_{yy} + \varepsilon_{zz}\right) + 2G\varepsilon_{xx} \qquad [2\text{-}11]$$

$$\sigma'_{yy} = \frac{2G\mu}{1-2\mu}\left(\varepsilon_{xx} + \varepsilon_{yy} + \varepsilon_{zz}\right) + 2G\varepsilon_{yy} \qquad [2\text{-}12]$$

$$\sigma'_{zz} = \frac{2G\mu}{1-2\mu}\left(\varepsilon_{xx} + \varepsilon_{yy} + \varepsilon_{zz}\right) + 2G\varepsilon_{zz} \qquad [2\text{-}13]$$

$$\sigma'_{xy} = \sigma'_{yx} = 2G\varepsilon_{xy} \qquad [2\text{-}14]$$

$$\sigma'_{yz} = \sigma'_{zy} = 2G\varepsilon_{yz} \qquad [2\text{-}15]$$

$$\sigma'_{zx} = \sigma'_{xz} = 2G\varepsilon_{zx} \qquad [2\text{-}16]$$

where δ_{ij} is the identity tensor (Kronecker delta), μ is the Poisson's ratio reflecting the change in the normal strain in a specific direction due to the change in a unit strain orthogonal to it, and G is the shear modulus reflecting the change in shear stress due to the change in a unit shear strain.

To solve the elastic problem in three-dimensional conditions, the equilibrium equations need to be constructed. Under the equilibrium conditions, at any point within the medium, the force and momentum balance in both the horizontal and vertical directions should be satisfied. The equilibrium equations are given in index notation as:

$$\sigma'_{ji,j} + f_i = 0 \qquad i,j = 1,2,3 \qquad [2\text{-}17]$$

where f_i is the body force vector. The Cartesian coordinates for the three-dimensional case are:

$$\frac{\partial\sigma'_x}{\partial x} + \frac{\partial\sigma_{yx}}{\partial y} + \frac{\partial\sigma_{zx}}{\partial z} + f_x = 0 \qquad [2\text{-}18]$$

$$\frac{\partial\sigma_{xy}}{\partial x} + \frac{\partial\sigma'_y}{\partial y} + \frac{\partial\sigma_{zy}}{\partial z} + f_y = 0 \qquad [2\text{-}19]$$

$$\frac{\partial\sigma_{xz}}{\partial x} + \frac{\partial\sigma_{yz}}{\partial y} + \frac{\partial\sigma'_z}{\partial z} + f_z = 0 \qquad [2\text{-}20]$$

Where the only body force is the weight of material, this vector has the non-zero component ρg in the z direction and zero components in x and y directions. The quantity ρg is the unit weight of material.

The unified effective stress equation (Eq. [2-5]) can be written in index form as:

$$\sigma'_{ij} = \sigma_{ij} - \sigma^s\delta_{ij} \qquad i,j = 1,2,3 \qquad [2\text{-}21]$$

Implementing the unified effective stress Eq. [2-21] into Eq. [2-17] yield:

$$\sigma_{ji,j} - \sigma^s_{,i} + f_i = 0 \qquad i,j = 1,2,3 \qquad [2\text{-}22]$$

The Cartesian coordinates in the three-dimensional case are:

$$\frac{\partial \sigma'_x}{\partial x} + \frac{\partial \sigma_{yx}}{\partial y} + \frac{\partial \sigma_{zx}}{\partial z} = -f_x + \frac{\partial \sigma^s}{\partial x} \qquad [2\text{-}23]$$

$$\frac{\partial \sigma_{xy}}{\partial x} + \frac{\partial \sigma'_y}{\partial y} + \frac{\partial \sigma_{yz}}{\partial z} = -f_y + \frac{\partial \sigma^s}{\partial y} \qquad [2\text{-}24]$$

$$\frac{\partial \sigma_{xz}}{\partial x} + \frac{\partial \sigma_{yz}}{\partial y} + \frac{\partial \sigma'_z}{\partial z} = -f_z + \frac{\partial \sigma^s}{\partial z} \qquad [2\text{-}25]$$

Equation [2-8], [2-10] and [2-22] include the equations required to compute the unknown variables in an elastic medium. In the three-dimensional case there are 15 equations with 15 variables (6 total stress, 6 strains, and 3 displacements). Conversely, in the two-dimensional case this involves 8 equations with 8 variables (3 total stress, 3 strains, and 2 displacements). The numerical solution of these equations is implemented in the coupled hydro-mechanical FE code with proper boundary conditions for displacements and stresses.

Chapter 3 : Prediction of Expansive Soil Response to Changes in Soil Moisture using Single Stress State Variable Framework

3.1. Abstract

The volume change behavior of expansive soils in response to changes in soil moisture caused by climate cycles can cause severe structural damage. This damage is more pronounced for lightweight structures, buried infrastructure and pavements. Hence, prediction of expansive soil deformation in response to changes in soil moisture is valuable to geotechnical engineers.

The generalized consolidation theory based on two-stress state variable framework has been utilized in many previous studies to predict the volume change behavior of unsaturated soils under mechanical stress and matric suction changes. This approach requires a constitutive surface that relates the soil void ratio to net stress and soil matric suction. Several mathematical functions have been proposed to describe the void ratio constitutive surface. The constants of void ratio surface function for a given soil are normally determined by fitting the equation to the laboratory test data. A large number of fitting parameters are typically required to obtain a two-variable void ratio surface function with adequate accuracy. In this study, a single stress state variable framework was adopted to describe the void ratio as a function of effective stress for soils in the unsaturated state. The proposed approach was used to fit single variable void ratio curves to the laboratory test data for two different expansive soils under a range of mechanical stress and matric suction using fewer fitting parameters. Moreover, a finite element model that couples variably-saturated flow and stress-strain analysis was developed to simulate the volume change behavior of expansive clay subject to long-term climate data. The finite element model utilizes suction stress-based effective stress to calculate the effective stress field. The model equipped with a power law equation incorporates the dependency of soil modulus on volumetric water content of soil. The equation

parameters were obtained from the best-fit power law curve matched to the calculated elastic modulus based on the proposed relationship between void ratio and effective stress.

The developed numerical model was validated against a benchmark problem in which a layer of Regina expansive clay is subjected to a constant infiltration rate. The results obtained indicate the capability of the proposed model in simulation of expansive soil deformations subject to varying moisture conditions over time.

3.2. Introduction

Expansive soils experience significant volume change in response to changes in soil moisture content. Climate is a key factor influencing the soil moisture content fluctuations. Climatic drying/wetting cycles may cause expansive soil to undergo significant swelling/shrinking that may ultimately lead to considerable damage to the lightly loaded buildings, buried utilities and pavements.

Several analytical / numerical methods have been proposed to predict the movement of expansive soils. These methods typically include two main components: (i) the range of water content or soil suction fluctuations as a function of time and (ii) the constitutive law that relates the soil state variables (i.e., water content, soil suction, or mechanical stress) to the volume change movement of the soil (Briaud et al., 2003). Adem and Vanapalli (2015) reviewed the various methods proposed for predicting the in situ volume change movement of expansive soils over time. They have categorized the available methods into three groups:

(i) Consolidation theory-based methods in which the transient water flow and the soil volume change processes are solved using the coupled consolidation theory of unsaturated soils. These methods utilize volume change constitutive relations for unsaturated soils including elastic models (e.g., Vu and Fredlund (2004) and Zhang (2004)) and elastoplastic models (e.g., Alonso et al., 1990).

(ii) Water content-based methods in which the soil movement due to environmental changes over time is related to soil water content rather than soil suction (e.g., Briaud et al. (2003) and Overton et al. (2006)). In contrast to the coupled models, these methods only consider the soil movements due to change in soil moisture.

(iii) Suction-based methods in which the soil movements associated with the expansive soils response to environmental changes are evaluated by estimating or predicting soil suction condition (e.g., Mitchel (1980), Wray et al. (2005) and Adem and Vanapalli (2013)).

Alonso et al. (1990) developed the Barcelona Basic Model (BBM), which correlates soil hardening with suction, to simulate the unsaturated soil stress-strain behavior. Later, Alonso et al. (1999) extended the original model for expansive soils by including a conceptual fabric representation, where elastic deformations in the microstructure and plastic deformations in the macrostructure are taken into consideration. They validated the extended constitutive model, known as Barcelona Expansive Model (BExM) using laboratory test data to understand the combined effect of vertical stress and soil suction on net volumetric strains.

Vu and Fredlund (2004, 2006) developed an elasticity-based model for unsaturated expansive soils that simulates the non-linear stress-strain behavior by using the coefficient of compressibility as a function of net normal stress and soil suction. They used the constitutive relationships that have been originally proposed by Fredlund and Morgenstern (1976). The following equations indicate the soil structure constitutive relation associated with the volumetric strain as well as the constitutive equation for the water phase which define water volume change in the soil element for any change in the total stress and matric suction:

$$d\varepsilon_v = d\varepsilon_x + d\varepsilon_y + d\varepsilon_z = \frac{3(1-2\mu)}{E} d(\sigma_m - u_a) + \frac{3}{H} d(u_a - u_w) \quad [3\text{-}1]$$

$$\frac{dV_w}{V_0} = \frac{3}{E_w} d(\sigma_m - u_a) + \frac{1}{H_w} d(u_a - u_w) \quad [3\text{-}2]$$

where ε_v is the volumetric soil strain, ε_x, ε_x and ε_x are the normal strains in the x-, y- and z-directions, respectively, σ_m is the mean total stress, μ is the Poisson's ratio, E is the modulus of elasticity for the soil structure with respect to a change in the net normal stress, H is the modulus of elasticity for the soil structure with respect to a change in matric suction, V_w is the volume of water in the soil element, V_0 is the initial overall volume of soil element, E_w is the water volumetric modulus associated with a change in net normal stress and H_w is the water volumetric modulus associated with a change in matric suction. Vu and Fredlund (2004, 2006) examined the developed model using coupled and uncoupled approaches for several examples and indicated that the results from an uncoupled analysis compares well with those obtained from a coupled analysis.

Ito and Hu (2011) developed a coupled numerical model to predict the hydraulic and mechanical behaviour of Regina expansive clay. The initial and final soil suctions derived from the model were used as the input stress conditions for the displacement model. The displacement model is based on the two elasticity parameters E and H.i.e. elasticity modulus with respect to net normal stress and suction, respectively. They indicated that their model resulted in acceptable agreement with the field observations. Later, Ito et al. (2014) developed a two-stage two-dimensional finite element model for moisture-induced deformations in expansive soils. They included a coupled soil-atmosphere model for seepage through the soil and suction-based displacement model to capture the behavior of expansive soil using normal stress and soil suction using a general partial differential equation solver named FlexPDE (FlexPDE, 2017). They validated the developed model using field monitoring data, reported by Hu et al. (2010).

Adem and Vanapalli (2013) proposed a simple method for predicting the vertical movements of unsaturated, expansive soils with respect to time. This model, which is referred as modulus of elasticity-based method (MEBM), integrates Fredlund and Morgenstern (1976) constitutive equation for unsaturated soil structure along with the soil-atmosphere model VADOSE/W (Geo-Slope, 2007) to predict the variation of expansive soil movement over time. Adem and Vanapalli (2015) further extended this model for estimating the modulus for unsaturated expansive soils using a semi-empirical model originally proposed by Oh et al. (2009). They employed the MEBM for several case studies to study expansive soil response for moisture variation with time (Vanapalli and Adem, 2012; Adem and Vanapalli, 2013; Vanapalli and Adem, 2013; Adem and Vanapalli, 2015).

Karunarathne et al. (2018) developed a numerical model to estimate the ground movements in expansive soils for two sites in Melbourne, Australia. They used VADOSE/W software to simulate the soil moisture variation due to climate. Unsaturated hydraulic conductivity function for the model was estimated using the Fredlund-Xing method (Fredlund and Xing, 1994). Initial soil suction profile was determined based on the measured volumetric water content profile and soil water characteristic curve (SWCC). The predicted soil moistures from the VADOSE/W model were then used to predict the ground movements using the software FLAC3D. They used the model to estimate variation of ground movements due to long-term climate conditions. In this study, the model validation was conducted by comparing the field measured and model predicted volumetric water content values. From the model sensitivity analysis, it was found that the thermal properties of expansive clays have extremely low sensitivity for the variation in volumetric water content. In their study, they simulated the soil moisture changes and ground movements over 70 years i.e., 1945 to 2015. They also investigated the same models subjected to predicted weather data for wet and dry periods for the period of 2015–2018. They generated the wet and dry climate data set by replicating the climate condition from the historical data.

Zhang et al. (2019) used the HYDRUS 2D software package to perform a one-year simulation of water infiltration into a road embankment. They used the climate specific suction profiles generated by the HYDRUS 2D to compute vertical movement of pavements using the suction-based constitutive law proposed by Lytton (1994) that relates the change in height of a soil layer to the change in suction. Based on a series of sensitivity analyses Zhang et al. (2019) showed that initial moisture condition and hydraulic conductivity has the most significant effect on the vertical movement of the pavement while the evaporation rate has a minimal impact on vertical movement calculations. Their results also indicated that vertical movement can increase two-fold under an extreme rain event.

Previous numerical models have used two independent stress state variable approach in which the soil constitutive law is defined based on net normal stress and soil suction. Such approach requires two sets of constitutive parameters to predict the expansive soil response to mechanical and environmental loadings. For example, the contributing material properties in the elasticity-based methods within the two-stress state framework include elasticity modulus with respect to net normal stress (E) and elasticity modulus with respect to suction stress (H).

In this study, a two-dimensional finite element model that incorporates a transient variably-saturated seepage analysis and an elastic-based effective stress-strain analysis was used to simulate the volumetric behavior of expansive clay subject to soil moisture variation. The finite element model utilizes suction stress to calculate the effective stress field as a single stress state variable.

The proposed method requires one elastic modulus to model the expansive soil deformation behavior under mechanical and environmental loadings compared to the two-stress state variable framework that requires two elastic moduli. The power law equation proposed by Lu and Kaya (2014) was employed to incorporate the dependency of soil modulus on volumetric water content of soil. The developed numerical model was used to model a benchmark problem of a partially paved Regina expansive clay surface subjected to a constant infiltration rate for 175 days, and the results were compared with those reported by others including Hamberg (1985), Vu and Fredlund (2006), Zhang and Briaud (2010) and Adem and Vanapalli (2013).

3.3. Void Ratio Constitutive Relation

In general, the hydro-mechanical modeling of the expansive soil response to changes in soil moisture due to climatic variables requires a transient variably saturated seepage model coupled with a mechanical strain-stress model The seepage model needs to be equipped with the soil-atmospheric boundary and the mechanical model requires to incorporate an unsaturated soil mechanics framework. The dependency of mechanical properties of an expansive soil on its moisture content requires an appropriate constitutive model to simulate the volumetric deformation behavior of expansive soil. The volume change behavior of expansive soils can be represented by constitutive relationships that relate the deformation state variables (e.g., void ratio, e) to the stress state variable(s).

3.3.1. Two Stress State Constitutive Surface

Two independent stress state approach using net normal stress and matric suction has been extensively used to explain the volume change and shear strength behavior of soils. In this approach, soil volume can change due to a change in mechanical stress and change in matric suction. Therefore, the constitutive relationships needs be defined in the form of a constitutive surface in void ratio-net normal stress-matric suction space.

Several mathematical equations for description of void ratio constitutive surface have been proposed in the literature. Fredlund (1979) suggested that the void ratio constitutive surface for an unsaturated soil can be linearized over a wide range of stress using the logarithm of the stress state variables using the following equation:

$$e = a + b\log(\sigma - u_a) + c\log(u_a - u_w) \qquad [3\text{-}3]$$

where a, b and c are the equation constants and other variables are as described earlier.

Lloret and Alonso (1985) investigated several mathematical equations for description of the volume change constitutive surface of unsaturated soils under different loading conditions by comparing best fit to experimental results on different soil types, and proposed the following equations:

$$e = a + b\log(\sigma - u_a) + c\log(u_a - u_w) + d\, log(\sigma - u_a)\log(u_a - u_w) \qquad [3\text{-}4]$$

where a, b, c and d are the equation constants.

Fredlund (2000) proposed the following equation for an overconsolidated soil:

$$e = a + b\, ln\left[1 + \left(\frac{\sigma}{c}\right)^2\right] + d\, ln\left[1 + \left(\frac{\sigma}{f}\right)^2\right] \qquad [3\text{-}5]$$

where $a = a_1 + a_2(u_a - u_w)$, $b = b_1 + b_2\ln(u_a - u_w)$, $d = d_1 + d_2\ln(u_a - u_w)$ and a_1, a_2, b_1, b_2, c, d_1, d_2 and f are six fitting parameters.

Vu (2003) evaluated six different mathematical equations to define a void ratio constitutive surface for Regina clay. The following six-parameter equation was shown to provide an optimal constitutive surface:

$$e = a + b\ log\left[\frac{1+c(\sigma-u_a)+d(u_a-u_w)}{1+f(\sigma-u_a)+g((u_a-u_w)}\right] \qquad [3\text{-}6]$$

where a, b, c, d, f and g are the equation constants. Vu (2003) proposed a=1.183, b=-0.283, c=0.015, d=0.045, f=0, and g=0.00534 for Regina clay using laboratory test data obtained by Shuai (1996).

A constitutive surface can be simplified as a plane surface assuming linear relationship between the state variables. If linear relationship between void ratio and logarithm of net stress and logarithm of matric suction is considered, the plane constitutive surface can be explained by the following equation:

$$\frac{\sigma_m-u_a}{10^{(\frac{e-b}{a})}}+\frac{u_a-u_w}{10^{(\frac{e-d}{c})}}=1 \qquad [3\text{-}7]$$

where a, b, c and d are the equation constants. However, the constant void ratio curve for the void ratio constitutive surface does not necessarily have to be a straight line. Zhang (2004) indicated that a quadratic constant void ratio curve could be a better assumption to explain the volume change behavior of soil. Based on this assumption, Zhang (2004) proposed the following mathematical expression for the void ratio constitutive surface:

$$(\sigma_m - u_a)10^{[y_1-b_1\ln\left(\frac{a_1}{e-x_1}-1\right)]} + (u_a - u_w)10^{[y_2-b_2\ln\left(\frac{a_2}{e-x_2}-1\right)]} = 1 \qquad [3\text{-}8]$$

where a_1, a_2, b_1, b_2, x_1, x_2, y_1 and y_1 are the equation constants (i.e., fitting parameters). Zhang (2004) used the above equation to establish the constitutive surface for an expansive clay from a site at Arlington, Texas in the United States. The regression parameters proposed by Zheng (2004) to fit the equation to the available laboratory testing data are presented in Table 3-1.

Table 3-1- Regression Parameters for Arlington expansive clay (Zhang 2004)

	a	b	x	y
e vs $(\sigma - u_a)$	0.6641	-0.6811	3.3957	0.1731
e vs $(u_a - u_w)$	0.3604	-0.5073	2.7015	0.4740

The reviewed literature indicates that most of the proposed mathematical equations for void ratio surface normally requires three to eight equation constants to provide the best fit to the experimental data. In general, a larger number of fitting parameters for explaining the mathematical expressions for constitutive relations results in better representation of the experimental data. However, this may lead to rapid loss of the physical interpretation of the parameters used in the equations (Lloret and Alonso, 1985).

3.3.2. Proposed Single Stress State Constitutive Relationship

The relationship of void ratio (e) versus logarithm of effective stress (σ') has been extensively utilized for saturated soils. For unsaturated soil conditions, laboratory testing to determine soil deformation behavior is normally carried out under controlled net total stress and controlled soil suction separately. In this study, the following equation was considered to relate the variation of void ratio and change in mean effective stress:

$$e = a + b\ ln\left[1 + (\frac{\sigma_m{'}}{c})^2\right] \qquad [3\text{-}9]$$

where a, b and c are the equation constants, and $\sigma_m{'}$ is mean effective stress. These constants were determined based on the available void ratio constitutive surface for two expansive soils that were described in the previous section i.e., Texas expansive clay reported by Zhang (2004) and Regina expansive clay reported by Vu (2003).

MATLAB was employed for regression analysis using Multiple Linear Regression (MLR). The fitted curves for these two expansive clays are shown in Figure 3-1 and Figure 3-2. The regression parameters are presented in Table 3-2. The regression model performance was validated using several regression indices including R-Squared (R^2), mean square error (MSE) and root mean square error (RMSE). The obtained values for these indices are presented in Table 3-2.

Table 3-2- Regression parameters for two expansive clays

	a	b	c	R^2	MSE	$RMSE$
Regina Clay	1.183	-0.032	8.475	0.960	1.79e-04	0.0134
Texas Clay	0.829	-0.038	45.697	0.993	4.76e-05	0.0069

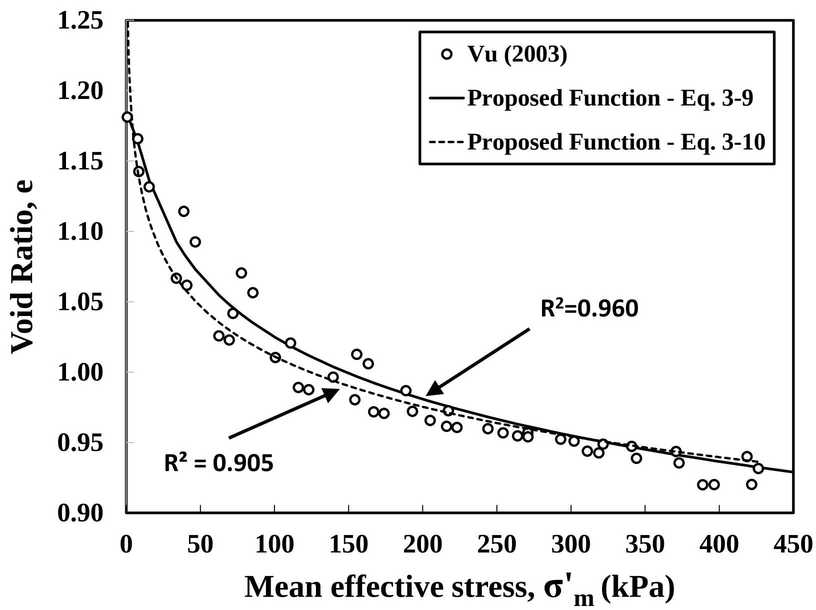

Figure 3-1- Fitted curve for Regina expansive clay reported by Vu (2003)

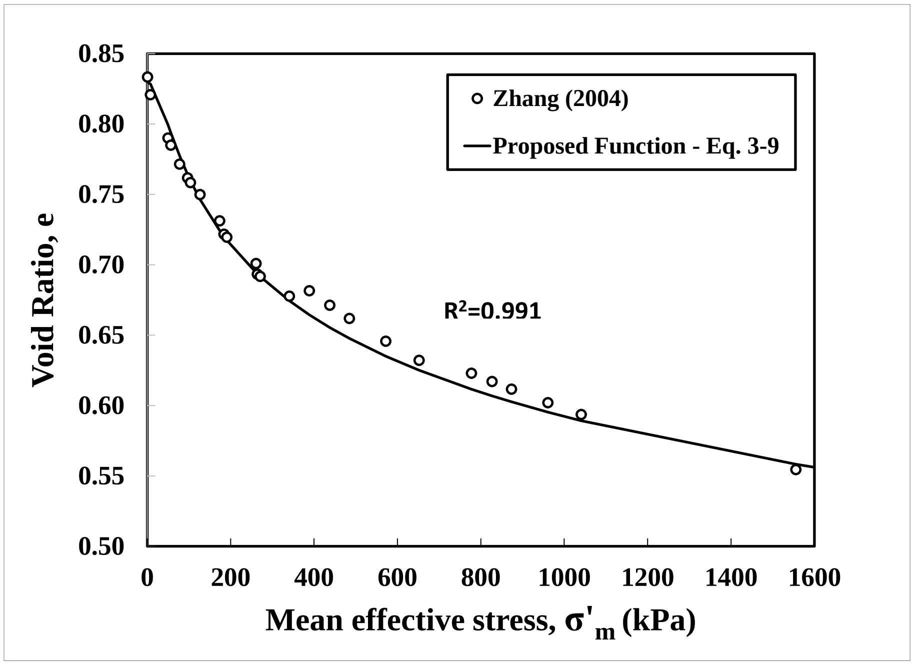

Figure 3-2- Fitted curve for Texas expansive clay reported by Zhang (2004)

In addition to Eq. 3-9, the following equation with two fitting parameters was also examined to relate void ratio and mean effective stress for Regina expansive clay:

$$e = a + bLn[\sigma_m{}']$$ [3-10]

The fitted curve based on the above equation (a =1.52 and b=-0.052) is also depicted in Figure 3-1. R-Squared (R^2) value of approximately 0.906 was obtained which is less than R^2=0.960 for Eq.3-9.

The regression analysis for fitting the best curve to the void ratio vs mean effective stress determines three constant parameters used in Eq.3-9 and two parameters in Eq.3-10. However, calculation of effective stress also requires α and n that should be determined by fitting the van Genuchten's (1980) equation to the soil water characteristic data. The computer program RETC (van Genuchten et al., 1991) was utilized to obtain the soil water characteristics parameters for the two expansive clays as presented in Table 3-3. SWCC curves considered for these two soils are presented in Figure 3-3.

Table 3-3- SWCC parameters α and n

	α (1/kPa)	n
Regina Expansive	1.2350	1.10
Texas Expansive	0.0029	1.27

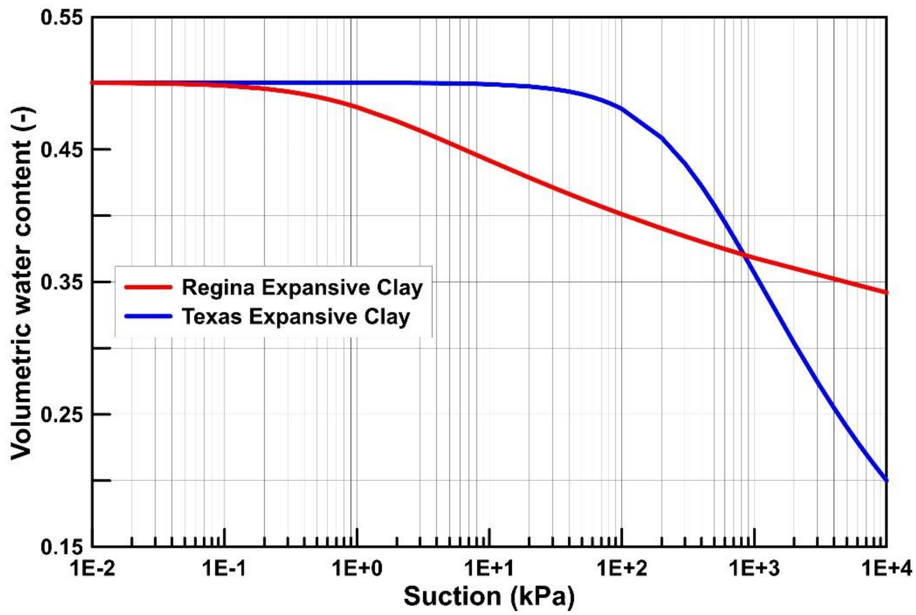

Figure 3-3- SWCC curves for two expansive clays

3.4. Variable Soil Stiffness

The relationship of void ratio (e) versus logarithm of effective stress (σ') has been extensively utilized for saturated soils. For unsaturated soil conditions, laboratory testing to determine soil deformation behavior is normally carried out under controlled net total stress and controlled soil suction separately. In this study, a mathematical model was developed to relate the variation of void ratio and effective stress change based on available soil constitutive data in terms of two stress variables i.e., net total stress (σ_{nt}) and soil suction (h).

Assuming that void ratio is defined as a function of net total stress and soil suction i.e., $e = f(\sigma_{nt}, h)$, the differential of this function is given by:

$$de = \frac{\partial f}{\partial \sigma_{nt}}\, d\sigma_{nt} + \frac{\partial f}{\partial h}\, dh \qquad [3\text{-}11]$$

The single stress state approach suggests that void ratio can be defined as a function of effective stress that is identified as $e = g(\sigma')$ in this study. Similarly, the deferential of this function can be expanded as below:

$$de = \frac{\partial g}{\partial \acute{\sigma}}\, d\acute{\sigma} = \frac{\partial g}{\partial \acute{\sigma}}\, (d\sigma_{nt} - d\sigma_s) \qquad [3\text{-}12]$$

The change in net normal stress, where the soil deformations under climate variables is studied, can be ignored. Moreover, net normal stress change where the soil is subject to light loads such as pavements or light buildings is normally minimal. Therefore, one can assume that the soil deformation can be largely due to changes in matric suction. In this study, the net normal stress is assumed constant in the development of the mathematical model ($d\sigma_{nt} = 0$). This assumption has been considered in the previous studies (e.g., Adem and Vanapalli, 2013). Therefore, Eq. 3-11 and Eq. 3-12 reduce to the following equations:

$$de = \frac{\partial f}{\partial h}\, dh \qquad [3\text{-}13]$$

$$de = -\frac{\partial g}{\partial \acute{\sigma}} d\sigma_s \qquad [3\text{-}14]$$

The above equations can be combined to obtain an equation for the change of a void ratio with respect to soil suction at a given total net stress:

$$\frac{de}{d\acute{\sigma}} = -\frac{\partial f}{\partial h} \times \frac{1}{\frac{d\sigma_s}{dh}} \qquad [3\text{-}15]$$

The first derivative of suction stress with respect to soil suction is given by (Lu et al., 2010):

$$\frac{d\sigma_s}{dh} = -\frac{1}{(1+[\alpha h]^n)^{\frac{n-1}{n}}} + \frac{(n-1)[\alpha h]^n}{(1+[\alpha h]^n)^{\frac{2n-1}{n}}} \qquad [3\text{-}16]$$

In this study, Eq. 3-15 was used to calculate the soil deformation modulus for the effective stress-strain analysis.

A number of previous studies have utilized elastic moduli to simulate the heave behavior of expansive soils. In general, an incremental procedure using small increments of stress and strain can be used to apply the linear elasticity formulation to model the non-linear stress-strain behavior of soil (Vu, 2003). Two elastic moduli are normally employed to calculate the soil deformations induced by change in net normal stress and matric suction within the two-stress state framework. This framework was originally proposed by Fredlund and Morgenstern (1976). However, the coefficient of volume change with respect to a change in effective stress can be considered in an effective stress analysis as follows:

$$m_v = \frac{1}{1+e_0}\frac{de}{d\acute{\sigma}} \quad [3\text{-}17]$$

For K0-loading condition, the coefficient of volume change is related to elastic modulus using:

$$E = \frac{(1+\mu)(1-2\mu)}{(1-\mu)m_v} \quad [3\text{-}18]$$

where μ is soil Poisson’s ratio.

The dependency of elastic modulus on effective stress is well established for the saturated soils. Under unsaturated conditions, the previous experimental studies confirm the dependency of elastic modulus on soil volumetric water content (e.g., Sawangsuriya et al. (2009); Ng et al. 2009; Schuettpelz et al. 2010 and Khosravi and McCartney 2011). It has been observed that a soil elastic modulus can increase up to several orders of magnitude from fully saturated to dry conditions due to soil water retention mechanisms i.e., adsorption and capillarity (Zhang et al., 2022).

Eq. 3-15, Eq. 3-17 and Eq.3-18 were used in the current study to obtain the variation of elastic modulus with soil suction at a given net total stress level. The soil water characteristic curve (SWCC) using van Genuchten’s (1980) equation was utilized to calculate the elastic modulus variation with volumetric water content.

Several semi-empirical models for predicting the variation of elastic modulus with soil volumetric water content or soil matric suction under unsaturated conditions have been proposed in the literature (e.g., Sawangsuriya et al. (2009); Oh et al. (2009); Lu and Kaya (2014) and Zhang et al., 2022). In this study, the following power law equation for soil elastic modulus as a function of volumetric water content was utilized in the numerical analysis:

$$E(\theta) = E_d + (E_w - E_d)\left(\frac{\theta-\theta_d}{\theta_w-\theta_d}\right)^m \quad [3\text{-}19]$$

where $E(\theta)$ is the elastic modulus, $E(\theta) = E_d$ for the drying state when $\theta = \theta_d$ usually measured at the residual saturation state; and $E(\theta) = E_w$ for the wetting state, when $\theta = \theta_w$ usually measured at the fully saturated state; and m is an empirical parameter.

3.5. Development of the Numerical Model

In this study, HYDRUS (2D/3D) version 3.04.0140 (Šimŭnek et al. 2006) together with Slope Cube module (Lu et al. 2016) were utilized to simulate two-dimensional transient fields of soil moisture, soil suction, suction stress, total and effective stresses and deformation. HYDRUS 2D is a finite element software that numerically solves a modified version of the Richards' equation for movement of water flow in variably saturated soils. Slope Cube simulates stresses and deformation from transient variably saturated flow analysis from HYDRUS. Slope Cube, which was originally developed to analyze the initiation and locations of landslide occurrences under rainfall conditions, is an effective stress-based finite element module that is capable of calculating soil deformations due to changes in suction stress field as described in previous Section. Moreover, the module utilizes the power law equation to consider the variation of elastic modulus with soil moisture.

At each time step, the pore pressure distribution affected by infiltration is updated by seepage analysis (HYDRUS 2D). This information is used by Cube module to calculate the suction stress and effective stress field and the resultant soil deformations.

3.6. Case Study

3.6.1. Problem Statement

Figure 3-4 illustrates a 5 m layer of Regina expansive clay which is partially covered by a impervious cover. The uncovered portion of the ground surface is subject to a constant infiltration rate equal to 1.73 mm/s. The initial matric suction is taken to be constant throughout the depth and equal to 400 kPa. The hydraulic boundary conditions are also depicted on this Figure.

The finite element stress-strain analysis was carried out with the left and right boundaries free to move in the vertical direction; while the bottom boundary is fixed in both vertical and horizontal directions. Figure 3-5 illustrates the finite element mesh and mechanical boundary conditions used in this study. The finite-element model consists of 10,124 triangular elements. Finer mesh was generated near the unpaved surfaces to provide appropriate resolution within the infiltration zone. This example was first simulated by Vu (2003) and has been considered in later publications (e.g., Vu and Fredlund 2006, Adem and Vanapalli 2015). The variation of soil moisture conditions during 175 days was simulated using the developed numerical model.

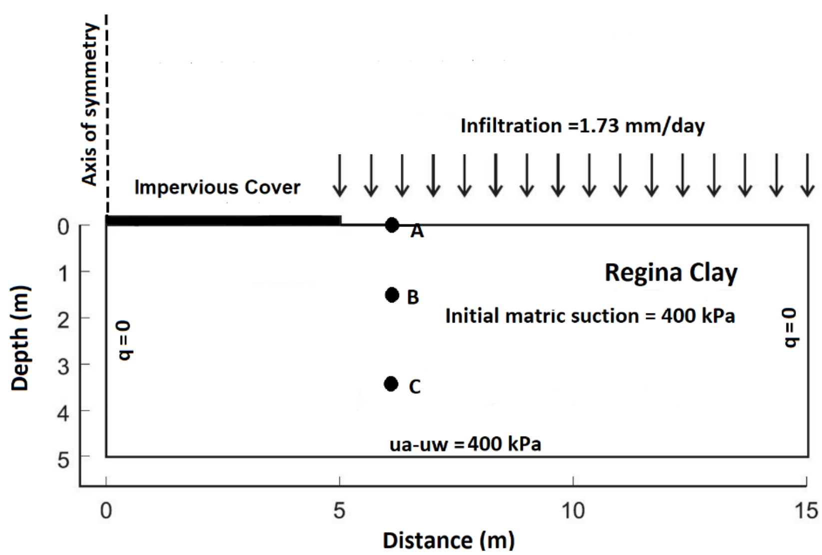

Figure 3-4- Geometry and hydraulic boundary conditions

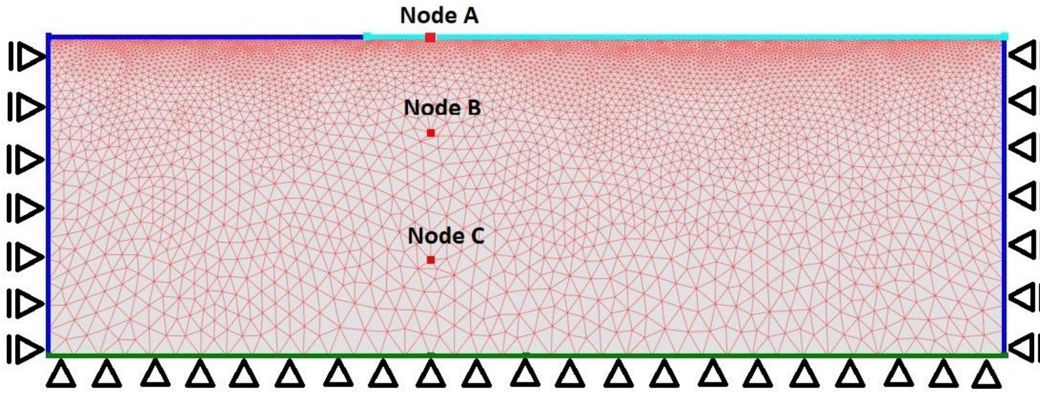

Figure 3-5- Finite element mesh and mechanical boundary conditions

3.6.2. Regina Clay Parameters

Figure 3-6 shows the soil water characteristic curve (SWCC) and unsaturated hydraulic conductivity function (HCF) for Regina clay, obtained from Vu (2003) and Adem and Vanapalli (2013). HYDRUS Cube module utilizes α and n parameters based on SWCC curve using the mathematical model suggested by van Genuchten (1980) to calculate the suction stress. These parameters are required to calculate suction stress using Eq. 2-5.

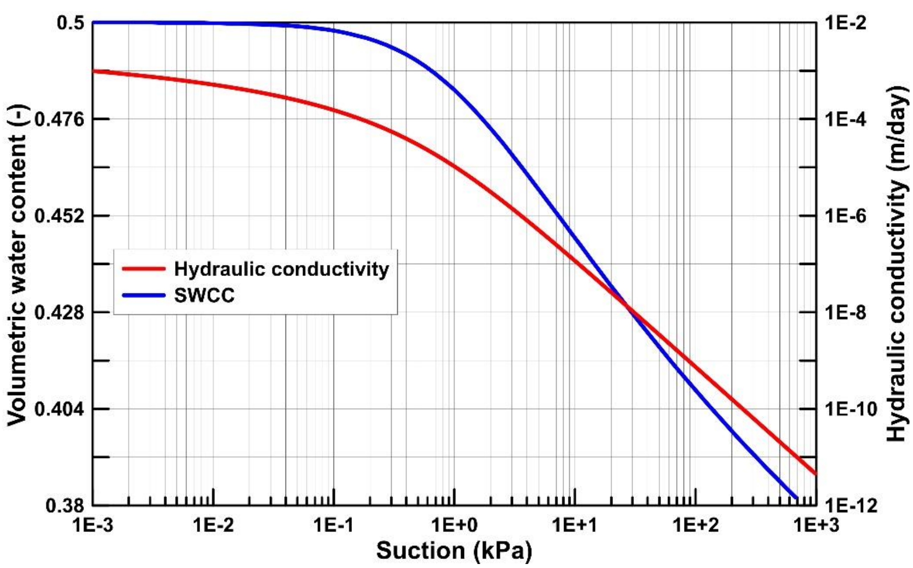

Figure 3-6- SWCC and HCF curves used for Regina clay in this study

The soil elastic moduli for dry and saturated conditions used in this study are presented in Table 3-4. These values were obtained from the best-fit power low curve matched to the calculated elastic modulus versus soil moisture data for the range of suction between 0 and 400 kPa. It should be noted that the saturated elastic modulus for Regina clay was estimated Esat (MPa)=1.1 MPa by Adem (2015) which is greater than the value used in this study.

Table 3-5 presents the physical parameters assumed for Regina clay in his study.

Table 3-4- Regina clay- elastic parameters used in this study

E_d (MPa)	E_w (MPa)	m	μ
51.2	0.32	0.11	0.4

Table 3-5- Regina clay- physical parameters used in this study

e_0	G_s	γ_t (kN/m)
0.955	2.83	17.27

3.6.3. Results and Discussions

The variation of matric suction distribution as well as horizontal and vertical soil deformation profiles were computed under 175 days infiltration at the unpaved ground surface using HYDRUS Cube module.

Figure 3-7, Figure 3-8 and Figure 3-9 illustrate the distribution of suction head, vertical and horizontal deformations at the day 175. The infiltration caused the matric suction to reduce from its initial value of 400 kPa (40.78 m) up to approximately 6 m at the vicinity of the unpaved ground surface. As one can expect, the decrease in the matric suction resulted in soil heaving. The maximum heave after 175 days is approximately 50 mm which occurred at the farthest left side of the domain at the ground surface. In addition to heaving, the asymmetric infiltration conditions caused lateral movements in the expansive soil. The numerical results indicate that the maximum horizontal deformation at the corner of the paved area is approximately 13 mm. The obtained values are in good agreement with those reported by Vu (2003).

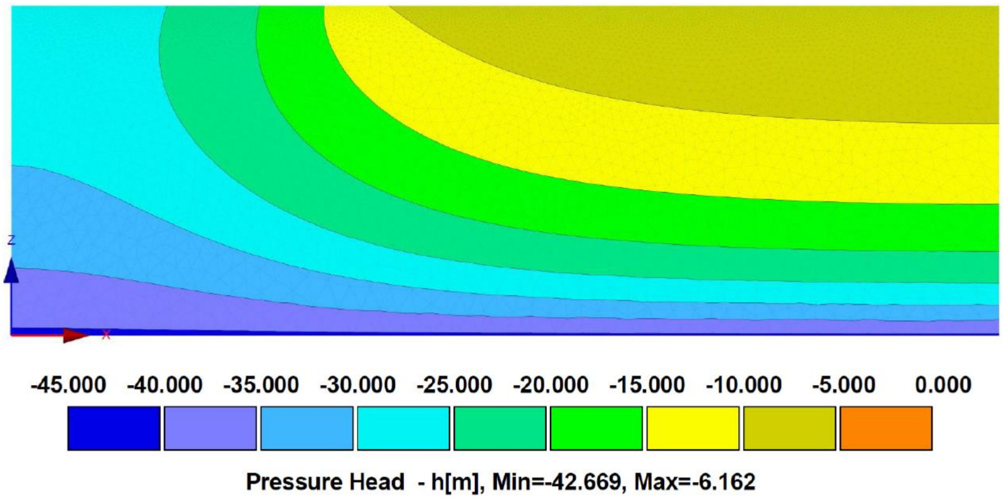

Figure 3-7- Suction head distribution at day 175

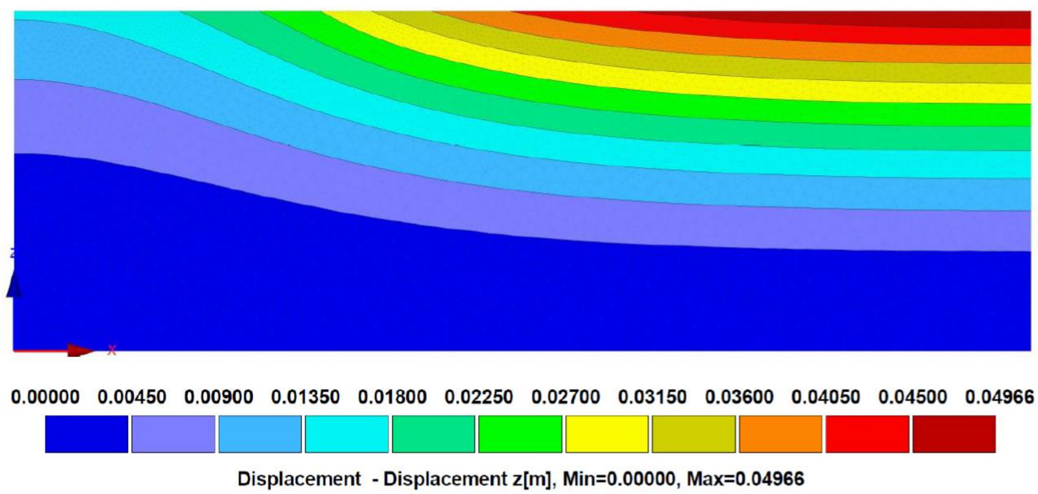

Figure 3-8- Vertical displacement distribution at day 175

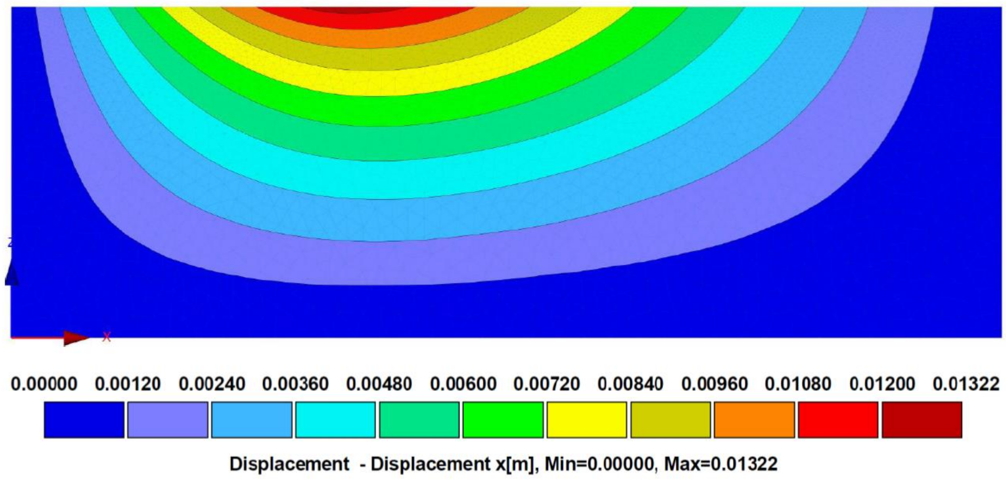

Figure 3-9- Horizontal displacement distribution at day 175

Figure 3-10 and Figure 3-11 illustrate the comparison of predicted matric suction and heave at the three locations (Nodes A, B, and C) over time using the developed numerical model and the results obtained by Vu and Fredlund (2006) using a coupled approach. The observation nodes A, B and C are located 1m away from the paved area at depth 0, 1.5 m and 3.5 m, respectively. Although the anticipated matric suction at node C is approximately 20% less than what was reported by Vu and Fredlund (2006), the matric suction compares well at shallower depths (Nodes A and B).

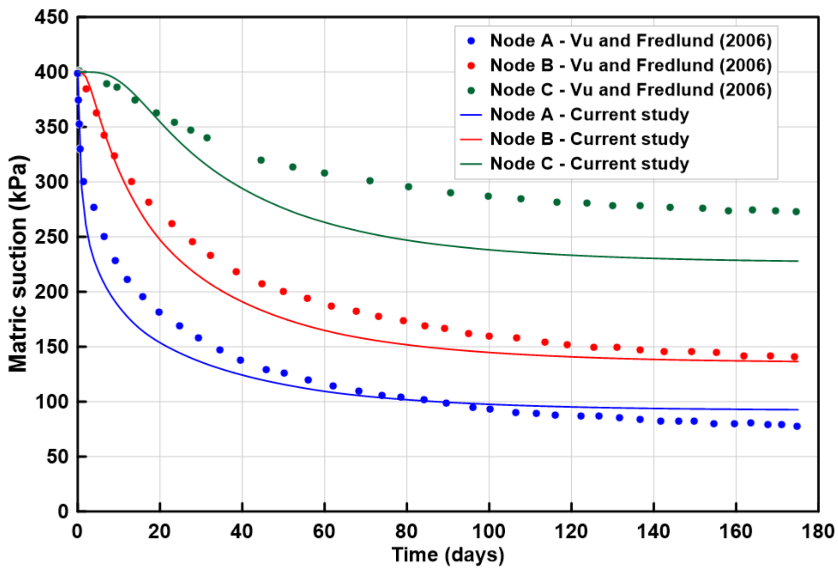

Figure 3-10- Matric suction development with time at points A, B, C

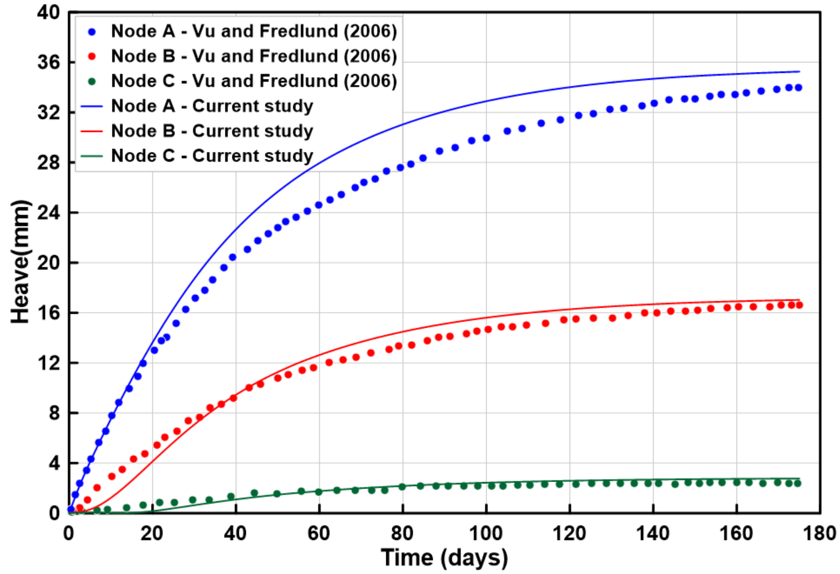

Figure 3-11- Vertical displacement (heave) with time at points A, B, C

The anticipated variation of heave with time indicates good agreement between two studies. The heave profile with depth (Figure 3-12) and the ground surface profile (Figure 3-13) at three different days i.e., day 13, day 53 and day 175 also confirm the good agreement between the results obtained from two studies despite different unsaturated soil mechanics formulations. The results show that more than 75% of the total heave is completed over 53 days.

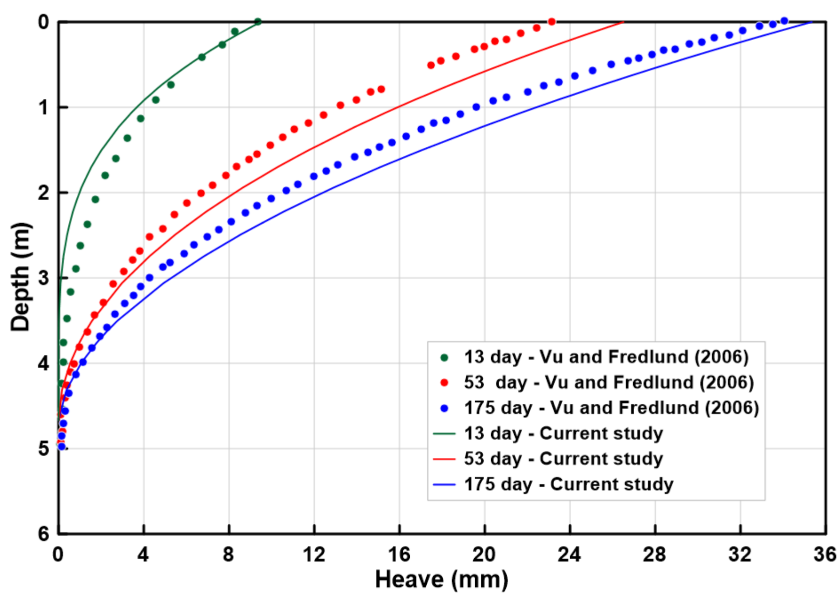

Figure 3-12- Vertical displacement (heave) with depth at different times

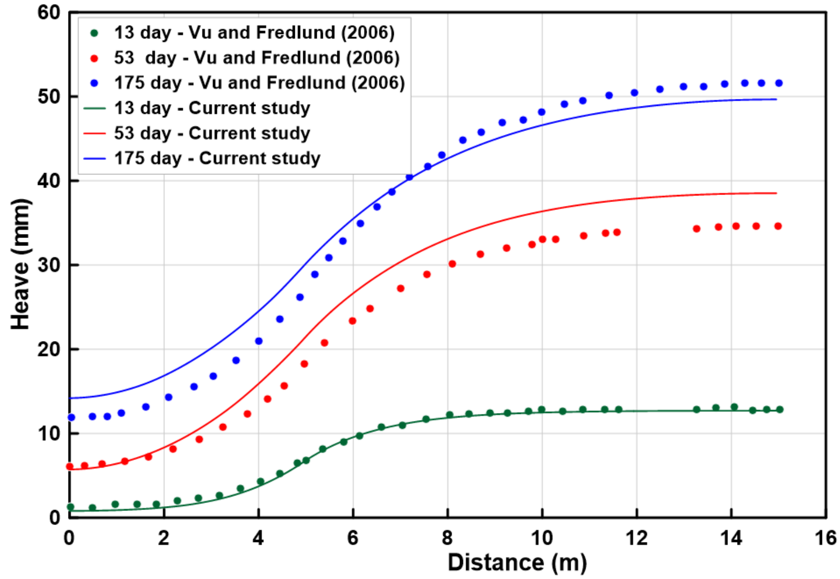

Figure 3-13- Ground surface heave profile at different times

Adem and Vanapalli (2013) carried out a comparison study for estimating the heave for the same benchmark problem using three different methods: Hamberg (1985), Zhang and Briaud (2010) and MEBM. Table 3-6 presents a summary of the maximum heave at ground surface (Node A) after 175 days using these three methods and the results obtained from effective stressed based analysis in this study. It should be noted that these three methods consider one dimensional heave, whereas the numerical model of Vu and Fredlund (2006) and the numerical model developed in the current study include two-dimensional deformation analysis. And results from the current study compare better to Vu and Fredlund (2006) by using fewer fitting parameters.

Table 3-6. Maximum heave at Node A after day 175

Method / Study	Maximum Heave (mm)	Comparison*
Vu and Fredlund (2006)	34	1.00
Adem an Vanapalli (2013)	41	1.21
Hamberg (1985)	71	2.09
Zhang and Briaud (2010)	58	1.71
This study	35	1.03

* with respect to Vu and Fredund (2006)

3.7. Concluding Remarks

In this study, a single stress state variable framework was adopted to describe the void ratio as a function of effective stress for soils in unsaturated state. The proposed approach was used to fit single variable void ratio curves to the laboratory test data for two different expansive soils, i.e., Regina expansive clay and Texas expansive clay, under a range of mechanical stress and matric suction. Two different logarithm functions with two and three constant parameters were selected to examine the relationship between void ratio and mean effective stress in unsaturated conditions. Multiple Linear Regression (MLR) was employed to obtain the best fitted curves for constitutive relationship for two expansive clays. The regression analysis was validated using several regression indices.

A two-dimensional finite element analysis was employed to simulate transient variably-saturated seepage analysis and to estimate soil deformations under mechanical and environmental loadings using elastic-based effective stress-strain analysis. The effective stress field is updated based on the changes in suction stress which is a function of matric suction and soil water characteristic curve. A mathematical approach was utilized to obtain the elastic modulus from the void ratio constitutive surface data. A power law equation was then employed to incorporate the dependency of soil modulus on volumetric water content of soil in the analysis.

The developed numerical model was used to model a problem of a Regina expansive clay layer, which is partially covered by a impervious pavement, and the uncovered ground is subjected to a constant infiltration rate over 175 days. The results obtained indicate the capability of the proposed model in simulation of expansive soil deformations subject to varying moisture conditions over time. In contrast to the available one-dimensional methods, the proposed model can simulate the two-dimensional distribution of suction head, vertical and horizontal soil deformations with time.

Such vertical and horizontal soil deformations can cause significant differential movements over time. The numerical results are in good agreement with those reported by Vu and Fredlund (2006) with fewer fitting parameters.

The obtained results indicate the capability of the proposed model in simulation of expansive soil deformations under climate data over time. The validation of the developed model to simulate the expansive soil response to long term climate considering climate change will be discussed in the next chapter.

Chapter 4 : Expansive Ground Response to Climate Change

4.1. Abstract

Expansive soils experience significant volume change due to soil moisture fluctuations caused by changes in climatic conditions. This may lead to considerable damage to the structures constructed on the expansive soils. The global climate change is predicted to impact the climate cycles over this century and therefore, the expansive ground response to soil-atmosphere interaction is expected to be intensified in future.

In this study, numerical simulation of the climate change impact on the long-term deformation behaviour of Regina expansive clay in the City of Regina is presented. For this purpose, a two-dimensional coupled hydro-mechanical model equipped with a soil-atmosphere boundary has been developed to simulate the moisture dynamics in the near- surface zone of the expansive clay. The developed model is capable of simulating the impact of climate induced moisture changes on volumetric change behavior of expansive clay. The mechanical model utilizes an elastic-based stress-strain finite element analysis based on a proposed single stress state unsaturated soil mechanics framework.

In this study, a three-staged approach has been proposed to select critical future climate scenario to quantify the expansive soil behavior. The ground movements due to soil moisture fluctuations were simulated for historical climate as well as the selected critical scenario for the future climate. The results of numerical model were statistically analyzed to quantify the impact of climate change, and to capture the relationship between ground movement and climatic variables based on daily, monthly and yearly basis. In general, the results indicate that the excessive ground deformation response is not necessarily correlated with moisture indices or the maximum daily precipitation events, but rather with the sequence of extreme precipitation events and their

concurrency within colder months with minimal evaporation. The comparison study indicated that the frequency of large expansive ground heaving events is considerably higher under future climate change predictions for the city of Regina.

4.2. Introduction

The expansive soils are clayey soils found mostly in arid and semi-arid regions around the world. These soils exhibit significant shrinkage and swelling when subjected to water content changes. Their swelling and shrinkage behaviour is due to the presence of expansive clay minerals, such as Montmorillonite (Mitchell and Soga, 2005). Larger percentage of the clay minerals generally equate to greater swelling/shrinkage potential.

Climate is a key factor influencing the soil moisture content fluctuations and therefore, climatic drying/wetting cycles may cause expansive soil undergoing significant swelling/shrinking that may ultimately lead to considerable damage to the lightly loaded buildings, buried utilities and pavements. Moreover, the global climate change process is actively underway and is expected to continue over the century. It has been predicted that the climate variables such as precipitation and potential evaporation, which are key factors affecting the soil moisture content, will change significantly over the course of this century.

In recent years, the impact of climate change on expansive soils behaviour has received some attention from researchers. Harrison et al. (2012) investigated the relationship between the climate change and the shrinkage/swelling behaviour of London clay in south-east England. Their study focused on enhancing the understanding of the potential consequence of projected changes in precipitation and temperature on ground movement over the next century. This study highlighted the potential value of the subsidence claims data from the Association of British Insurers as a proxy for shrinkage/swelling geo-hazard in the UK. A preliminary geographical information system

(GIS) model was built to quantify the susceptibility of shrinkage and swelling as a result of climate change. The model used subsidence claims data, historical climate data from the United Kingdom Meteorological Office (UKMO), future climate change scenarios from UKC1P02 climate model, and the British Geological Society's (BGS) GeoSure national geo-hazard database. High and low emissions climate change scenarios were considered in their assessment. Their 2020 projection modelling indicates that for high emission scenario much larger area with significantly greater susceptibility to shrink-swell is expected in comparison to low emissions scenario. Their 2080 projection indicates that even for low emissions scenario, almost all of the area with clay-rich formations will be susceptible to increased shrink and swell. One of the shortcomings of their study is the use of precipitation and temperature data as proxies instead of using the moisture deficit information.

Mitchell (2013) quantified the climate change effects on expansive soil movements for the Australian cities of Adelaide, Melbourne, Sydney, and Perth for the years 2030 and 2070. His approach entailed the calculation of Thornthwaite (1948)'s Moisture Index (TMI) for the years 2030 and 2070 based on the predicted temperature increases for these years. The change in the estimated TMI for the future years was related to the expansive soil movements using the empirical approach described in Australian Standard AS 2870-2011 (Standards Australia 2011). According to his estimates, continuing revisions of footing standards are required to take into account the climate change. One of the limitations of his approach is the use of regional monthly average temperatures for the estimation of potential evaporation (PE) using Thornthwaite (1948) equation. A more rigorous approach, such as by Penman (1948) or Monteith (1965), that takes into account the effect of relative humidity, air temperature, wind speed, and net radiation on PE, might have resulted in more refined estimates. It should also be noted that it is the actual evaporation (AE) that influences the suction behaviour of soil as opposed to the PE, which assumes a limitless supply of water. Moreover, predictions of future temperatures were based on a single emission scenario (AIB emission scenario for 2030 and AIFI emission scenario for 2070). IPCC 2000 recommends that a number of different scenarios with a variety of assumptions regarding driving forces should be used in any analysis.

Laeo (2014) used GIS to produce a map of potential risk of damage to residential buildings from expansive soil ground movement due to climate change. The map combines information on soil moisture changes related to climate and population growth in the state of Victoria, Australia. The absolute changes in TMI between the years 2001 and 2011 were used to quantify the severity of moisture deficiency. Changes in TMI between 6-10 and greater than 10 were considered medium and high, respectively. Similarly, the population between 5,001-15,000 and greater than 15000 were considered medium and high, respectively. After combining the attributes of TMI and population change, Laeo (2014) concluded that medium to high potential risk for expansive soil, damage exists for 11% of the state of Victoria. Most of the at-risk areas are located in the urbanized portions of the state, including metropolitan Melbourne and the surrounding regions.

Karunarathne et al. (2018) developed a numerical model to estimate the ground movements in expansive soils for two sites in Melbourne, Australia. They used VADOSE/W to simulate the soil moisture variation due to climate. Unsaturated hydraulic conductivity function for the model was estimated using the Fredlund-Xing method (Fredlund and Xing, 1994). Initial soil suction profile was determined based on the volumetric water content profile and soil water characteristic curve (SWCC). The predicted soil moistures from the VADOSE/W model were used to predict the ground movements using FLAC3D. The developed formulation in FLAC model is based on the assumption of isotropic free swelling behaviour of soil in which the linear swelling strain is related to the change in moisture content. They used the model to estimate the variation of ground movements due to long-term climate conditions. In this study, the model validation was conducted by comparing the field measured and model predicted volumetric water content values. From the model sensitivity analysis, it was found that the thermal properties of expansive clays have extremely low sensitivity for the variation in volumetric water content. Karunarathne et al. (2018) investigated the soil moisture change and ground movements over 70 years i.e., 1945 to 2015. They also investigated the same models subjected to predicted weather data for wet and dry periods for the period 2015–2018. No real climate change scenario was used in their analysis, and they generated the wet and dry climate data set by replicating the climate condition from the historical data.

Assadollahi and Nowamooz (2020) developed a transient hydro-thermal model of the soil-vegetation-atmosphere interaction (SVA) to calculate the variation of soil water content and suction in the soil medium. The HYDRUS 2D software package was used in their study for the unsaturated water flow analysis considering the influence of the water uptake by vegetation in the source term of the unsaturated water flow model. They used a linear void ratio – log suction model proposed by Nowamooz et al. (2013 and 2016) based on the drying-wetting tests to predict the volume change behavior of an unsaturated soil due to the variation of the soil suction. They assessed the established methodology by comparing the simulation results with the provided data from an instrumented site. Assadollahi and Nowamooz (2020) also utilized their proposed model to assess the future evolution of the soil movements subjected to the projected climatic variables until 2050 using three RCP scenarios i.e., RCP 2.6, 4.5 and 8.5. They concluded that in the long-term evaluation, the RCP 8.5 scenario could potentially have more impact on the soil movements and the differential soil movements close to trees are considerable in all three scenarios.

The above review of the published literature about the effects of climate change on expansive soil behaviour indicates that most of the studies to date have used indicators of soil moisture supply to quantify the expansive soil behaviour. There are only a few reported studies where the dynamics of drying and wetting have been articulated in terms of climate change and expansive soil behaviour (e.g., Karunarathne et al. (2018) and Assadollahi and Nowamooz (2020)). These studies employed simple linear relations between void ratio and either matric suction (Assadollahi and Nowamooz, 2020) or soil moisture content (Karunarathne et al., 2018) to estimate the expansive soil movements. These studies are limited to a small number of climate change scenarios.

The present study looks at the effects of climate change on the behaviour of Regina Clay in the city of Regina, province of Saskatchewan, Canada. A two-dimensional coupled hydro-mechanical soil-atmosphere model has been developed to investigate the moisture dynamics in the near-surface zone of the expansive clay deposit. The model utilizes an elastic-based effective stress-strain finite element analysis to simulate the volumetric behavior of expansive clay subject to soil moisture variation. In the effective stress analysis, suction stress was used to calculate the effective stress field as a single stress state variable. The proposed method requires one moisture dependent elastic modulus to model the expansive soil deformation behavior under mechanical and environmental loadings comparing to the two-stress state variable framework that requires two elastic moduli. The model was employed to quantify the expansive soil movements in response to variation of soil moisture due to long-term climate data.

The severity and the spatial extent of the ground movements due to soil moisture fluctuations were quantified not only for historical climate (1996-2010) but also for a selected climate change scenario for the next 90 years (2010-2100). The future climate data based on the latest climate models provided by the Pacific Climate Impacts Consortium (PCIC) was considered in this study.

A three-staged methodology was developed to select a critical future climate scenario for the city of Regina. The selected future climate data was used as in the developed numerical models to assess the impact of climate change on the long-term expansive Regina clay behavior.

4.3. Methodology

4.3.1. Numerical Model

In this study, HYDRUS (2D/3D) version 3.04.0140 (Šimůnek et al. 2006) together with Slope Cube module (Lu et al. 2016) were utilized to simulate two-dimensional transient fields of soil moisture, soil suction, suction stress, total and effective stress and soil deformation.

The model geometry, finite element mesh, and mechanical boundary conditions that were used in the case study (Section 3.6.) were modified for simulation of ground deformation response to the compiled long-term historical and future climate. The soil hydraulic properties i.e., SWCC and HFC proposed by Vu (2003) for Regina clay, which were obtained based on laboratory testing measurements, have been used in this study. The proposed SWCC and HFC were also considered in several previous studies (e.g., Adem, 2015).

At the uncovered portion of the ground surface in the model, a system-dependent boundary condition was applied to simulate the soil-atmosphere interaction at the ground surface. This boundary condition is capable of estimating actual evaporation, net infiltration, and surface runoff using climatic records of precipitation and potential evaporation together with model predicted transient soil-moisture conditions. The properties of the soil-atmosphere boundary as well as the initial conditions considered in the numerical model will be discussed in Section 4.5.1.

Fifteen years of historical climate data and thirty years of selected future climate data, comprising of daily values of precipitation and potential evaporation, was considered as input for the soil-atmosphere boundary at the top of the uncovered soil column. In all numerical models, the daily precipitation records were uniformly distributed over the day. The climate data used in this study as well as the seasonal considerations that were taken into account in the compilation of soil-atmosphere boundary input will be discussed in the following sections.

4.3.2. Climate Data

The Pacific Climate Impacts Consortium (PCIC) is a regional climate service centre at the University of Victoria that provides practical information on the physical impacts of climate variability and change in the Pacific and Yukon Region of Canada. PCIC offers statistically downscaled daily Canada-wide climate scenarios, at a gridded resolution of 300 arc-seconds (0.0833 degrees, or roughly 10 km) for the simulated period of 1950-2100. The variables available include minimum and maximum temperature, and precipitation.

PCIC has offered a coupled model intercomparison project in two phases i.e., phase 5 (CMIP5) and phase 6 (CMIP6). In phase 5, the downscaled scenarios were constructed from 27 Global Climate Models (GCMs) and 3 Representative Concentration Pathways (RCPs) (van Vuuren et al., 2011) from CMIP5 (Taylor et al., 2012) using the BCCAQv2 downscaling method. In phase 6, the downscaled scenarios were constructed from 26 GCMs and 3 Shared Socioeconomic Pathways (SSPs) (Riahi et al., 2017) from CMIP6 (Eyring et al., 2016) using the BCCAQv2 downscaling method. For both CMIP5 and CMIP6 scenarios can be selected from any combination of models, SSPs, and time period.

The CMIP6 database for Regina, Saskatchewan has been considered in this study. The predicted daily data for minimum and maximum, temperature, and precipitation from 1981-2100 for different 26 GCMs and 3 climatic scenarios (SSP1-2.6, SSP2-4.5, SSP5-8.5) were downloaded and compiled. The time period between 1981-2010 and 2010-2100 were assumed as historical and future climate periods. A proposed three-stage approach, which will be described in Section 4.6.

was employed to select the critical future climate scenario It should be noted that the predicted daily data for 1981-2010 were only utilized for validation of climate models. The numerical analysis for historical conditions was carried out using from the measured historical climate data obtained from Environment and Climate Change Canada (Environment and Climate Change Canada, 2019).

4.3.3. Seasonal Considerations

In winter, both atmosphere and ground could remain frozen for several months. Therefore, partitioning of the climate into active and inactive periods simplifies the estimation of water balance. In the active period, the ground condition remains thawed, and water can enter the ground surface and flow. In the inactive period, both the atmosphere and ground are frozen. It can also be assumed that in the inactive period little to no water enters the ground, and there is no flow in the upper soil layers. In order to reduce the computation time and unnecessary complexities related to ground freezing, development, and thawing of the snowpack, the inactive periods was ignored in the numerical model developed in this study. This approach has been proposed by e.g., Fredlund et al. (2012) and used by others (Bashir et al. (2016), Pk (2017), Baninajarian (2020) and Bashir et al. (2022)).

The inactive period starts with the date of freeze and ends with the date of thaw. The freezing and thawing dates can be found by analyzing the air temperature data. Historical and future daily mean air temperature data for the city of Regina was analyzed to estimate the average freezing and thawing dates and the length of active and inactive periods. The average active period of 215 and 241 days was obtained for historical and selected critical future climate scenarios, respectively. Based on the conducted analysis, the average thawing and freezing dates for historical climate were identified to be in early April and early November, respectively. However, these dates are found to be in mid April and early December, for selected critical future climate scenario. The longer active period in the future is consistent with observations from others for other locations (e.g., Pk, 2017; Baninajarian 2020).

As mentioned above, the atmosphere as well as the ground are frozen during the inactive period. The precipitation in inactive periods commonly comes in the form of snow and accumulates over the ground surface. A portion of this snow is moved away by the wind, and rest of it remains at the ground surface. At the beginning of the spring, when the temperature rises above freezing and the ground thaws, a portion of the accumulated precipitation of inactive period infiltrates into the ground and the rest of it flows over the ground as surface runoff (Pk, 2017). Therefore, it is reasonable to distribute a portion of the accumulated precipitation in inactive period at the beginning of the active period in the numerical model. In this study, 50% of the accumulated precipitation in inactive period was uniformly distributed over first two weeks of active period. This approach was used to adjust the compiled climate data for both historical and future periods. This amount is consistent with the prairie hydrological processes and reasonable for the city of Regina (Pomeroy et al., 2005).

4.4. Ground Deformation Response to Historical Climate

4.4.1. Monthly Basis

Figure 4-1 presents the range of ground surface vertical displacement for each month over a 15 year period from 1996 to 2010 in the form of a box and whisker plot. In this figure, the box shows Interquartile Range (or IQR) which is defined as the middle 50% of data (i.e., the range between the 25^{th} and 75^{th} percentiles), and the whiskers show the range between 1.5× IQR below 25^{th} percentile and 1.5× IQR above 75^{th} percentile. Based on this Figure, the median (50^{th} percentile) of the ground surface movement data for different months is negative indicating that the ground experienced shrinkage with exception of the month of April in which the median and mean values are slightly above zero indicating swelling behavior. The graph also shows that the range of first and third quartile for the obtained ground displacement data (25^{th} and 75^{th} percentile) ranged between -4.5 mm and 1.0 mm in different months except in April that its range is approximately between -1.1 mm to 12.3 mm. The maximum anticipated shrinkage is about -4.7 mm, and the maximum heave value is approximately 44.7 mm. In general, a smaller range of variation for ground vertical displacement is observed in summer (July, August, and September). It is noteworthy that the mean value is greater than the median for all months indicating the ground movement data distribution is positively skewed.

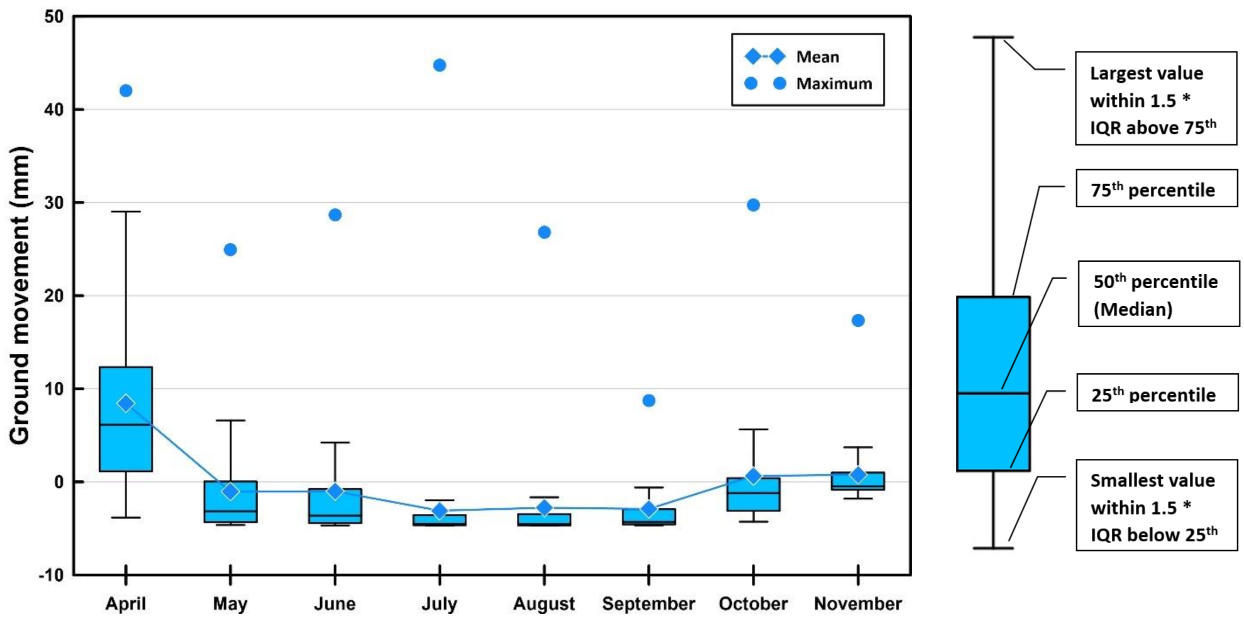

Figure 4-1- Ground vertical displacement in different months over 15 years from 1996 to 2010

Figure 4-2 illustrates the monthly variations of precipitation (P), potential evaporation (PE) as well as the potential surface flux (PE-P) over 15 years from 1996 to 2010. As can be seen, the lowest PE-P occurred in April and November. However, the expansive ground experienced greater swelling heave in April compared to November (Figure 4-1). This implies that potential surface flux (PE-P) alone is not a representative of expansive ground displacement behavior. In fact, the ground movement is a function of change in soil moisture that depends on the amount of water infiltrating into the soil (net infiltration) rather than the potential surface flux. The amount of net infiltration (*NI*) primarily depends upon precipitation (*P*), runoff (*RO*), and actual evaporation (*AE*):

$$NI = P - AE - RO \qquad [4\text{-}1]$$

Figure 4-2 also indicates that the average precipitation in November (active days) is much less than April. Moreover, the maximum potential evaporation is observed in summer months with maximum potential surface flux in July. This corresponds to the most sever shrinkage behavior in July as shown in Figure 4-1.

The box and whisker plots in Figure 4-3 and Figure 4-4 are presented to provide more details on the precipitation and potential evaporation averaged over different months over 15 year period from 1996 to 2010, respectively. As can be seen, a large range of precipitation can be observed in the months of April and June, in comparison to other months that have smaller range in precipitation. It should be noted that the precipitation in April include spring freshet event and the small precipitation in November can be attributed to fact that the inactive period starts in November reducing the number of active days. It can also be observed that mean *PE* values increase from the months of April to July with the highest value in month of July with values decreasing thereafter.

It should be noted that the inactive period, during which almost no water infiltrates into the frozen ground, ends in early April as described in Section 4.3.3. . The relatively considerable swelling response obtained for the month of April is not only due to the higher monthly precipitation and lower PE, but also as the result of higher soil moisture from the winter snow melting that enters the ground at the beginning of active period (spring freshet event).

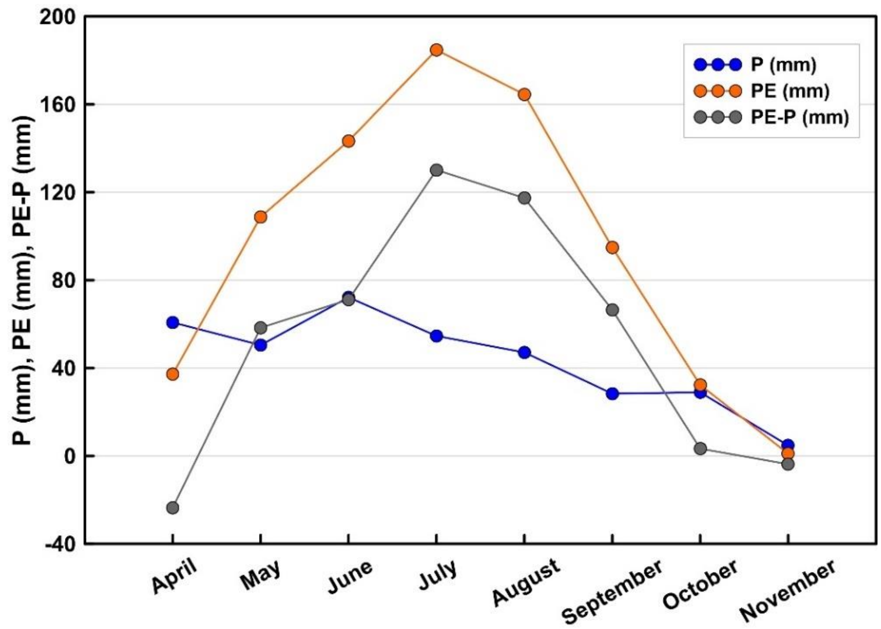

Figure 4-2- Variation of monthly precipitation and potential evaporation over 15 years from 1996 to 2010

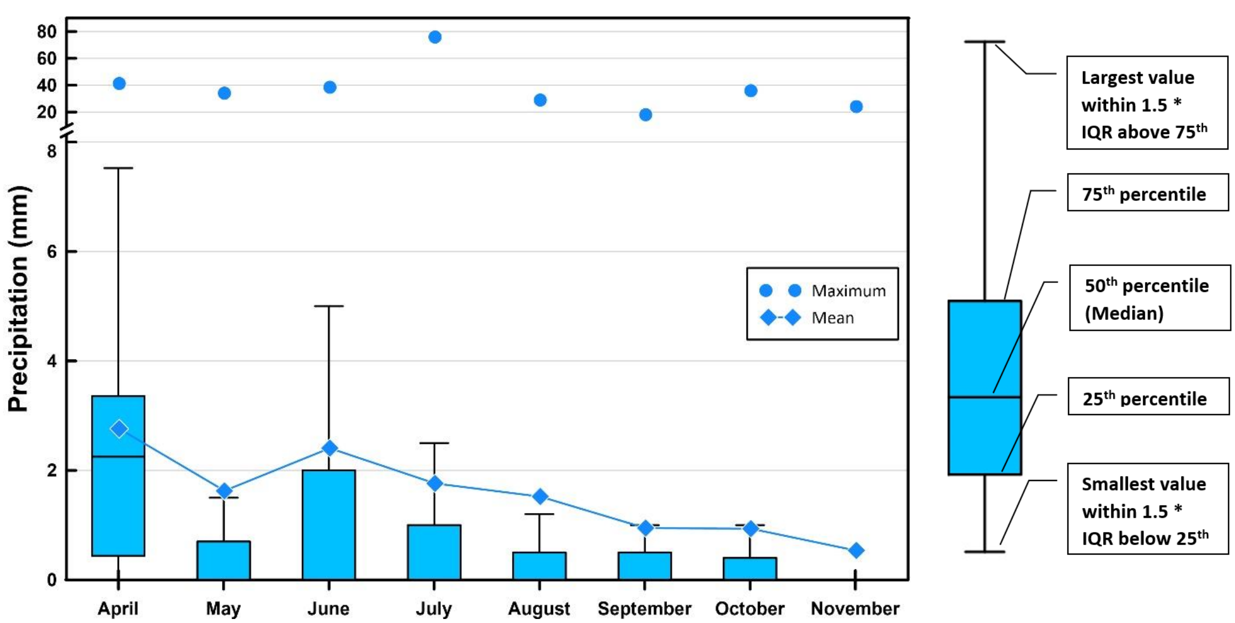

Figure 4-3- Variation of precipitation in different months over 15 years from 1996 to 2010

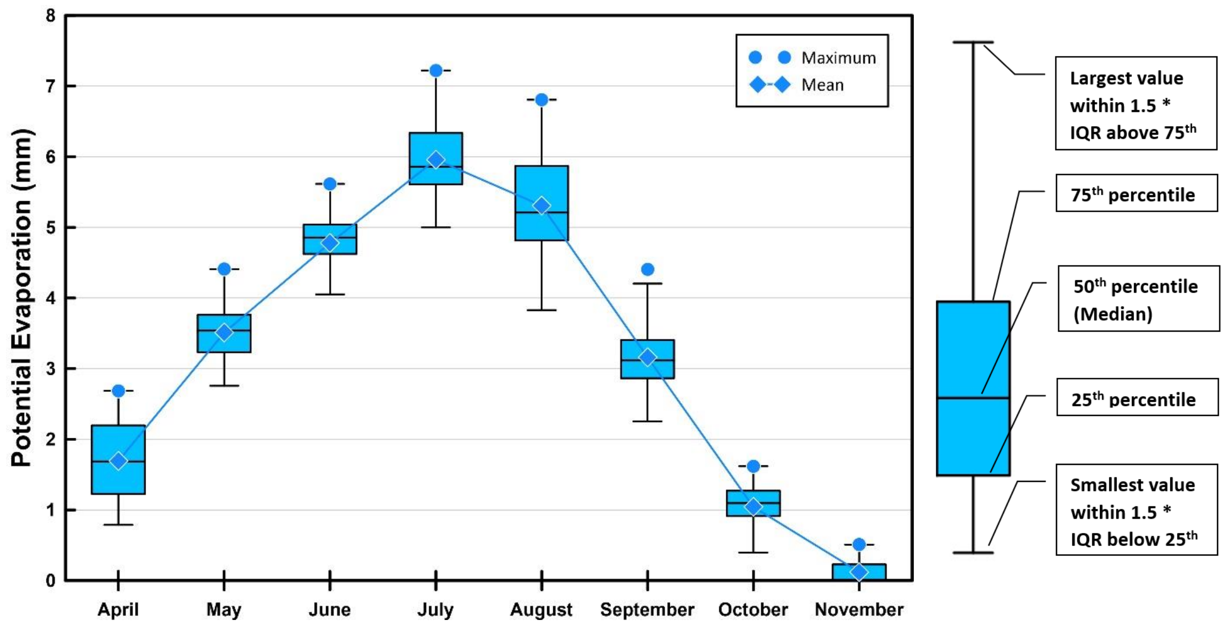

Figure 4-4- Variation of precipitation in different months over 15 years from 1996 to 2010

The expansive soil deformation in response to climatic conditions can be related to seasonal trend of precipitation and potential evaporation. In general, the soil is moist and tends to remain that way throughout the year in humid climates. This is because the periods of greatest evaporation and transpiration (the summer months) also coincide with the greatest rainfall. The climate in North Carolina in United States, as shown in Figure 4-5a, is typical of this pattern. Because the variations in moisture content are small, very little shrinkage or swelling will occur. However, some problems have been reported during periods of extended drought when the soil dries and shrinks (Hodgkinson, 1986). Most of the problems with expansive soils occur in arid, semi-arid, and monsoonal areas because the seasonal distribution of precipitation and evaporation/transpiration causes wide fluctuations in the soil moisture content. Most of the precipitation in arid and semi-arid areas occurs during the winter and spring when evaporation and transpiration rates are low. Thus, the moisture content of the soil increases. Then, during the summer, precipitation is minimal, and evaporation/transpiration is greatest, so the soil dries. Thus, the soil expands in the winter and shrinks in the summer. The climate in Los Angeles, shown in Figure 4-5b, displays this pattern

(Coduto et al., 2001). Figure 4-5c presents a similar graph based on the climate data between 1996 and 2010 for the city of Regina. The climate for the City of Regina has been typically classified as semi-arid (Yoshida et al., 1983; Bashir et al., 2022). The results presented above (Figure 4-1 to Figure 4-4) confirm that shrinkage is the dominant deformation behavior of Regina clay during the summer months (i.e., July, August and September). The results also indicate that the swelling is more likely to occur in spring (i.e., April, May and June) and colder months (i.e., October and November).

From an unsaturated soil mechanics perspective, expansive soil deformations due to climatic cycles occur due to change in suction head. Figure 4-6 illustrates the variation of average suction head at the ground surface in different months over 15 year period from 1996 to 2010. In general, the suction head results typically follow the trend of climatic data i.e., precipitation and potential evaporation as discussed earlier. As can be seen, April, May, June and October show the largest range of suction head values. A smaller range of suction head values has been obtained in the remaining months. It should be noted that the minimum suction head at the ground surface was limited to -300 m in the numerical analysis. A sensitivity analysis on this assumption has been carried out and the results are presented in Ssection 4.5. The variation of suction head with depth will be discussed in the following section.

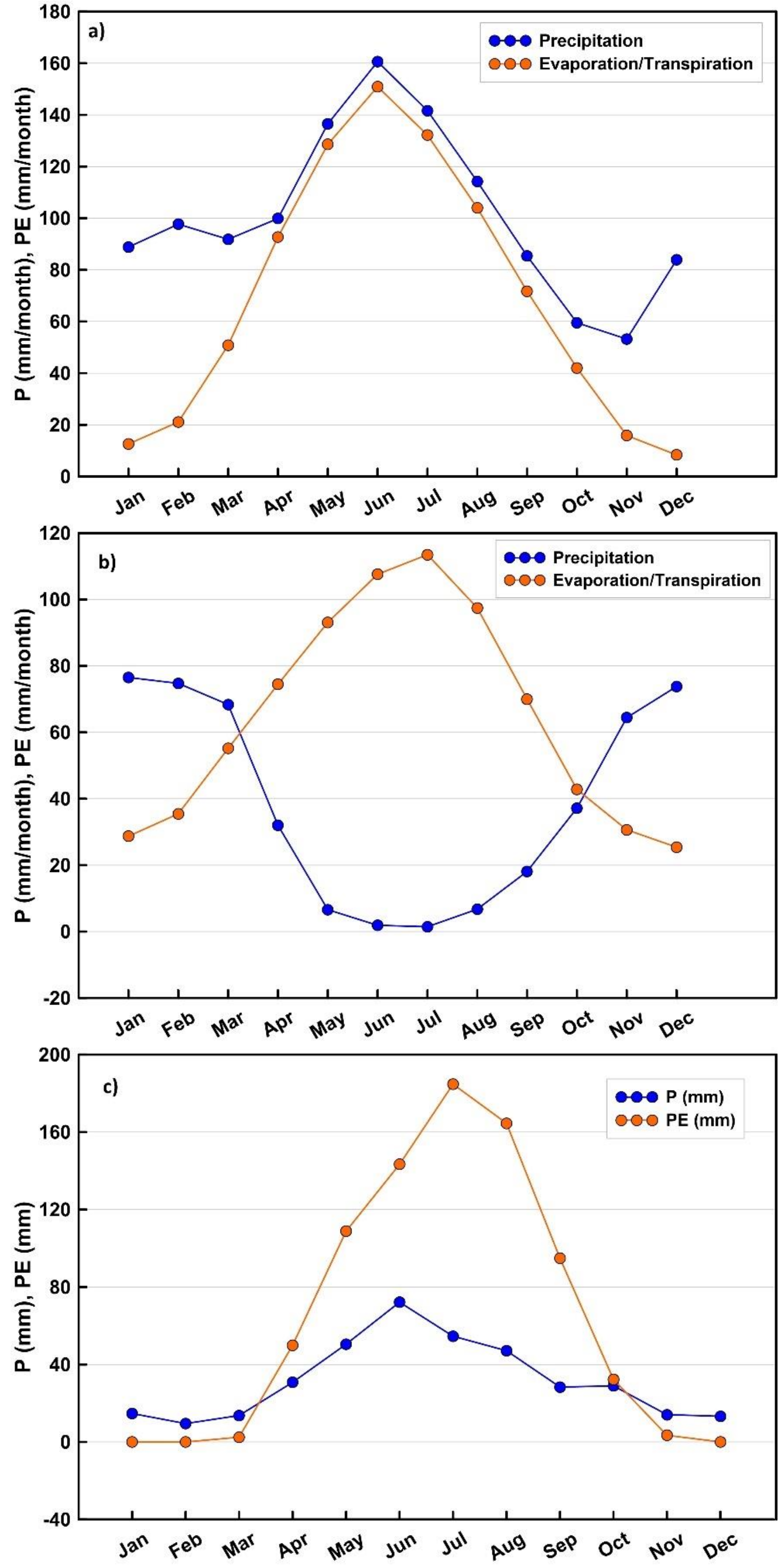

Figure 4-5- Annual distribution of precipitation and potential evaporation/transpiration in (a) Willand, North Carolina, (b) Los Angeles, California (Coduto, 2001- adapted from Thornthwaite, 1948), and (c) City of Regina (between 1996 and 2010)

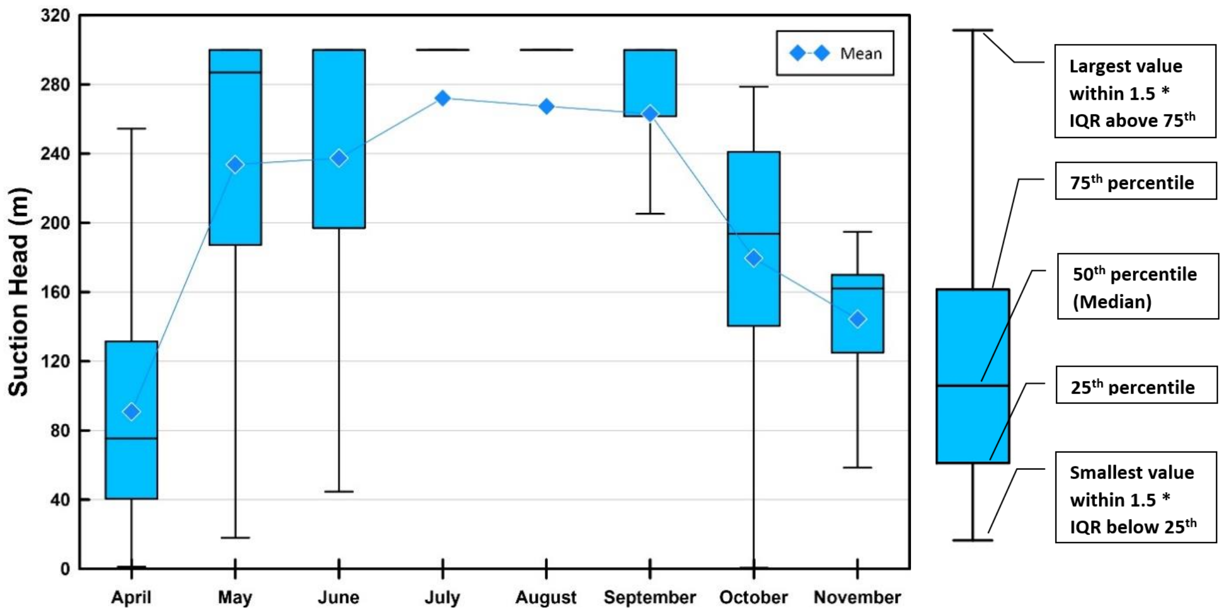

Figure 4-6- Variation of suction head at ground surface in different months over 15 years from 1996 to 2010

4.4.2. Yearly Basis

Figure 4-7 presents the results for ground surface movement and annual moisture index over the 15 years period i.e., 1996-2010. Figure 4-7a shows the variation of ground vertical displacement over different years. According to this figure, the largest swelling/shrinkage interquartile range over the 15-year period appears to have occurred in the year 1998. The first and third quartile for 1998's displacements were estimated to be approximately -4.6 mm and 4.1 mm, respectively. Moreover, the maximum shrinkage and swelling would have been approximately 4.7 mm and 29.9 mm in this year respectively, resulting in approximately 35 mm of maximum differential vertical ground surface movement. Conversely, the smallest swelling/shrinkage interquartile range would have occurred in 2003. In this year, the maximum shrinkage and swelling are estimated as approximately -4.7 mm and 15.9 mm respectively. This indicates, approximately 20.6 mm maximum differential vertical ground movement in 2003 which is slightly less than 60% of the value obtained for the year 1998.

Figure 4-7b presents the variation of precipitation, potential evaporation, and annual moisture index (I_m) over the 1996-2010 period. The annual moisture index can be estimated after Thornthwaite and Hare (1955) as:

$$I_m = 100(\frac{P}{PE} - 1) \quad [4\text{-}2]$$

In above equation, I_m is calculated based on total annual precipitation (P) and total annual potential evaporation (PE) . The annual moisture index was originally developed from limited climatic data collected in the United States. However, it forms an adequate basis for establishing the climatic type and variations in climate which has become a globally accepted for climate classification. Table 4-1 presents climate classification based on annual moisture index (Fredlund and Rahardjo, 1993). Based on the calculated values for I_m, all fifteen years of Regina climate can be categorized as arid or semi arid. The maximum and minimum I_m are obtained as -38 and -69 in the years 2010 and 2003, respectively. The climate classification for years 1998 and 2003, which were shown to experienced largest and smallest interquartile range of vertical ground movement, can be identified as semi-arid and arid. respectively.

Table 4-1- Classification of climate using the I_m

I_m	Category of Climate
>100	Perhumid
20-100	Humid
0-20	Moist humid
-33-0	Dry subhumid
-67 to -33	Semiarid
-100 to -67	Arid

Figure 4-8 presents the results for precipitation and potential evaporation over the 15 years period i.e., 1996-2010. Figure 4-8a and Figure 4-8b show the variation of precipitation and potential evaporation over 1996 to 2010. The peak median value for precipitation and potential evaporation is observed in years 1998 and 2003, respectively. The maximum precipitation is approximately 76 mm that has occurred in 2001. The maximum daily potential evaporation over the historical period varies between 53 mm and 72 mm.

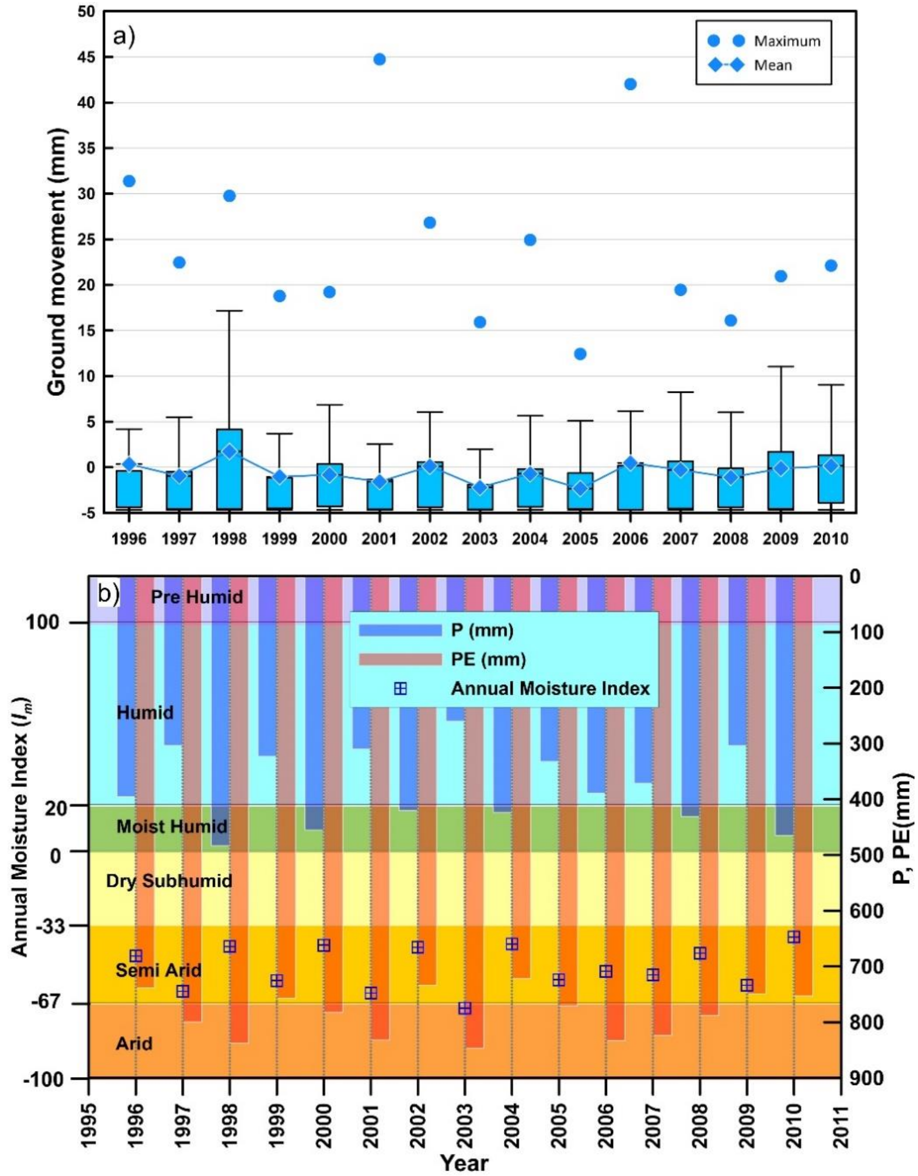

Figure 4-7- Variation of a) ground surface movement; and b) annual moisture index over 15 years from 1996 to 2010

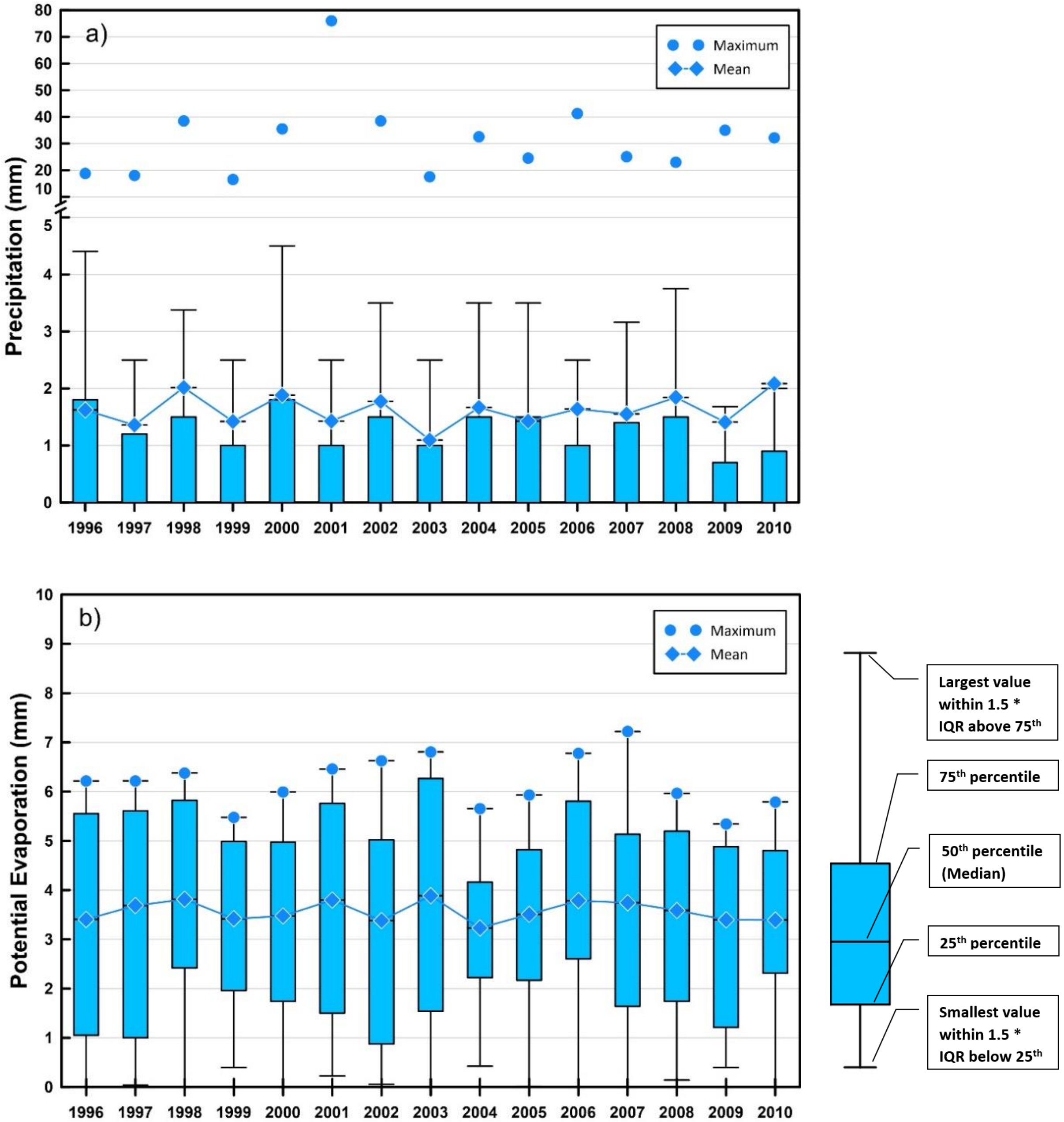

Figure 4-8- Variation of a) precipitation; and b) potential evaporation over 15 years from 1996 to 2010

4.4.3. Daily Basis

Figure 4-9 illustrates the daily data for ground movement, precipitation, and potential evaporation for the years 1998, 2003 and 2010. These years were selected based on the results presented in the previous section: a) 1998: largest differential ground movement (based on data interquartile range),

b) 2003: smallest differential ground movement as well as minimum annual moisture index, and

c) 2010: maximum annual moisture index.

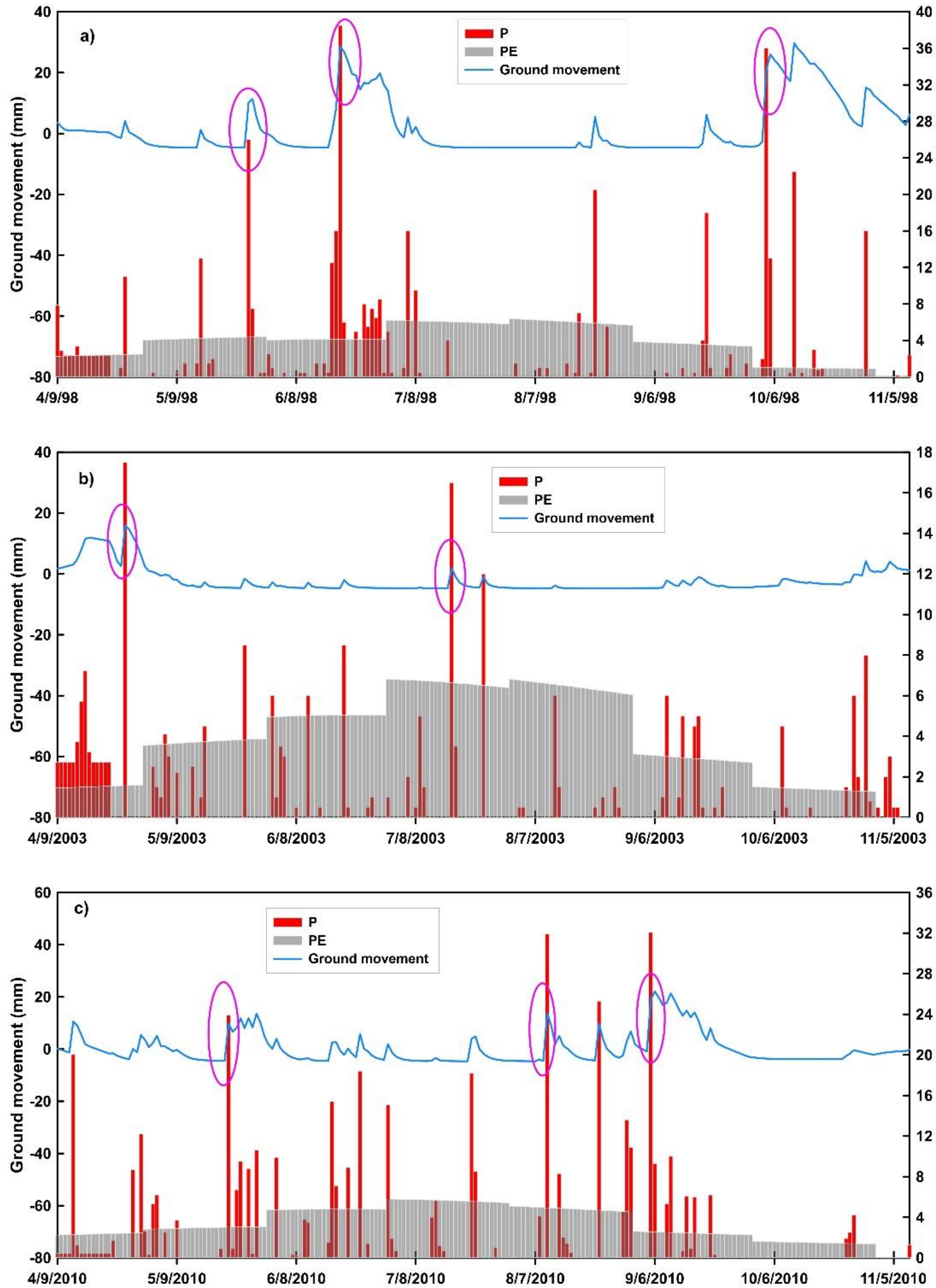

Figure 4-9- Daily precipitation, potential evaporation and ground surface movement over (a) 1998, (b) 2003 and (c) 2010

As can be seen in all three graphs, the fluctuation of ground movement is typically associated with the fluctuation in daily precipitation. The sharp changes in the ground surface movement generally correspond to days following extreme precipitation events. Some samples of these sharp transitions from shrinkage to swelling are marked up on the graphs. Similar trend can be observed in 2010's graph. However, rapid shrinkage to swelling transition is less considerable for dryer year 2003.

Figure 4-10 presents the profile of the mean value of suction head data with depth for different months. The general shape of suction head profile throughout the depth is similar for all months except April and colder months of October and November. The results for April shows lower suction head with the depth that can be attributed to the higher water infiltration during this month. It should be noted that the suction head value was limited to 300 m in the conducted numerical models. Moreover, the constant suction value of 150 m (approximately 1470 kPa) was assumed at the depth of 5 m in all numerical models. Further discussion on this is presented in Section 4.5.2. There are several studies (Fityus et al., 1998; Walsh et al., 1998; Fox, 2000; McManus et al., 2004; Chan and Mostyn, 2008) that have focused on the effect of climate on the depth of suction change (H_s) and have tried to relate it to the TMI (Thornthwaite moisture index as cited by Thornthwaite (1948). Those studies were based on field investigations of H_s. Mitchell (2008) provides a summary of those studies. Figure 4-11 shows a graphical representation of the relationship between H_s and TMI given by Mitchell (2008). These studies confirm that depth of suction change ranges between 4 m and 6 m for semi-arid and arid that is consistent with the assumption made in this study i.e., constant suction at the bottom of 5 m soil column.

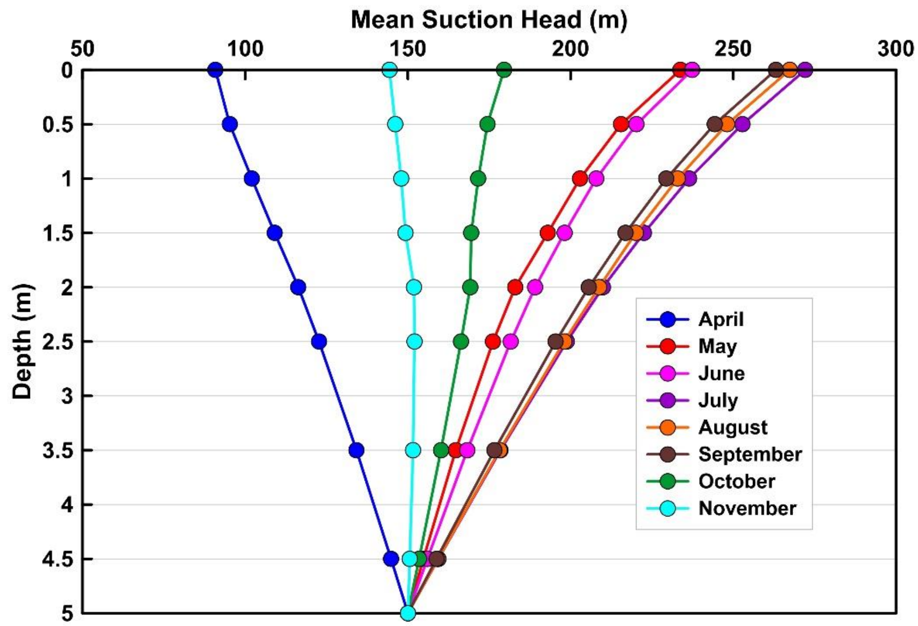

Figure 4-10- The variation of mean value of suction head data with respect to depth for different months over 15 years from 1996 to 2010

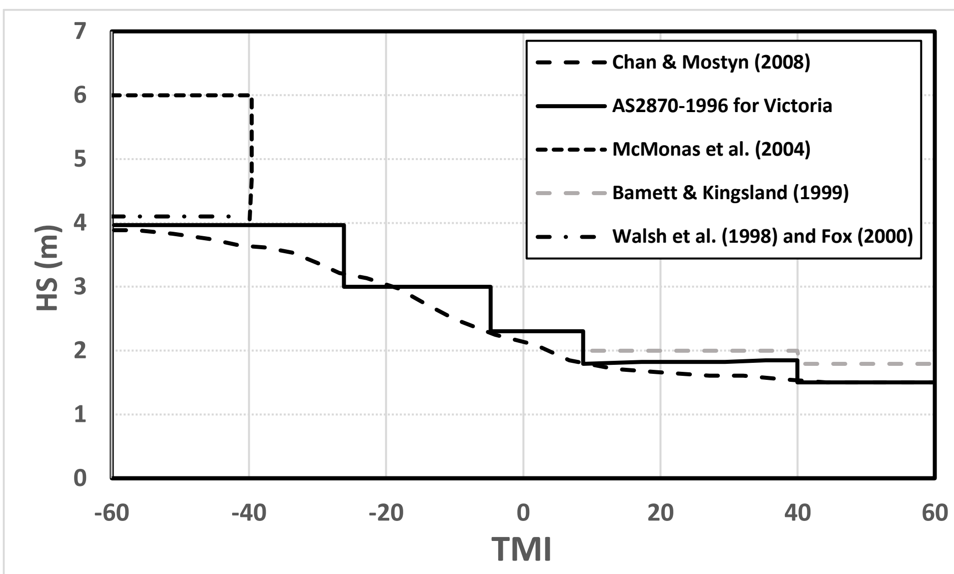

Figure 4-11- Relation between Hs and annual moisture index (modified from Michell,2008)

The numerical suction head profiles based on the 25th and 75th percentiles of the suction head data for April, August and November are plotted in Figure 4-12. In practice, soil suction profile can be obtained from suction measurements at different depths during wet and dry periods. The observed wet and dry suction values usually decrease rapidly with depth (Fityus et al., 2004).

Mitchell (1980) assumed a "trumpet" shaped suction profile (Figure 4-13) to derive concept of swelling of expansive soil. Suction profile is approximated to a triangular shape in AS2870 (1996 and 2011). The difference in suction head (*Δu*) decreases linearly with depth from a maximum value at the ground surface to zero at the depth of design suction change (H_s), below which it is assumed that the changes in soil suction can be ignored. The soil suction change at the ground surface based on the numerical profiles presented in Figure 4-12 is approximately 260 m.

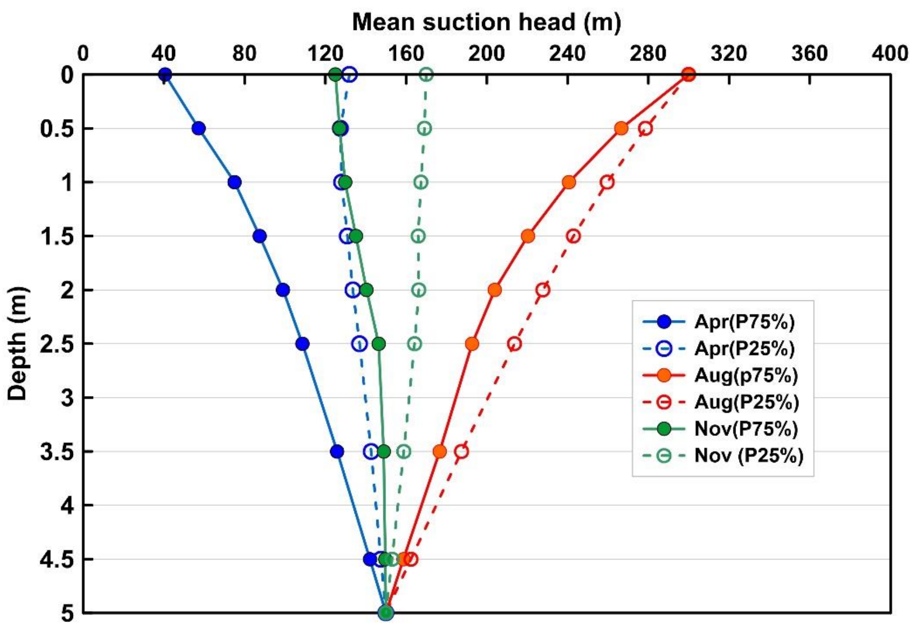

Figure 4-12- Suction head profiles based on the 25th and 75th percentiles of suction data for different months over 15 years from 1996 to 2010

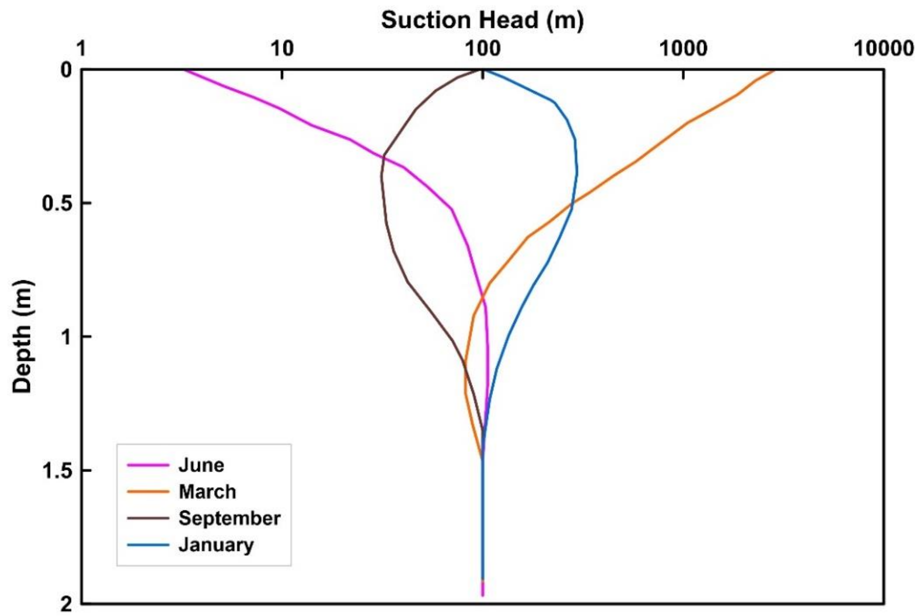

Figure 4-13- Theoretical suction profiles (adopted from Mitchell (1980))

4.5. Sensitivity Analysis

4.5.1. Selected Variables

In general, the prediction of ground movements subject to long term climate using numerical model is influenced by various factors including the stiffness and hydraulic parameters of soil as well as mechanical and hydraulic boundary conditions of the model. Vu et al. (2007) performed a parametric study to determine the significance of each of the environmental and soil parameters to the predicted infiltration rates in Regina clay. Their results suggest that change in soil properties, including the SWCC (drying and wetting curves) and hydraulic conductivity (within a range of one order of magnitude), have minor effects on the predicted results, and the parameters that have the most significant effect on the predicted cumulative infiltration are the net radiation and precipitation. Similarly, from a model sensitivity analysis, Karunarathne et al. (2018) found that precipitation is the main influence on soil moisture changes followed by evaporation and relative humidity. They also indicated that the SWCC is more influential than hydraulic conductivity and thermal conductivity on soil moisture variation.

For the current research, a power law equation for soil elastic modulus as a function of volumetric water content was utilized in the numerical analysis. This equation includes three parameters i.e., elastic modulus for dry state (E_d), elastic modulus for saturated state (E_w), and an empirical parameter (m). Lu and Kaya (2014) proposed a practical three-point testing procedure to determine a single fitting parameter that defines the power law for any type of soil. The procedure involves measuring elastic moduli at three states of water content: dry, wet (nearly saturated), and the middle points. They used the proposed approach to obtain these three parameters for 16 different soils from sandy to silty to clayey soils. The value of these parameters for Regina clay are not available in the literature and these parameters were obtained from the best-fit power low curve matched to the calculated elastic modulus versus soil volumetric soil moisture data. To understand the impact of the selected values on the ground response to the climatic variables, a series of sensitivity analyses on the power law equation parameters were also considered in this study.

The actual evaporation (AE) along with the precipitation are two key factors controlling the water balance at the ground surface, and consequently the soil moisture content and ground deformations. Actual evaporation is the actual amount of water that can be evaporated from the soil surface. The AE from a soil surface might be considerably lower than the PE (Fredlund et al. 2011). The AE rate from a saturated soil surface can be assumed equal to the PE. However, when the soil begins to dry, it tries to hold onto the water more strongly and therefore, the soil suction increases as the soil dries. The tendency of soil to hold the water depends on its gradation because the water in larger pores is held less strongly compared to smaller pores. The actual evaporation rate from the soil surface gradually decreases with the increase in soil suction. Several methods have been proposed for AE calculations (Fredlund et al. 2012).

In HYDRUS 2D, which is utilized in this study, a system dependant boundary condition using an approach proposed by Neuman et al. (1974) is implemented to calculate the actual evaporation (Šimŭnek et al. 2016). In this approach, a maximum (critical) allowable suction head identified as h_{cr} is set at the ground surface. As long as the suction head at the soil surface is lower than h_{cr}, the actual evaporation rate is equal to the potential evaporation rate. Once the h_{cr} value is reached, the actual evaporation rate is decreased from the potential value since the soil is then considered to be too dry to deliver the potential evaporation rate. The h_{cr} value is usually specified in the range of 150 m to 1000 m. Numerically, h_{cr} is used to increase model stability as it is a lower bound for pressure head to prevent it from changing dramatically when there are small changes in the water content near residual. Šimŭnek et al. (2009) suggests selecting h_{cr} such that the corresponding water content is at least 0.005 higher than the residual water content rate. Sillers and Fredlund (2001) suggested a residual suction of 3000 kPa (approximately 305 m) as an estimate for most soils when the actual evaporation rate starts to decrease from potential evapoartion. A h_{cr} of 300 m was used in this study. This value is consistent with previous studies indicating the suction head at ground surface does not exceed 300 m in Regina expansive clay (Vu et al., 2007; Adem and Vanapalli, 2014). The impact of the assumed value for h_{cr} on the ground deformation response was studied in the conducted sensitivity analysis.

The initial soil suction profile and the expected depth of changes in soil suction due to variations of environmental factors are important in predicting the vertical movements of expansive soils (Adem and Vanapalli, 2016). According to AS 2870, the equilibrium soil suction for semi-arid climate can be considered as 4.4 pf (approximately 251 m). Vu e al. (2007) measured an initial suction of 1000 kPa to 2000 kPa within the upper 4 m of Regina clay in their parametric study. In this study, the constant value of 150 m (1471.5 kPa) was assumed as initial suction head at the depth of 5 m in all numerical models. As mentioned before, some previous studies confirm that depth of suction change ranges between 4 m and 6 m for semi-arid and arid that is consistent with the assumption made in this study. The impact of equilibrium suction head at depth (h_{eq}) on the ground deformation response was estimated through a series of sensitivity analyses.

4.5.2. Base Model

Five parameters as discussed in the previous section including three parameters for power law elastic equation (E_d, E_w and m), maximum (critical) allowable suction head at ground surface (h_{cr}) and initial suction head (h_{eq}) was considered in the conducted sensitivity analyses. As mentioned in the previous section, the values assumed for h_{cr} and h_{eq} in the "base" model are 300 m and 150 m, respectively. In Section 4.4. , the predicted ground response to 15 years historical climate data (1996-2010) were analyzed. Based on the obtained results, 1998 and 2003 were shown as years in which the Regina clay soil column experienced the largest and smallest differential ground movement (difference in swelling and shrinkage), respectively. To study the potential impact of the climatic condition on the influencing parameters under study, the sensitivity analyses were carried out for these two years. In each set of sensitivity analyses, each of the five parameters was changed by ± 50% and the results in terms of mean value of daily ground movement, maximum ground shrinkage and maximum ground heave were compiled. The obtained results are discussed in the following section.

4.5.3. Sensitivity of the influencing Parameters

Figure 4-14 illustrates the percent change of maximum ground heave and maximum ground shrinkage due to ± 50% changes in the soil stiffness parameters (E_d, E_w and m), equilibrium suction head at depth (h_{eq}) and maximum (critical) allowable suction head (h_{cr}) under climate conditions of two years i.e., 1998 and 2003.

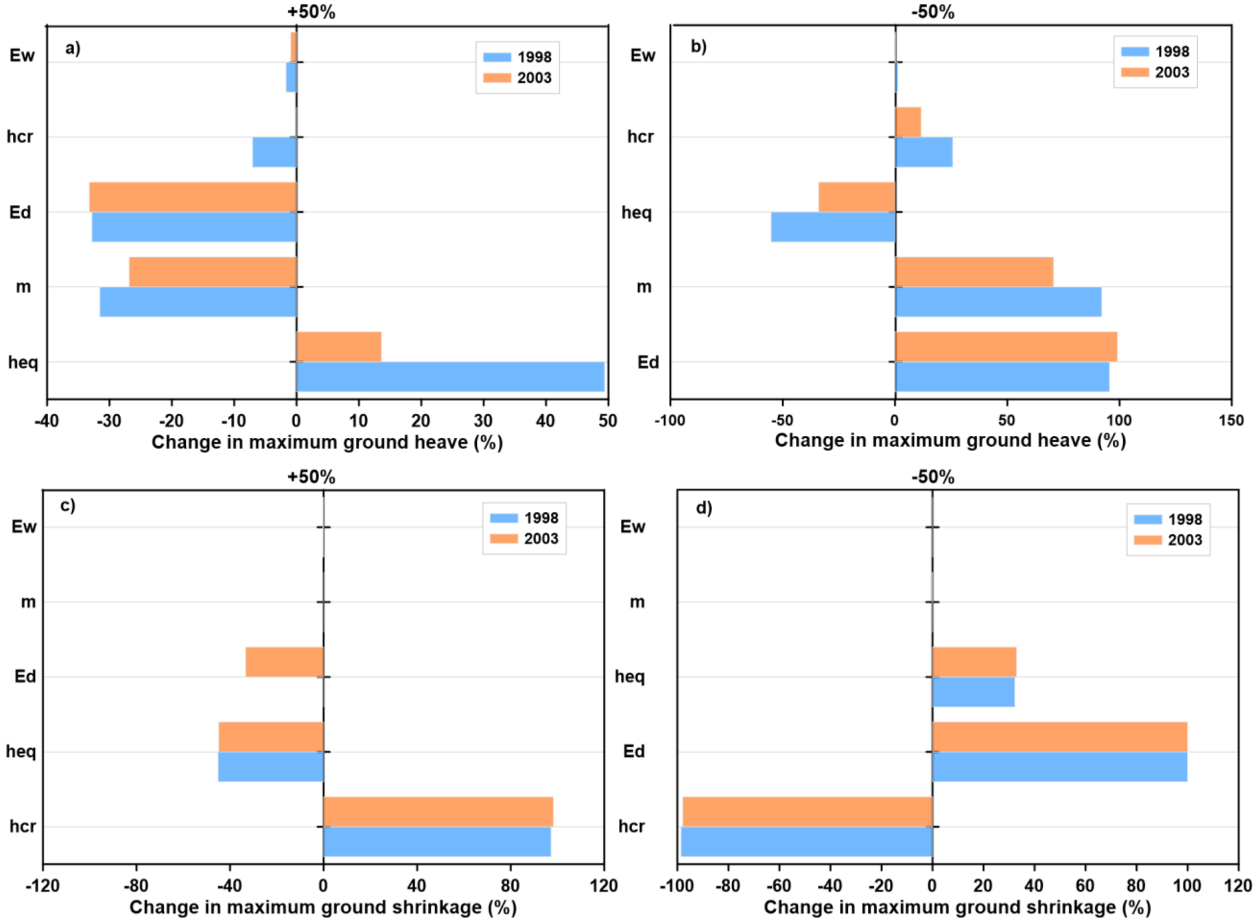

Figure 4-14- Percent change of (a) maximum ground heave; and (b) maximum ground shrinkage due to ± 50% changes in the selected input variables

Based on the results obtained, for the soil stiffness parameters, E_w has the minimal impact on the variations of ground movements. The results also indicate that m has negligible impact on shrinkage, but its impact on maximum ground heave is significant. The changes in ground movements due to change in soil stiffness parameters are almost identical for both climate parameters for the years 1998 and 2003.

As explained earlier, h_{cr} controls the actual evaporation in the numerical model. The obtained results confirm that although the impact of h_{cr} on maximum ground heave is small, 50% change in this parameter resulted in up to approximately 100% change in maximum ground shrinkage.

This is because h_{cr}, which is the maximum (critical) allowable suction head at the ground surface, is activated when soil dries and therefore shrinkage governs the expansive soil response.

The equilibrium suction at depth (h_{eq}) is shown to have impact on both maximum ground shrinkage and heave. The impact of 50% increase in h_{eq} on ground response is greater under 2003 climate input for maximum ground heave.

The extreme differential ground movement (maximum heave- maximum shrinkage) is an important factor where assessment of potential damage to lightly loaded structures supported on the expansive soils are subject to long term climate variation. Remarkably, the results show that in general a 50% increase/decrease in stiffness soil parameters causes decrease/increase in both maximum heave and shrinkage values obtained over the time period under consideration. Consequently, any increase in soil stiffness parameters will result in smaller difference in the extreme ground movements, while any decrease in soil stiffness parameter will cause larger difference in the extreme ground movements.

However, the results for h_{eq} and h_{cr} show a reverse trend i.e., a 50% increase/decrease in h_{eq} parameter causes increase/decrease in maximum heave while causing decrease/increase in maximum shrinkage values. Inversely, a 50% increase/decrease in h_{cr} parameter causes decrease/increase in maximum heave while causing increase/decrease in maximum shrinkage values.

The above discussion implies that the impact of change in soil stiffness parameters is amplified where the differential ground movement is of concern, while the impact of change in h_{eq} and h_{cr} reduces in this condition. Figure 4-15 illustrates a graph indicating the impact of change in different parameters on the extreme differential ground movement. The results show that the differential ground movement is more sensitive to the decrease in E_d and m compared to increase in these parameters and compared to increase or decrease in h_{eq} and h_{cr}. The impact of E_w on the differential ground movement is minimal. For dryer year 2003, the sensitivity of differential ground movement to change of h_{cr} is much greater than wetter year 1998.

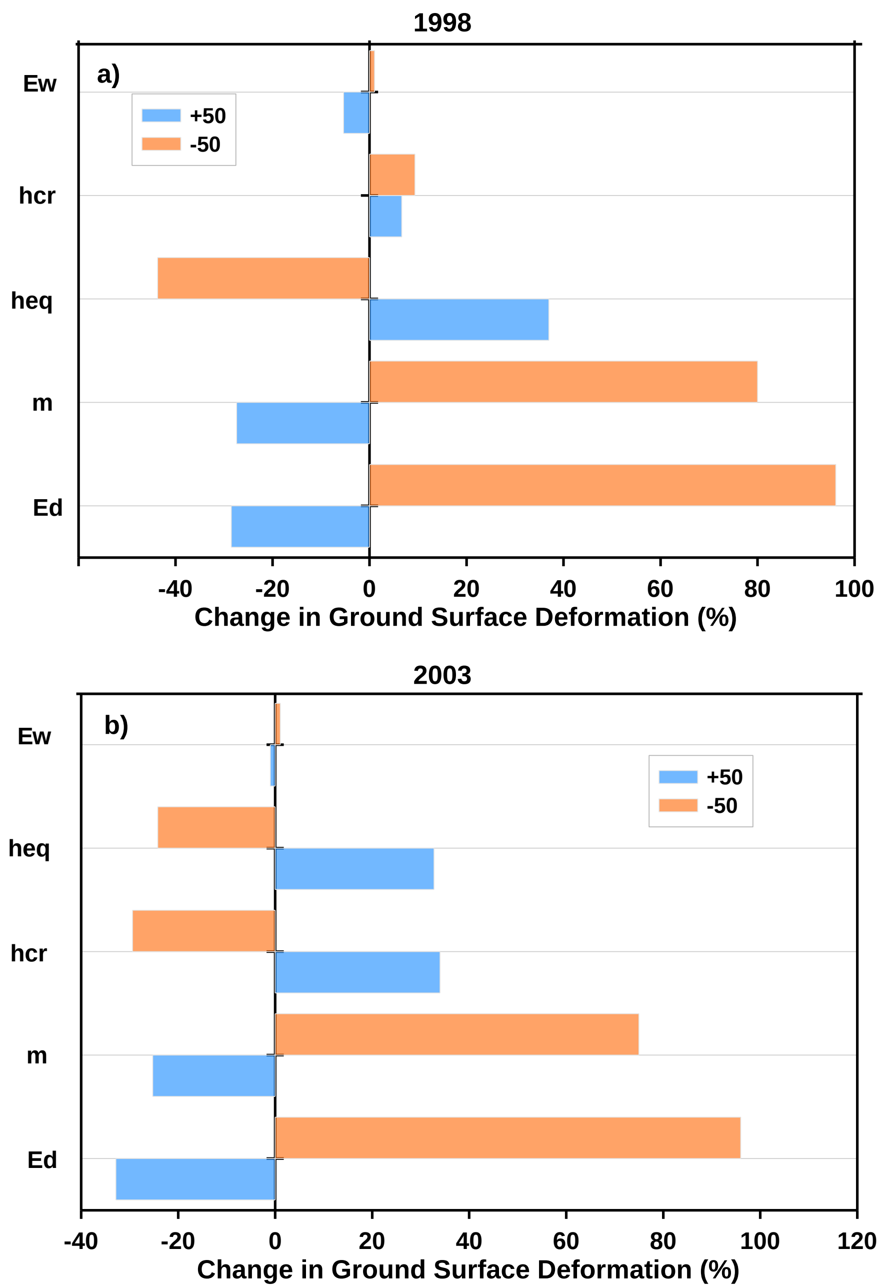

Figure 4-15- The impact of change in different parameters on the difference in the extreme ground movement for (a) 1998; and (b) 2003

In order to further study of the impact of h_{cr} on expansive soil response to soil-atmosphere interaction, the sensitivity analysis was extended to include the range of 300 to 1000 m for h_{cr}. The analysis was conducted for the years 1998 and 2003. Figure 4-16 indicates the variation of ground surface movement with increase in maximum allowable suction head at the ground surface. As expected, assuming higher values of h_{cr} in the analysis has negligible impact on maximum ground heave and mean ground movement. However, the maximum ground shrinkage (and therefore differential ground movement) shows relatively high degree of sensitivity with respect to increase in h_{cr}. The increase of h_{cr} from 300 m to 1000 m resulted in increase of differential ground movement from 36 mm to 47 mm for wetter year (1998) and from 14 mm to 34 mm for drier year (2003) indicating that the dryer year is more prone to shrinkage than wetter year.

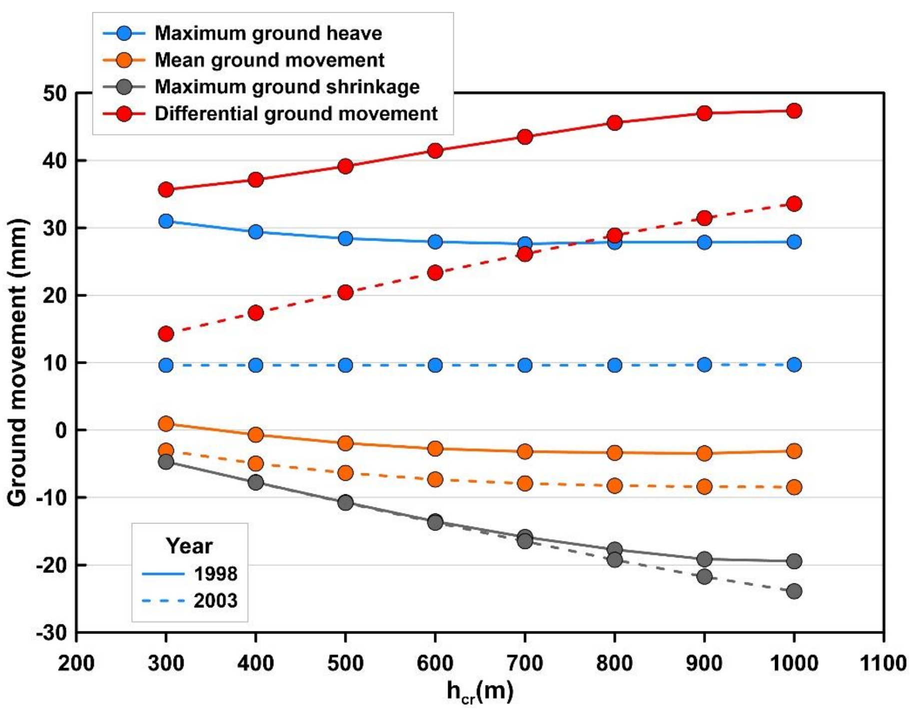

Figure 4-16- The variation of ground surface movement with increase in maximum allowable suction head at the ground surface

The findings of the conducted sensitivity analyses indicate that although the base numerical model can be utilized to predict the trend of ground movements subject to long-term climate, the sensitivity of the results to the selected parameters should be taken into consideration for any proper quantitative assessment.

4.6. Future Climate Selection

Prediction of future climate is an attempt to estimate the actual evolution of the climate. Global Circulation Models (GCMs) are the primary tool used for understanding and attribution of past climate variations and future predictions. Simulations by climate models provide the response of the climate system to emission or concentration scenarios of greenhouse gases or radiative forcing scenarios (IPCC 2007, 2013). The pathways of total radiative forcing or cumulative measure of human emissions of greenhouse gases from all sources are termed Representative Concentration Pathways (RCPs) (van Vuuren et al., 2011) or Shared Socioeconomic Pathways (SSPs) (Riahi et al., 2017). Every RCP or SSP number expresses a different cumulative radiative forcing by the year 2100. The increasing number in RCP or SSP indicates more accumulation of radiative force; the RCP 2.6 or SSP 2.6 represents the best-case scenario with the lowest concentration of radiative forces by the end of 2100, whereas RCP 8.5 or SSP 8.5 shows the worst-case scenario where the concentration of radiative forces would be the highest at the end of 2100.

4.6.1. Proposed Scenario Selection Method

In a climate change impact study, it is crucial to carefully select the future climate scenario for the analysis. IPCC (2000) states that all future scenarios could be equally valid with no assigned probability of occurrence. Over last two decades, several climate models (GCMs) with various size, scope, scale, and complexity have been developed to provide projections of future climate change. Different greenhouse gas emissions scenarios for each GCM generates a large number of future climate projections. Hence, in most of the climate change studies, a strategy is employed to narrow the climate projections to a handful number of future climate scenarios.

In general, three approaches are typically taken in the climate change impact studies (Fenech et al, 2002):

a) Extremes (max/min) approach: The extremes (max/min) approach suggests that it is best to plan within the full range of possibilities considering all available future climate scenarios. The approach takes the projection for the maximum change, as well as the projection for the minimum change, and uses both as the range of consideration when planning;

b) Ensemble approach: The ensemble approach suggests that it is best to plan for the average change of all the models. The approach uses a mean or median of all the models (or many models) to reduce the uncertainty associated with any individual model; and

c) Validation approach: The validation approach suggests that those models that compare well to historical climate observations should be the ones used for planning. The approach takes the historical climate observations over a thirty-year period from a global gridded dataset (for example, the Environment Canada) and compares this against all models to see which ones reproduce the values best.

In this study, a three-staged approach was considered to select the future climate scenario among the 26 GCMs and 3 SSPs available in CMIP6 database for the city of Regina. First, the validation approach was used to identify 4 out of 26 GCM models that predicts the historical climate data with minimum error. Second, the expansive soil response under a sample one-year climate data was analyzed to assign a representative climate variable that has the greatest impact on the extreme ground movements (maximum differential ground movement over time). Third, a statistical analysis on the projected data for the identified representative climate variable was carried out to select a future climate ensemble (a 30-year period) that can result in the most critical ground movement response to the climatic conditions. The selected future climate ensemble as well as the historical climate data was then used in the developed hydro-mechanical model to evaluate the impact of climate change on the long-term expansive soil movement patterns.

4.6.2. GCM Models Validation

As the first step, the quality of the predicted daily climate data by different GCMs was assessed. For this purpose, the back predicted precipitation and temperature data were collected from a nearest grid to the city of Regina and compared with climate normals reported by Environment and Climate Change Canada (Environment and Climate Change Canada, 2019). Climate normals are used to summarize or describe the average climatic conditions of a particular location. In this study, the available climate normals in terms of precipitation, and minimum and maximum temperature from 1980 to 2021 were considered.

Figure 4-17 to Figure 4-19 show a comparison between monthly climate normals (1980-2020) (Environment Canada) and predictions made using 26 GCMs for 3 SSPs. In general, although all GCMs' predictions are in good agreement for maximum temperature, the models generally underestimate the minimum temperature. Also, the predicted precipitation shows more scatter as compared to the minimum and maximum temperature. This implies that the selection of future climate scenario can potentially be more sensitive to precipitation rather than temperature. It should be noted that the potential evaporation can be related to minimum and maximum temperature according to the mathematical model proposed by Pereira and Pruitt (2004), which also have been used in this study.

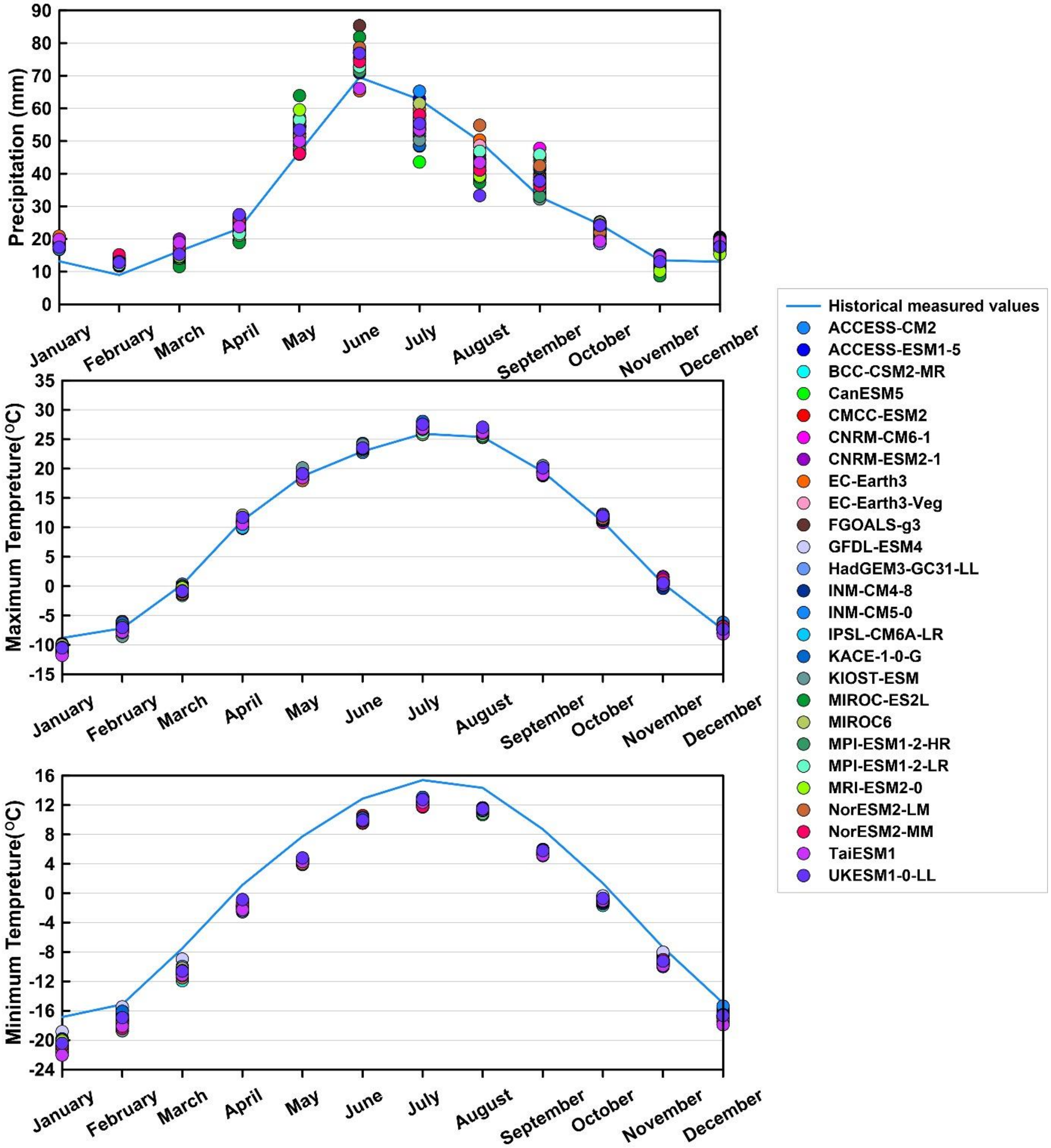

Figure 4-17- Comparison of projected future daily climate data using different GCMs with climate normal for Regina (SSP-2.6)

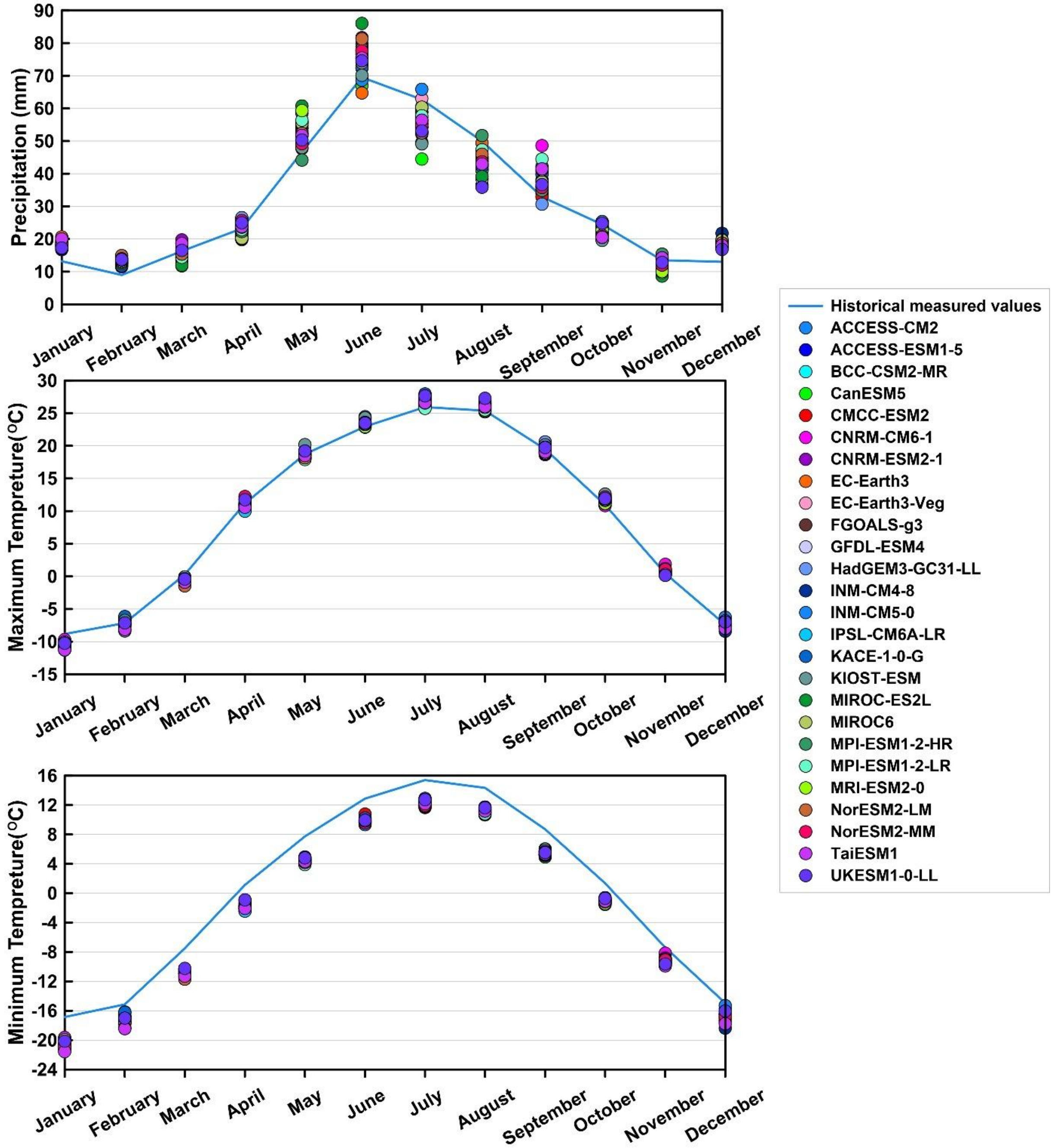

Figure 4-18- Comparison of projected future daily climate data using different GCMs with climate normal for Regina (SSP-4.5)

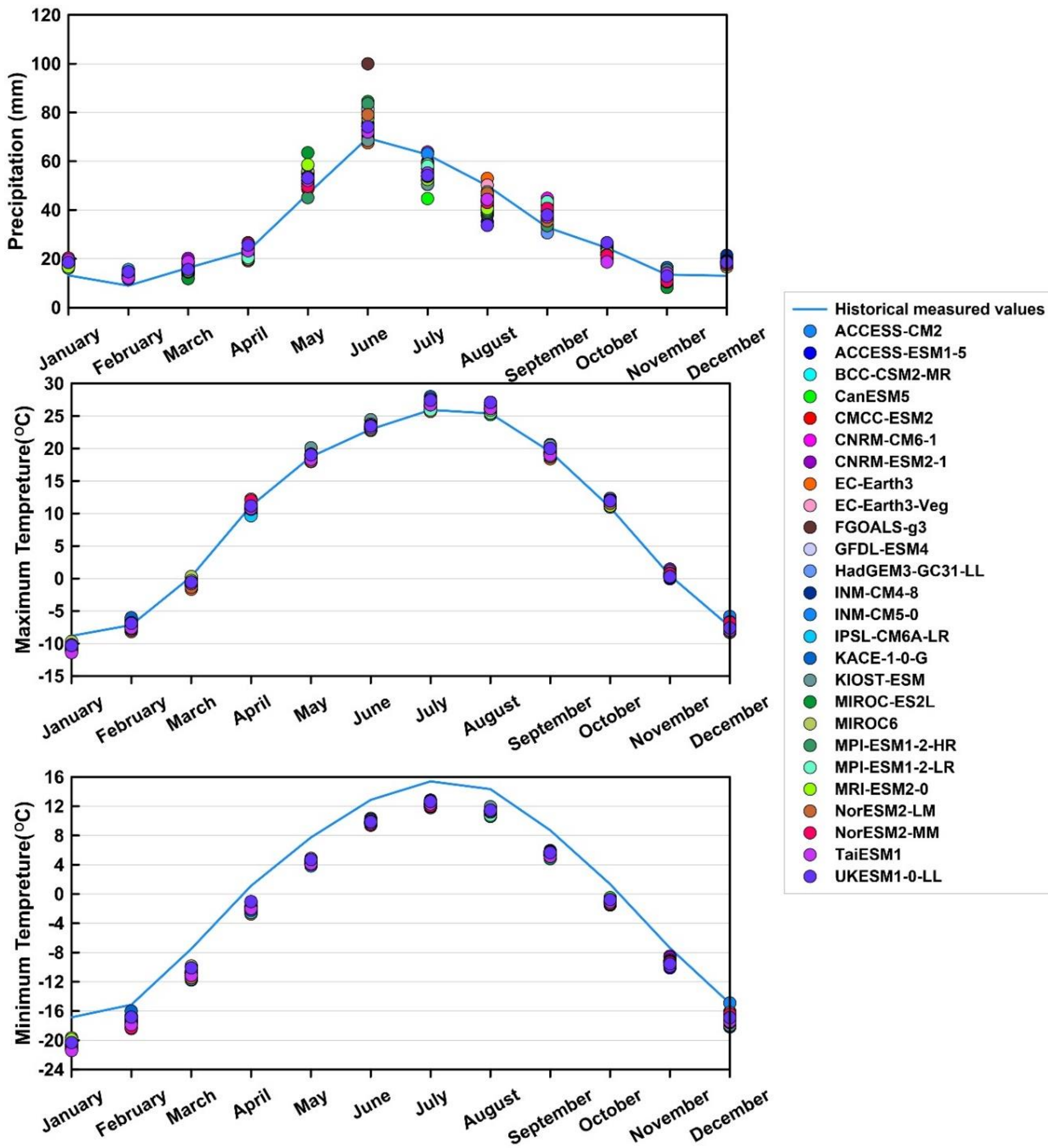

Figure 4-19- Comparison of projected future daily climate data using different GCMs with climate normal for Regina (SSP-8.5)

In order to assess the performance of various GCMs in predicting historical data (1981-2010), the square root of mean squared error (RMSE) between the reported climate normals by Environment and Climate Change Canada and the predicted from various GCMs were considered. The sum of RMSE values for minimum temperature, maximum temperature and precipitation were calculated for each GCM-SSP combination. In addition to precipitation, temperature was also considered in this analysis because the potential evaporation, which is estimated based on temperature, can potentially impact the quantity of water entering the ground. Table 4-2 presents the calculated values for all GCMs and SSPs considered in this study. In this table, the GCMs were ranked based on the average of the obtained RMSE values for three SSPs. Based on the obtained results, four GCMs i.e., MPI-ESM1-2-HR, INM-CM4-8, HadGEM3-GC3 and NorESM2-MM were selected for the next stage of future scenario selection.

Table 4-2- Calculated RMSE values for different GCMs

GCM	Sum of square root of mean squared error (RMSE) for minimum temperature, maximum temperature, and precipitation daily data			
	SSP1-2.6	SSP2-4.5	SSP5-8.5	Average
HadGEM3-GC31-LL	28.20	27.60	27.59	27.80
EC-Earth3-Veg	34.18	24.32	26.63	28.38
INM-CM5-0	30.09	29.14	27.70	28.98
INM-CM4-8	27.99	27.91	32.81	29.57
MPI-ESM1-2-HR	27.03	28.29	34.68	30.00
MIROC6	31.68	28.75	29.91	30.11
CNRM-ESM2-1	29.83	32.86	27.64	30.11
NorESM2-MM	28.87	30.21	31.56	30.21
BCC-CSM2-MR	30.09	27.58	33.33	30.34
EC-Earth3	29.20	30.94	32.55	30.90
ACCESS-CM2	33.20	30.90	31.01	31.70
CMCC-ESM2	35.17	29.26	31.26	31.90
TaiESM1	32.88	33.12	30.74	32.25
MPI-ESM1-2-LR	32.79	33.05	32.39	32.74
IPSL-CM6A-LR	34.09	33.16	32.58	33.28
NorESM2-LM	33.41	34.19	32.35	33.32
ACCESS-ESM1-5	32.39	32.91	36.53	33.95
KIOST-ESM	34.39	33.92	33.76	34.02
UKESM1-0-LL	35.45	32.21	35.22	34.29
GFDL-ESM4	32.90	34.73	35.49	34.37
MRI-ESM2-0	35.50	34.40	33.52	34.47
KACE-1-0-G	34.62	34.39	34.94	34.65
CNRM-CM6-1	34.93	37.72	31.77	34.80
CanESM5	36.73	35.03	35.40	35.72
FGOALS-g3	36.54	33.65	49.95	40.05
MIROC-ES2L	44.46	43.55	44.89	44.30

4.6.3. Representative Climate Variable

Expansive soils experience significant volume change in response to changes in the soil moisture content. Climate is a key factor influencing the soil moisture fluctuations. The climate condition can cause soil moisture changes up to a certain depth of soil over a given time period that is mainly dependent on the soil type (Karunarathne et al., 2018). Therefore, the selection of critical climate scenario based on the variation of moisture content through the soil mass with the influence depth seems a reasonable approach to assess the impact of changing climate on the expansive soil behavior. However, such approach requires conducting variably-saturated flow analysis over long term periods for all future climate scenarios. Alternatively, in this study, the statistical analysis of a representative climate variable that was shown to have the higher impact on the extreme ground movement is proposed for future climate scenario selection.

As shown in Figure 4-9, sharp increases in the ground surface movement typically corresponds to extreme precipitation events. Where an extreme event is followed by subsequent rainy days, the heave remained almost constant while subsequent dry days are shown to result in gradual ground shrinkage. The results presented in Section 4.4. also indicated that the maximum shrinkage remains relatively constant at -20 mm. This can be attributed to the maximum soil suction assumed in the numerical analysis.

The above discussion leads one to conclude that extreme precipitation event can be considered as the critical climate variable that may cause large differential ground movement. The extreme precipitation event is usually defined to be any event above a certain percentile of the daily precipitation data for a given region. For example, U.S. Global Change Research Program (USGCRP) defines the extreme precipitation events as days with precipitation in the top 1 percent of all days with precipitation. In this study, the compiled daily precipitation data for historical

(1981-2010) and different projected future climate ensembles (i.e., 2011-2040, 2041-2070 and 2071-2100) using different GCMs and SSPs are statistically analyzed, and the results are presented in the following section.

4.6.4. Statistical Analysis

Figure 4-20(a) and (b) compare the 99th percentile (P99) of the daily precipitation data for all climate ensembles. Only precipitation data during active period of the year were considered in the statistical analysis. The value of P99 for historical period is equal to 22 mm and is shown to be greater than P99 value for all future climate ensembles with exception of EC-Earth3-Veg-SSP1-2.6 (2011-2040), EC-Earth3-Veg-SSP2-4.5 (2011-2040), EC-Earth3-Veg-SSP5-8.5 (2011-2040), EC-Earth3-Veg-SSP2-4.5 (2041-2070), EC-Earth3-Veg-SSP2-4.5 (2071-2100) and EC-Earth3-Veg-SSP5-8.5 (2071-2100). The number of events with precipitation greater than this value are also presented in these figures.

Although considering P99 may be appropriate for comparing some aspects of various climate ensembles, it is more crucial to consider the water balance at the ground surface where the variation of soil moisture content is of importance. In reality, the intensity of the precipitation, together with the water-holding and conduction properties of the soil materials, would dictate the actual amount of water that enters the ground surface. For example, if one is to consider a daily resolution of precipitation data for water balance evaluation, the actual amount of water that enters the ground surface would be different if the sub-daily resolution of precipitation data is used. This is related to the infiltration capacity of the soil, which is a function of the hydraulic properties of the soil. Therefore, estimates of water balance are a function of temporal resolution of meteorological data, as also pointed out by others (Bashir and Pastora Chevez, 2018; Pk et al. 2018).

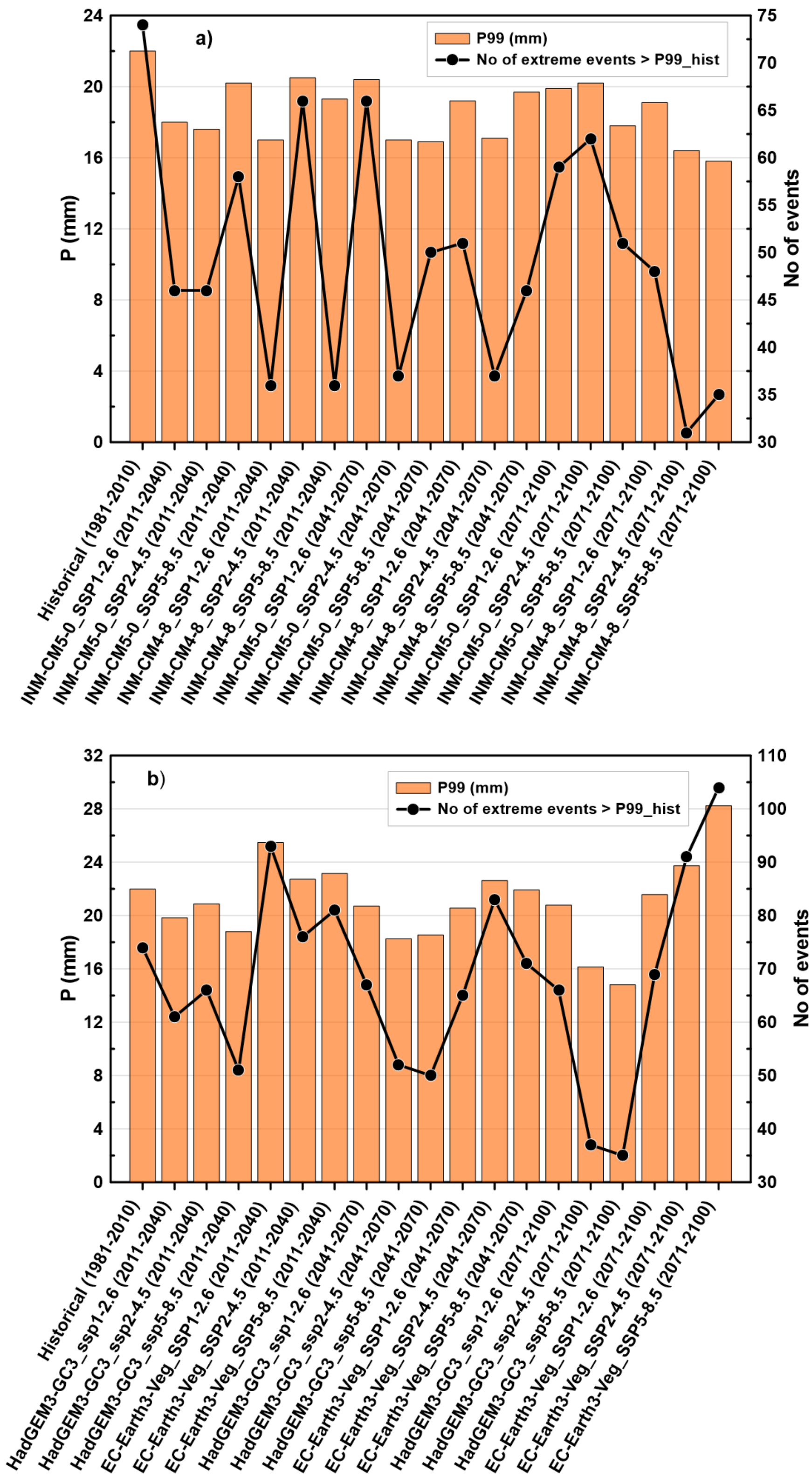

Figure 4-20- 99^{th} percentile of precipitation daily data for different future climate ensembles

Although the actual intensity of the event can vary form a few minutes to hours, historical and future climate data such as precipitation is normally only available at daily temporal resolution. In this study, the resolution of precipitation used in the numerical method is daily i.e., it is assumed that any daily precipitation occurs with uniform intensity over 24 hours. This will result in a conservative assessment of water entering the expansive clay with low saturated hydraulic conductivity.

The saturated hydraulic conductivity of Regina expansive clay under study was assumed equal to 5.23 mm/day which has been obtained from Vu (2003) and Adem and Vanapalli (2013). As can be seen in Figure 4-20, the amount of daily precipitation for extreme events identified by P99 is much larger than this threshold and such events are likely to produce large volume of runoff rather than increasing the soil moisture content at shallow depths. Therefore, 75th and 90th percentiles of the daily precipitation data (P75 and P90) were considered for the climate scenario selection in this study.

Figure 4-21(a) and (b) presents the 75th and 90th percentiles (P75 and P90) of the daily precipitation data for all analyzed climate ensembles (37 ensembles in total). The value of P75 and P90 for historical period is equal to 3.8 mm and 0.5 mm, respectively which are less than the saturated hydraulic conductivity of the Regina clay. The number of events with precipitation greater than the value of P90 of the historical period is also presented in these figures.

Figure 4-21 indicates that the value of P90 is larger than historical for 18 future climate ensembles. With exception of one future climate ensembles (i.e., HadGEM3-GC31-LL-SSP1-2.6 (2071-2100), the value of P75 of all other future climate ensembles data is greater than value of P75 for historical period. A summary of the results of the statistical analysis for the analyzed future climate ensembles together with the historical ensemble will be presented in the next section.

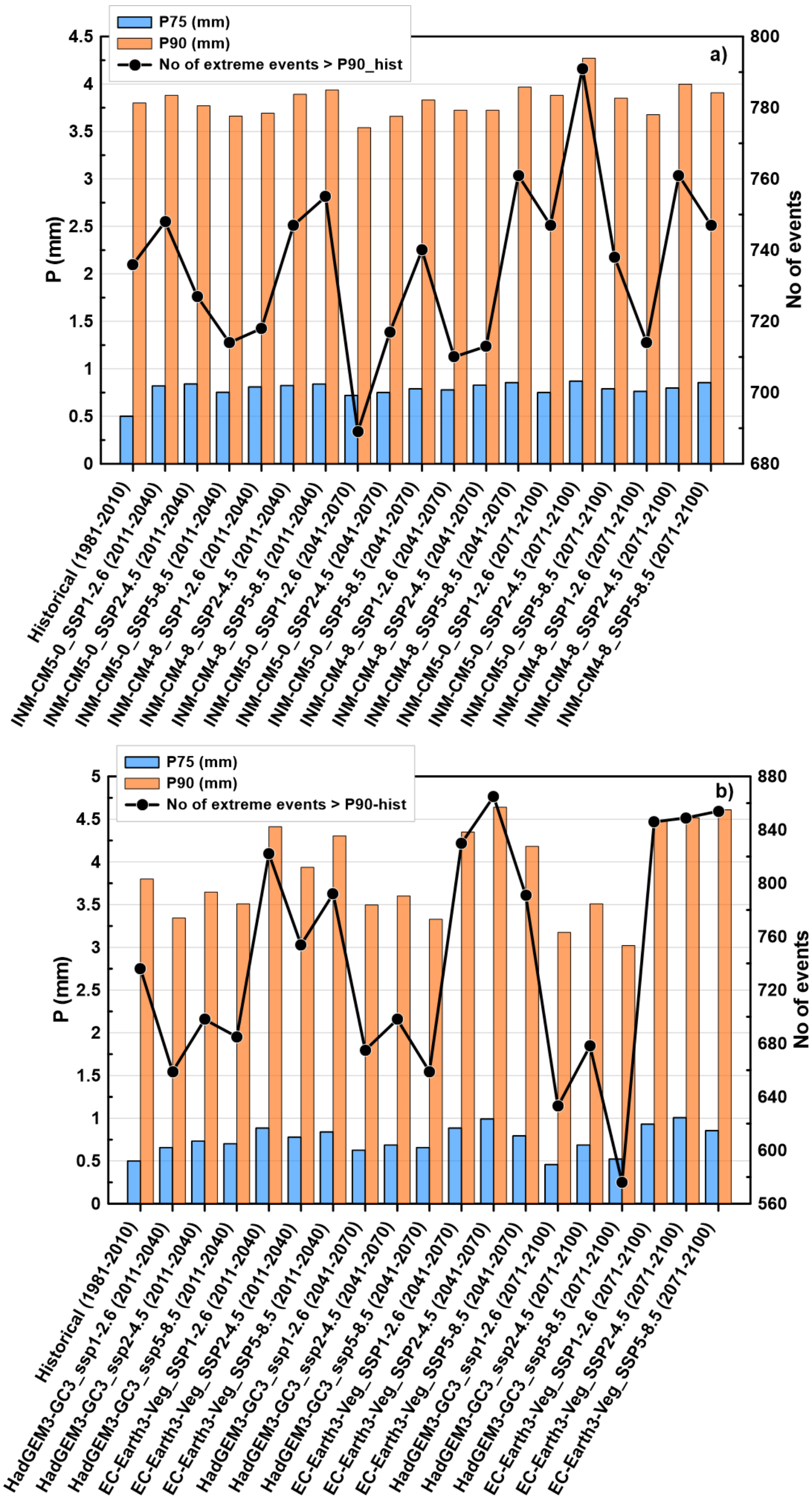

Figure 4-21- 75th and 90th percentiles of precipitation daily data for different future climate ensembles

4.6.5. Selected Scenario

Table 4-3 presents a summary of the statistical analysis. In this table, the future climate ensembles are sorted based on their P90 value. Also, the values for historical climate data are presented in the first row. Based on these results, EC-Earth3-Veg_SSP2-4.5 for the period 2041-2070 is selected for the numerical analysis of the expansive clay's response to future climate using the developed hydro-mechanical model in this study. Based on the results presented in Table 4-3, P75 and P90 for this future climate ensemble are shown to be approximately 98% and 22% higher than the historical period. Moreover, this future climate ensemble includes 865 events with daily precipitation greater than 90th percentile of the historical data.

It should be noted that the value of P99 for EC-Earth3-Veg_SSP2-4.5 during 2041-2070 has the 6th rank among the future climate ensembles and is 3% greater than the P99 of the historical data. Remarkably, the maximum daily precipitation for this future climate ensemble is 126.4 mm, which is greater than the corresponding value in the historical period (76 mm). Moreover, the maximum daily precipitation is ranked number 14 among the 36 future climate ensembles considered in this research. However, as it is discussed in the previous sections, extreme precipitation events identified by P99 or Pmax do not necessarily represent the critical (worse) climate scenario when the deformation behavior of expansive soil is to be considered.

4.7. Numerical Assessment of Climate Change Impact

The developed numerical model as described in Section 4.3.1. was used to assess the impact of climate change on expansive soil response to environmental loading in the form of the climate data. For this purpose, the compiled climate e data for selected future climate scenario was applied as input for the system-dependent boundary condition, which was defined at the uncovered portion of ground surface. The numerical results are discussed in the following sections and the anticipated ground response under selected future climate scenario is compared with the historical results.

Table 4-3- Summary of statistical analysis results

Climate Ensemble	P75 (mm)	P90 (mm)	P99 (mm)	Pmax (mm)	No of events P>P90-hist
Historical (1981-2010)	0.5	3.8	22.0	76.0	736
EC-Earth3-Veg_SSP2-4.5 (2041-2070)	1.0	4.6	22.6	126.4	865
EC-Earth3-Veg_SSP5-8.5 (2071-2100)	0.9	4.6	28.2	130.6	854
EC-Earth3-Veg_SSP2-4.5 (2071-2100)	1.0	4.5	23.7	98.2	849
EC-Earth3-Veg_SSP1-2.6 (2071-2100)	0.9	4.5	21.6	144.9	846
EC-Earth3-Veg_SSP1-2.6 (2011-2040)	0.9	4.4	25.5	162.5	822
EC-Earth3-Veg_SSP1-2.6 (2041-2070)	0.9	4.3	20.6	140.3	830
EC-Earth3-Veg_SSP5-8.5 (2011-2040)	0.8	4.3	23.2	109.3	792
INM-CM5-0_SSP2-4.5 (2071-2100)	0.9	4.3	20.2	116.7	791
EC-Earth3-Veg_SSP5-8.5 (2041-2070)	0.8	4.2	21.9	115.6	791
INM-CM4-8_SSP2-4.5 (2071-2100)	0.8	4.0	16.4	190.3	761
INM-CM4-8_SSP5-8.5 (2041-2070)	0.9	4.0	19.7	200.0	761
EC-Earth3-Veg_SSP2-4.5 (2011-2040)	0.8	3.9	22.7	173.3	754
INM-CM4-8_SSP5-8.5 (2011-2040)	0.8	3.9	19.3	200.0	755
INM-CM4-8_SSP5-8.5 (2071-2100)	0.9	3.9	15.8	113.4	747
INM-CM4-8_SSP2-4.5 (2011-2040)	0.8	3.9	20.5	150.6	747
INM-CM5-0_SSP1-2.6 (2011-2040)	0.8	3.9	18.0	200.0	748
INM-CM5-0_SSP1-2.6 (2071-2100)	0.8	3.9	19.9	126.0	747
INM-CM5-0_SSP5-8.5 (2071-2100)	0.8	3.9	17.8	104.9	738
INM-CM5-0_SSP5-8.5 (2041-2070)	0.8	3.8	16.9	104.1	740
INM-CM5-0_SSP2-4.5 (2011-2040)	0.8	3.8	17.6	120.5	727
INM-CM4-8_SSP1-2.6 (2041-2070)	0.8	3.7	19.2	118.2	710
INM-CM4-8_SSP2-4.5 (2041-2070)	0.8	3.7	17.1	119.8	713
INM-CM4-8_SSP1-2.6 (2011-2040)	0.8	3.7	17.0	113.0	718
INM-CM4-8_SSP1-2.6 (2071-2100)	0.8	3.7	19.1	106.4	714
INM-CM5-0_SSP5-8.5 (2011-2040)	0.8	3.7	20.2	103.5	714
INM-CM5-0_SSP2-4.5 (2041-2070)	0.8	3.7	17.0	112.9	717
HadGEM3-GC3_ssp2-4.5 (2011-2040)	0.7	3.6	20.9	109.8	698
HadGEM3-GC3_ssp2-4.5 (2041-2070)	0.7	3.6	18.3	190.8	698
INM-CM5-0_SSP1-2.6 (2041-2070)	0.7	3.5	20.4	94.7	689
HadGEM3-GC3_ssp5-8.5 (2011-2040)	0.7	3.5	18.8	118.7	685
HadGEM3-GC3_ssp2-4.5 (2071-2100)	0.7	3.5	16.1	85.5	678
HadGEM3-GC3_ssp1-2.6 (2041-2070)	0.6	3.5	20.7	151.7	675
HadGEM3-GC3_ssp1-2.6 (2011-2040)	0.7	3.3	19.8	117.3	659
HadGEM3-GC3_ssp5-8.5 (2041-2070)	0.7	3.3	18.5	46.8	659
HadGEM3-GC3_ssp1-2.6 (2071-2100)	0.5	3.2	20.8	345.0	633
HadGEM3-GC3_ssp5-8.5 (2071-2100)	0.5	3.0	14.8	83.1	576

4.7.1. Monthly Basis

Figure 4-22 compares the range of ground surface vertical displacement for each month under future climate (over 30 years period from 2041 to 2070) and historical climate (over 15 years period from 1996 to 2010). In general, the variation of ground vertical displacement in first two spring months i.e., April and May and fall months i.e., October, November and December are shown to be larger in future with higher mean and median values compared to historical period. Based on this Figure, the range of first and third quartile for the obtained ground displacement data (25^{th} and 75^{th} percentiles) for months of June, July, August and September falls below zero indicating that the ground would experience shrinkage. For the months of July and August, more severe shrinkage behavior is anticipated under future climate compared to historical climate. It should be noted that since the freezing date occurred in November for historical and is anticipated to occur in December for selected future climate scenario, results for December are only available for simulations for future climate data.

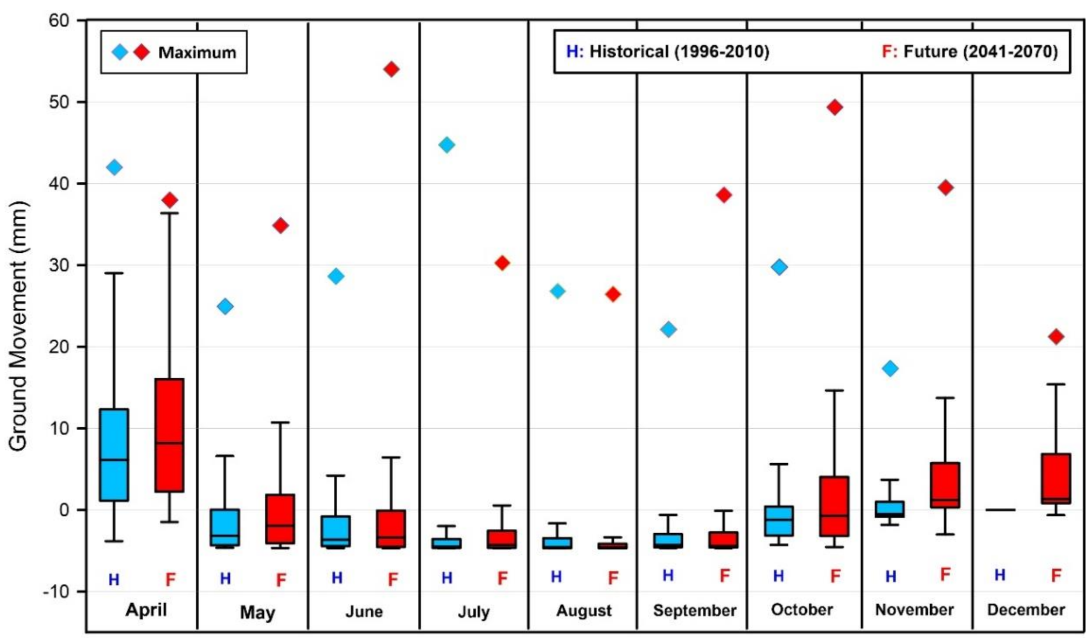

Figure 4-22- Ground vertical displacement in different months under historical and future climate

Figure 4-23 and Figure 4-24 present the variation of precipitation and potential evaporation data for historical and future climate. Larger heave values observed in April, May and June as well as in October, November and December (higher upper whisker with positive ground movement value) as shown in Figure 4-22 can be attributed to more precipitation for these months in future. Figure 4-22 also indicates that more severe shrinkage is expected to occur in future compared to historical for the month of August. Figure 4-25 compares the mean values of monthly potential surface flux (PE-P) for different months in historical and future periods. The figure confirms that the mean potential surface flux in the month of August is approximately 20% larger in future which implies drier conditions. For other months, the future mean potential surface flux is similar to the historical values. It should be noted that the extreme differential ground movement is not necessarily a function of monthly precipitation or potential surface flux (PE-P) and the amount and sequence of extreme precipitation events play a more critical role in this regard. This will be discussed further in the following sections.

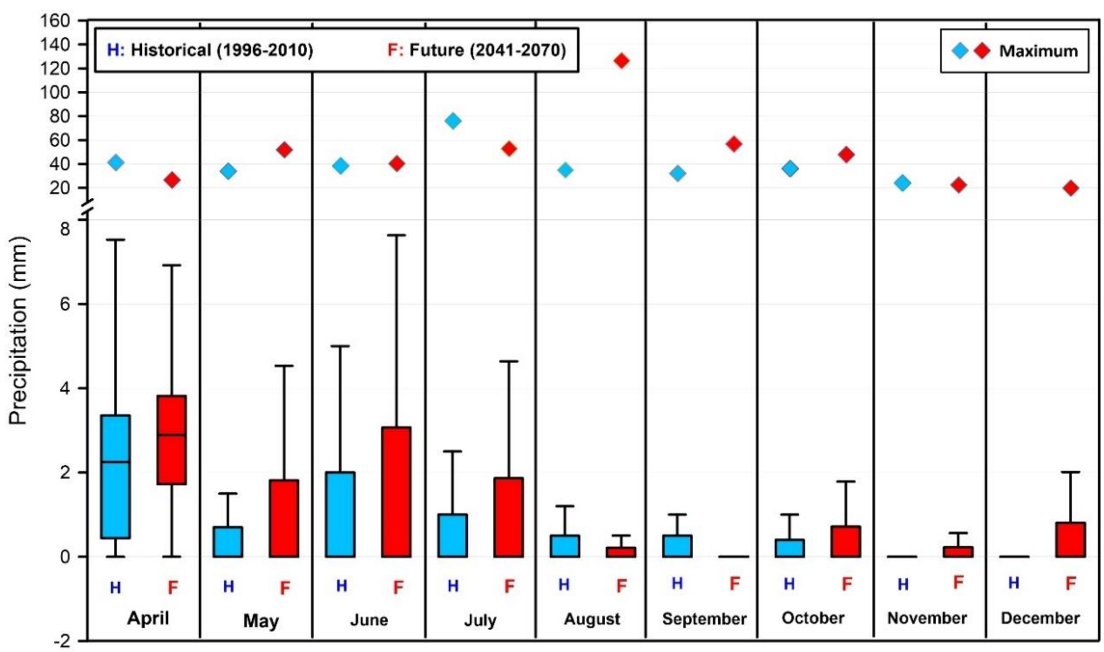

Figure 4-23- Variation of precipitation in different months under historical and future climate

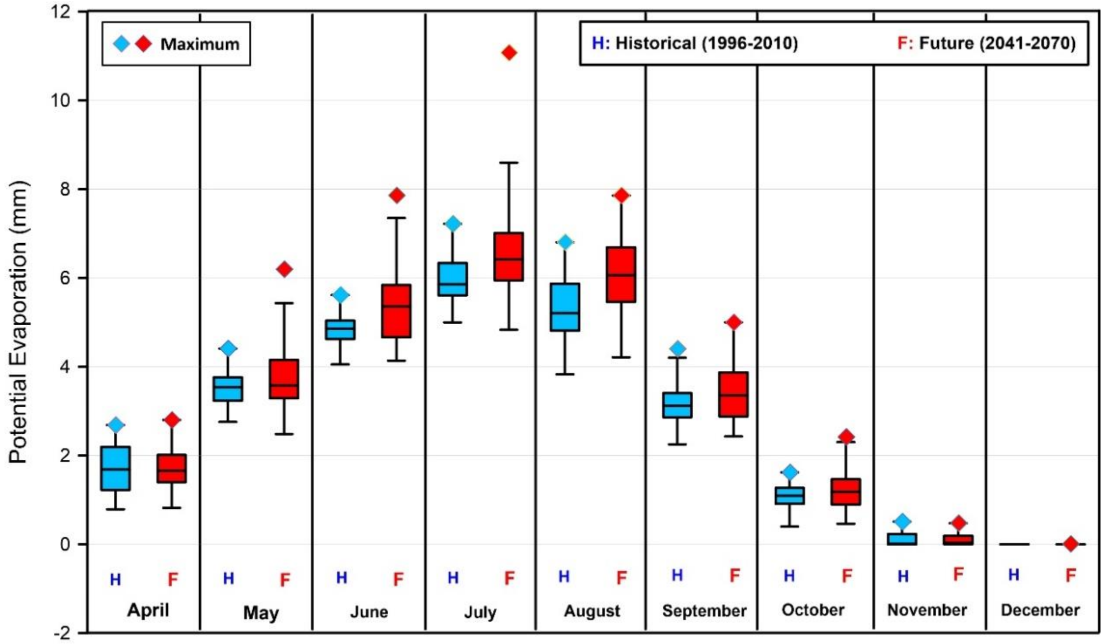

Figure 4-24- Variation of potential evaporation in different months under historical and future climate

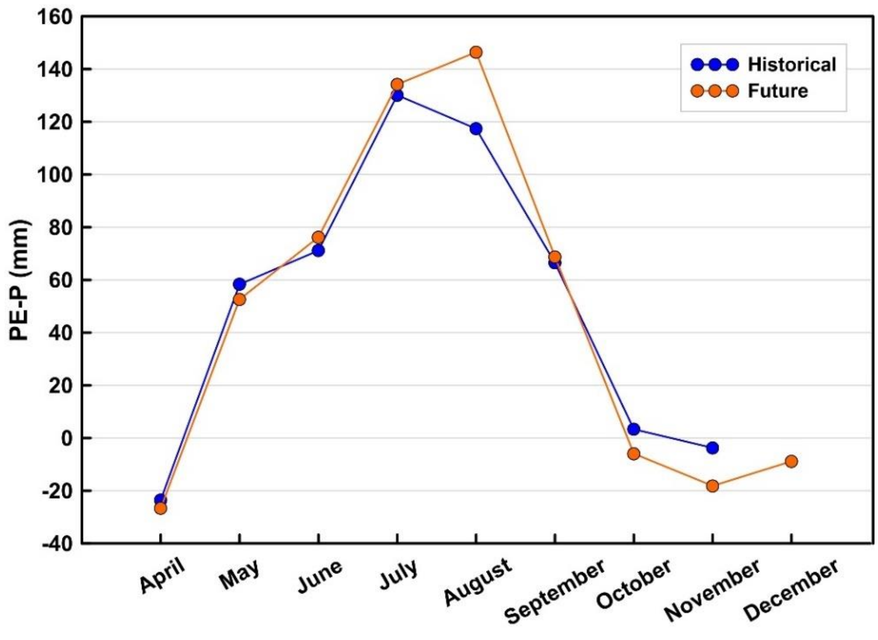

Figure 4-25- Variation of potential surface flux (PE-P) in different months under historical and future climate

4.7.2. Yearly Basis

Figure 4-26, Figure 4-27 and Figure 4-28 present the variation of ground surface movement, precipitation and potential evaporation over historical and future periods. Figure 4-26 indicates significant larger differential ground movements in future particularly after 2050. In contrast to historical period, the median values for future yearly data are generally positive that implies dominancy of swelling behavior of expansive soil in the future. The largest yearly differential ground movement (interquartile range) is observed in 2059, which is much higher than the critical year in historical period i.e., 1998. The maximum ground surface heave in the historical and future periods is approximately 45 mm (in 2001) and 54 mm (in 2063), respectively.

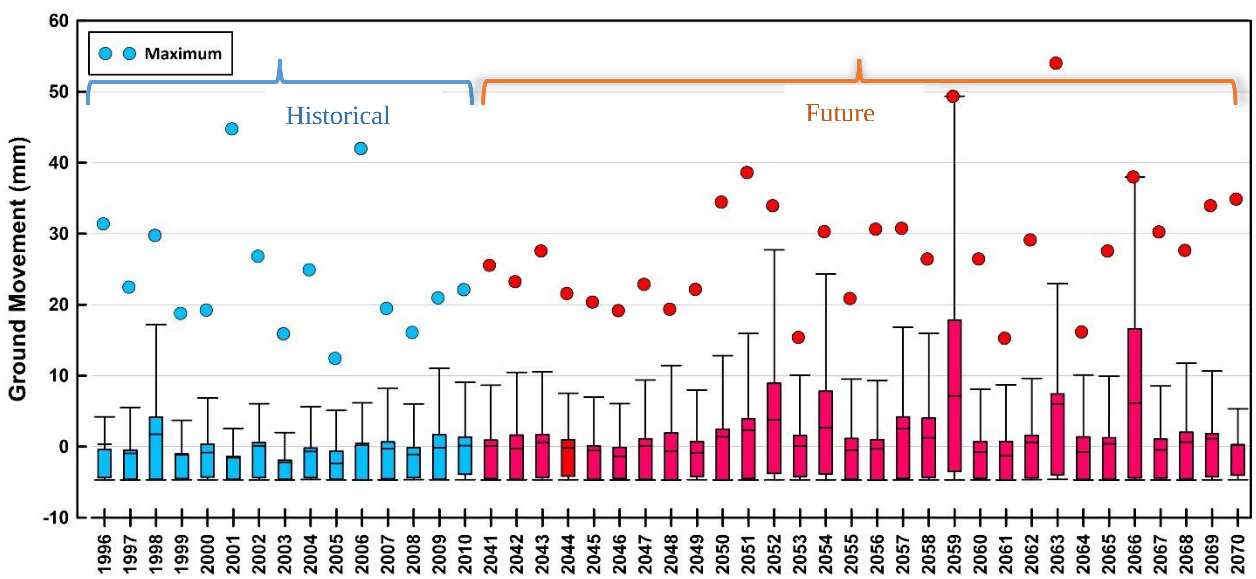

Figure 4-26- Ground vertical displacement in different years under historical and future climate

Figure 4-27 shows that generally the precipitation variations in future are larger than the historical (longer box in the graph) with considerably more extreme events (larger whisker extension). The maximum precipitation in the historical and future periods is approximately 76 mm (in 2001) and 126 mm (in 2058), respectively. A similar graph for potential evaporation is presented in Figure 4-28. This figure indicates that generally larger variation of potential evaporation is also anticipated in future.

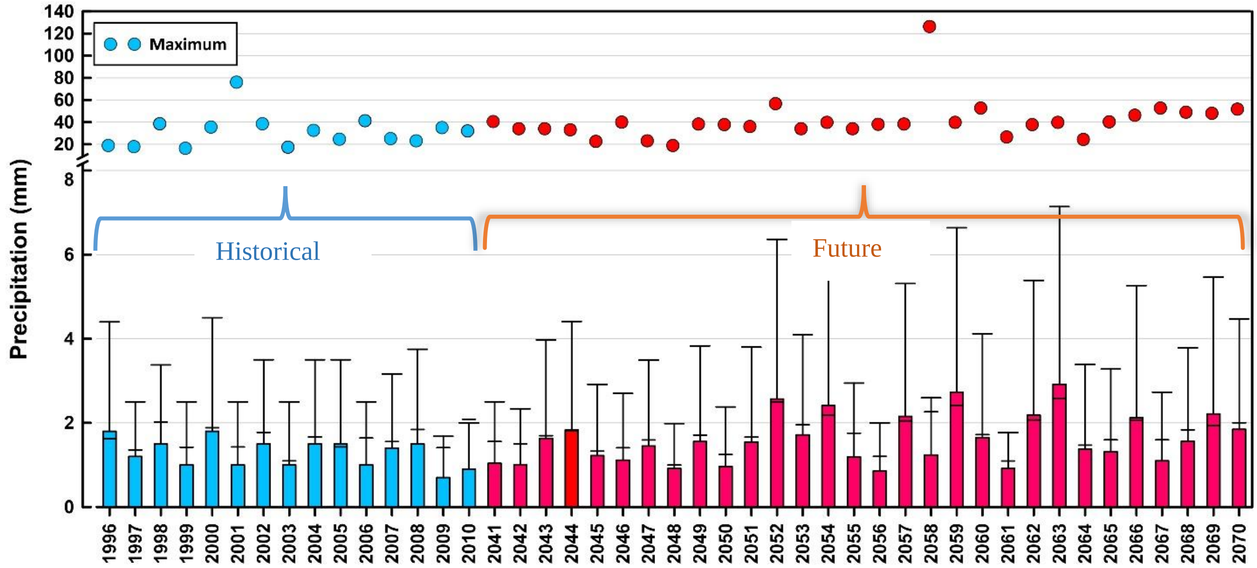

Figure 4-27- Variation of precipitation in different months under historical and future climate

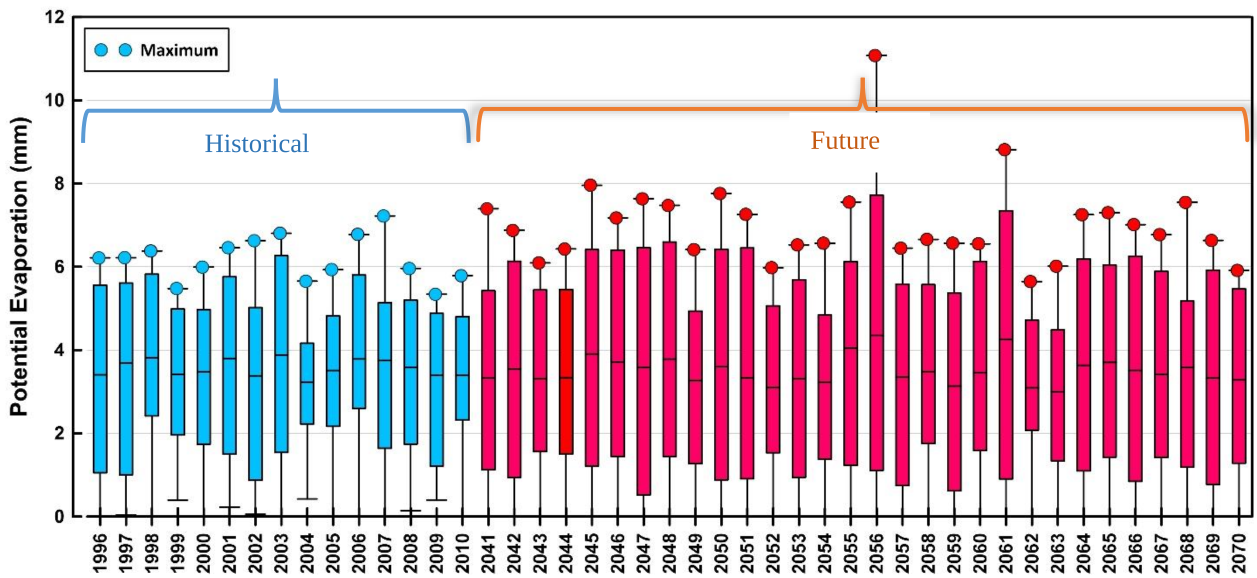

Figure 4-28- Variation of potential evaporation in different months under historical and future climate

4.7.3. Daily Basis

In Section 4.4.2. , the variation of annual moisture index over the historical period was presented. With exception of year 2003, which can be classified as arid, other years in the 1996-2010 period fall within semi-arid climate type. Similar graph based on the selected future climate is presented in Figure 4-29. As can be seen in this Figure, although most years are still anticipated to have semi-arid conditions, three years i.e., 2048, 2056 and 2061 are classified as arid and six years i.e., 2052, 2054, 2058, 2059, 2062 and 2063 are classified as dry-subhumid. This implies that future climate is likely to be associated with more wet years, and consequently higher potential for swelling response of expansive soils. The wetter dry-subhumid years in future has not been witnessed in historical period (1996-2010). Moreover, more drier years and larger year to year variation in climate is anticipated based on the selected future climate scenario.

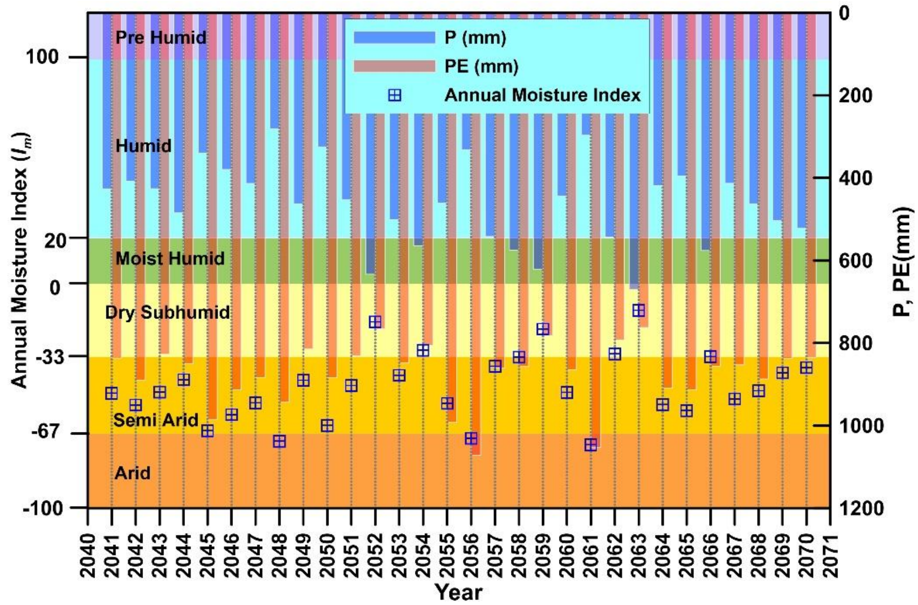

Figure 4-29- Variation of predicted precipitation, potential evaporation and annual moisture index over different years between 2041 and 2070

Figure 4-30 illustrates the daily data for ground movement, precipitation, and potential evaporation for the years 2059, 2061 and 2063. These years were selected based on the results that have been already presented in this section: a) 2059: dry-subhumid with largest differential ground movement (based on interquartile range), b) 2061: arid with minimum annual moisture index, and c) 2063: dry-subhumid with maximum annual moisture index.

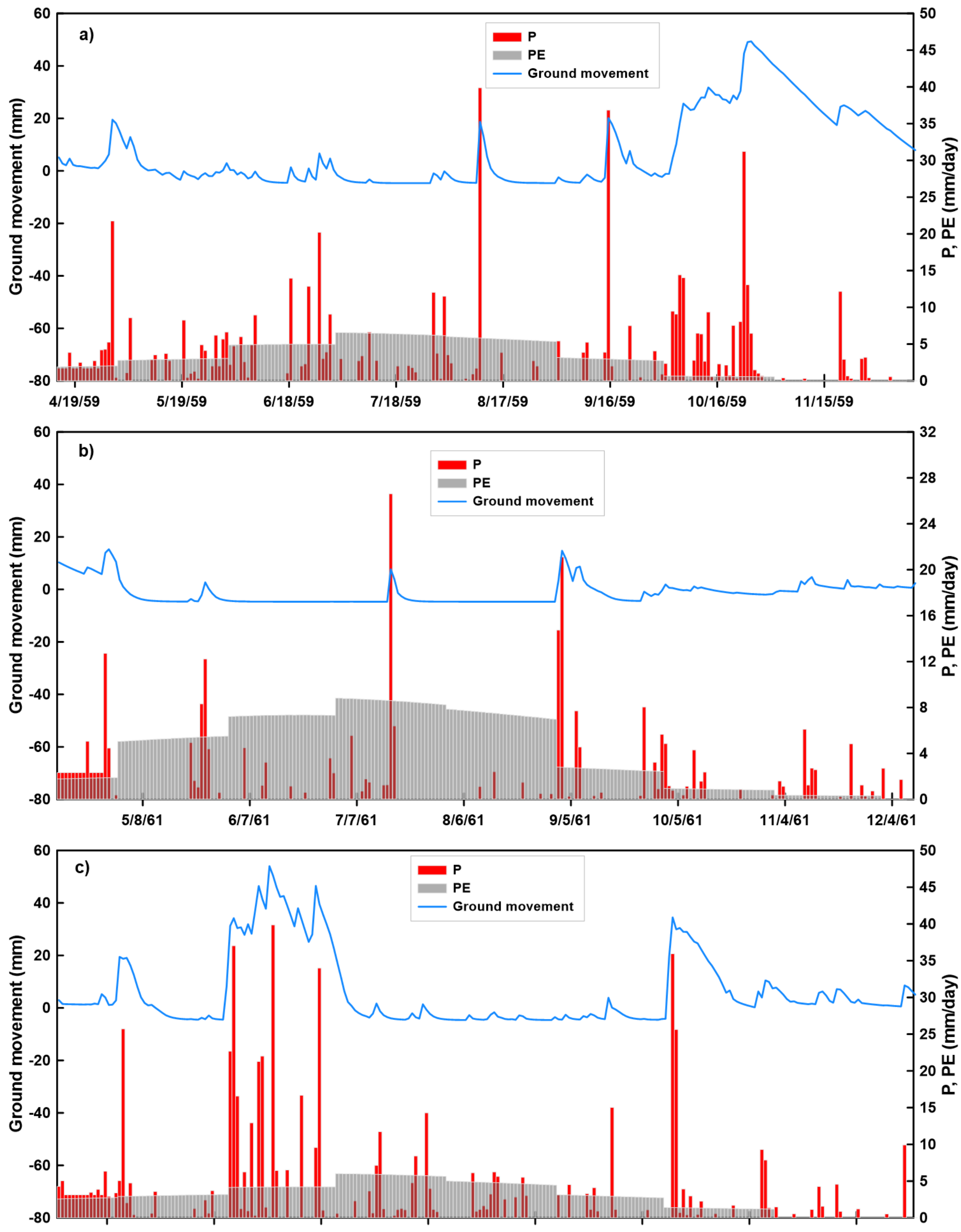

Figure 4-30- Daily precipitation, potential evaporation and ground surface movement over a) 2059, b) 2061 and c) 2063

In 2059, a significant ground heave is observed corresponding to consecutive extreme precipitation events in October when the potential evaporation is minimal. The maximum differential ground movement in arid year 2061 is approximately 20 mm, which is anticipated to occur in late April and early September following some extreme precipitation events. The dry-subhumid year 2063 indicates the maximum annual moisture index over the entire future period. The maximum differential ground movement is approximately 59 mm which is the largest differential ground movement anticipated under selected future climate scenario. The maximum ground heave can be observed to occur when several consecutive extreme precipitation events are anticipated in month of June.

The above-mentioned results suggest that the sequence of extreme precipitation events and their concurrency with colder months with minimal evaporation play a key role in causing significant ground heaving. Figure 4-31 presents frequency of number of events with potential infiltration (P-PE) greater than soil saturated hydraulic conductivity for three years 2059, 2061 and 2063.

As can be seen, smaller frequency of subsequent precipitation events is anticipated to occur in dry year 2061. The subsequent rainy days with P-PE greater than k_{sat} is not observed more than two days in 2061. In 2063 and 2059, three subsequent rainy days are anticipated to occur one time and two times over these years, respectively. Four subsequent rainy days that are observed in this graph for 2059 are anticipated to occur on October 3 to October 6 and October 22 to October 25. The latter is associated with approximately 50 mm heaving. The maximum heave over the entire historical and future periods is approximately 54 mm which is anticipated to occur in first half of June in 2063. The daily precipitation data indicate 9 days with $P>k_{sat}$ over two weeks.

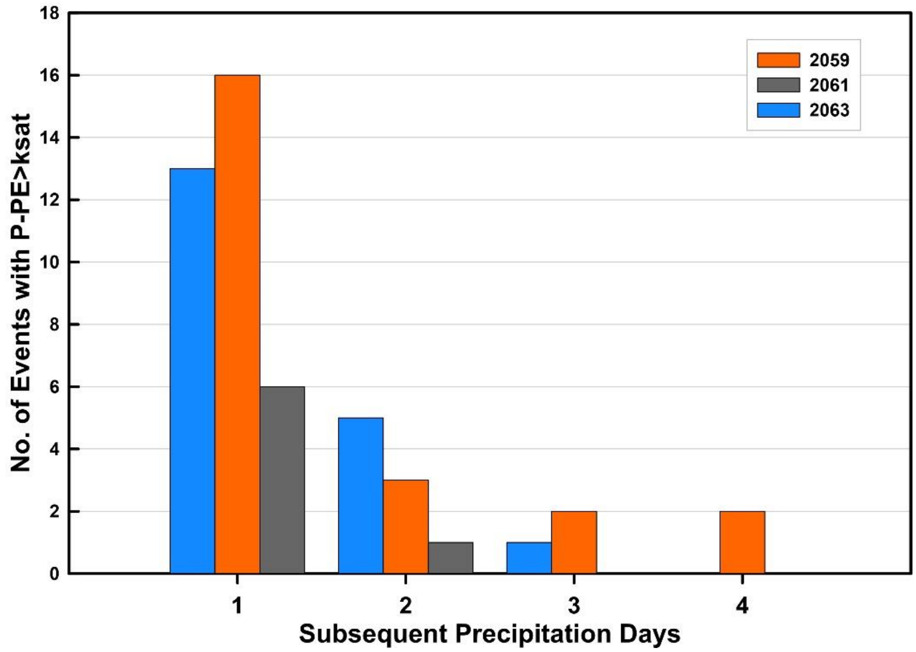

Figure 4-31- Number of subsequent events with P-PE greater than k_{sat} in mm/day in 2059, 2061 and 2063

4.8. Concluding Remarks

In this study, the impact of climate change on long-term behavior of Regina clay was studied using a two-dimensional hydro-mechanical coupled model. The model comprises of a finite element transient variably-saturated flow model and a mechanical finite element effective stress-based model. The mechanical model is equipped with a constitutive relationship that relates the change in void ratio to the change in effective stress in unsaturated soil state. The developed model has been validated against a benchmark problem and the results were presented elsewhere (Chapter 3).

The developed numerical model was used to analyze the expansive soil response to the historical climate (i.e., 1996-2010). The results of numerical model were statistically analyzed to establish the relationship between ground movement and climatic various variables on a daily, monthly and yearly basis.

A series of sensitivity analysis was carried out to study the impact of different influencing factors on expansive soil volume change response. The sensitivity analyses quantified the impact of selected factors including soil stiffness parameters, equilibrium suction head at depth and critical suction head at ground surface on the results. .

In this study, a three-staged approach has been proposed and used to select the future climate scenario among the 26 GCMs and 3 SSPs data in CMIP6 database for the city of Regina. The selected future climate ensemble (between 2041-2070 obtained from EC-Earth3-Veg_SSP2-4.5) as well as the historical climate data (1996-2010) was then used in the developed hydro-mechanical model. The numerical model results for the historical and future climate data were statistically compared to evaluate the impact of climate change on the long-term expansive soil movement patterns. Some of the key findings of the comparison study are summarized as follows:

- In contrast to historical period, the mean and median values for yearly future ground movement data indicates dominancy of the swelling behavior of expansive soil, this is in contrast to the historical conditions where shrinkage behavior is more prevalent. The largest yearly differential ground movement is observed to be 59 mm in the year 2063. This value is higher than what was estimated over the critical year in historical period i.e., 1998, which is calculated as approximately 44 mm.
- A summary of the comparison study is presented in Figure 4-32. As can be seen, although the 90th and 99th percentiles of future precipitation data are less than 20% greater than the corresponding values for historical period, the ground movement (heave) is anticipated to be considerably larger (more than 20%) than what is estimated value for the historical climate.

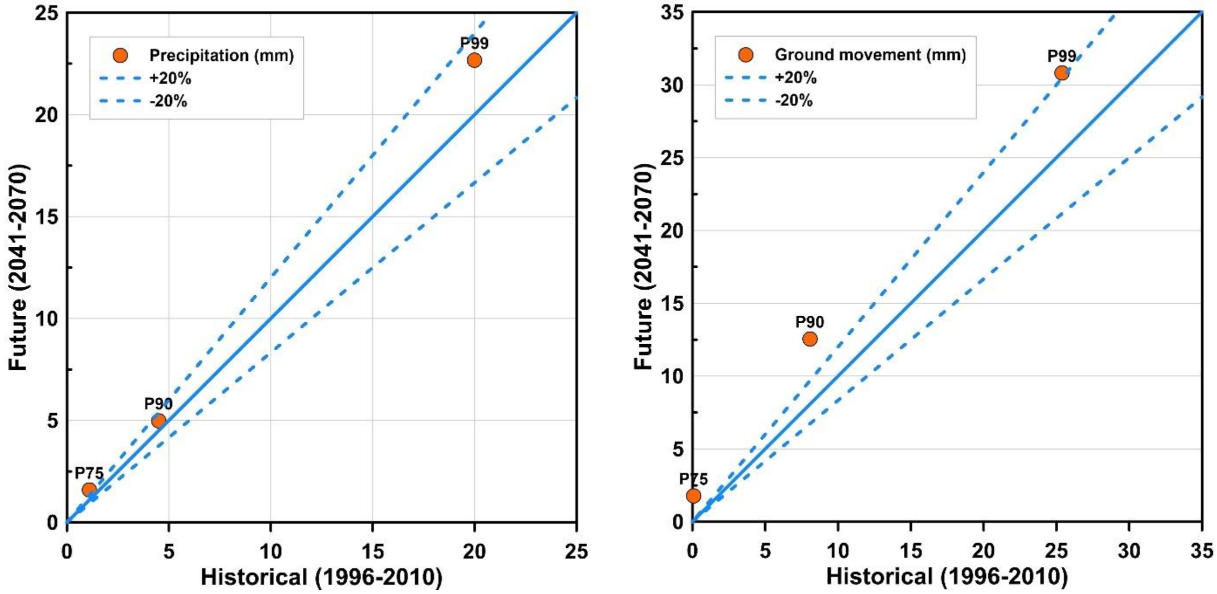

Figure 4-32- Comparison of historical and future climate impact in terms of percentiles of daily precipitation and ground movement data

- In general, the obtained results show that the ground deformation response is not necessarily correlated with the maximum daily precipitation events. The numerical results suggest that the sequence of extreme precipitation events and their concurrency with colder months with minimal evaporation are important factors influencing the expansive ground response to the long-term climate. Figure 4-33 presents a comparison between the frequency of events with potential infiltration (P-PE) greater than saturated soil hydraulic conductivity for critical historical (i.e., 1998) and future years (i.e., 2059 and 2063). In general, the frequency of subsequent precipitation events is anticipated to be higher in critical future years i.e., 2059 and 2063 compared to the critical historical year 1998. Four subsequent rainy days are predicted to occur from October 22 to October 25 in 2059 are shown to be associated with a ground heave of approximately 50 mm.
- Figure 4-34 presents a comparison of frequency distribution of ground movements greater than 5 mm in years 1998, 2059 and 2063. The results indicate that the frequency of larger ground heaving events is considerably higher under future climate. This leads to the

conclusion that changing climate increases the probability (and consequently the risk) of damage to the structures supported on expansive soil in Regina. It should be noted that the impact of climate change on the risk of structural damage should be considered in conjunction with existing structural conditions and structure damage criteria.

Based on the findings of the sensitivity analyses the numerical results are sensitive to selected soil mechanical and hydraulic parameters. Therefore, in spite of the capability of the proposed numerical model in prediction of expansive ground response to climate, the real ground movement in future may be different from those obtained in this study. This could be potentially due to the change in soil hydraulic and mechanical properties as a result of changing climate. Nevertheless, the current numerical study confirms the adverse impact of climate change on long-term expansive soil volume change and the increase of risk of damage to the lightweight structures and utilities constructed on expansive soil.

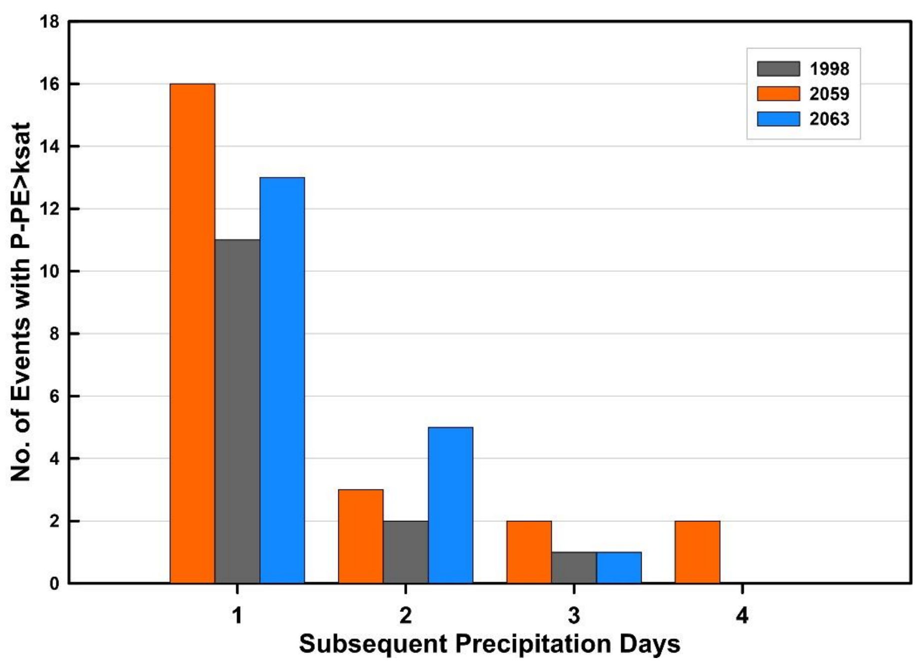

Figure 4-33- Comparison of number of subsequent events with P-PE greater than k_{sat} in mm/day in 1998, 2059 and 2063

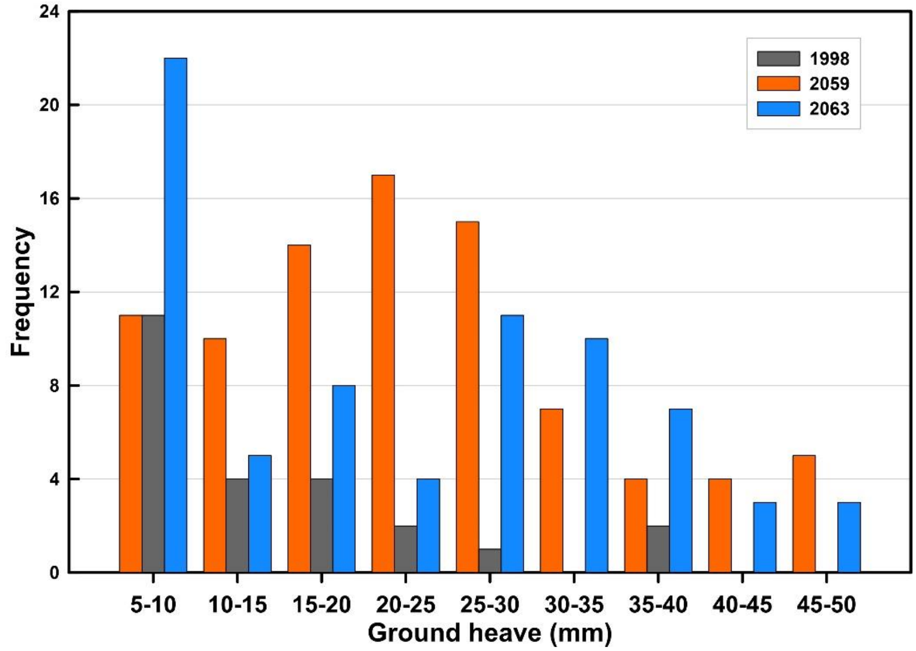

Figure 4-34- Comparison of frequency distribution of ground movements greater than 5 mm in years 1998, 2059 and 2063

Chapter 5 : Summary, Conclusions, and Recommendations for Future Research

5.1. Summary

In this study, a finite element model that couples variably-saturated flow and stress-strain analysis was developed to simulate the volume change behavior of expansive clay subject to change in soil moisture content. The two-dimensional coupled hydro-mechanical model utilizes a suction stress-based mechanical analysis to calculate the effective stress field. The model is equipped with a power law equation to incorporate the dependency of soil modulus on volumetric water content of soil. The power law equation was estimated from the proposed relationship between void ratio and effective stress that has been obtained from the measured soil constitutive data in terms of void ratio and two stress state variables i.e., net total stress and soil suction.

The developed model was utilized to quantify the expansive soil movements in response to variation of soil moisture due to long-term climate data including the historical climate (1996-2010) as well as a selected climate change scenario for the next 90 years (2010-2100). The future climate data was extracted from the latest climate models provided by the Pacific Climate Impacts Consortium (PCIC). A three-staged methodology was developed to select a critical future climate scenario for the city of Regina. The selected future climate data was used in the developed numerical models to assess the impact of climate change on the long-term deformation behavior of a Regina expansive ground.

In summary, the results indicate the more severe ground heaving events is anticipated to occur in future compared to the historical period. More details about the conclusions of this study are presented in the following section.

5.2. Conclusions

5.2.1. Validity of the Proposed Numerical Model

The developed numerical model was used to model a situation where Regina clay layer is partially covered by a impervious pavement and is subjected to a constant infiltration over a 175 day period. The results obtained indicate the capability of the proposed model, which is based on single stress state variable framework. In comparison with other approaches, it was found that the proposed model is capable of simulating the expansive soil deformations subject to varying moisture conditions over time. In contrast to the available one-dimensional methods, the proposed model can simulate the two-dimensional distribution of suction head, as well as vertical and horizontal soil deformations with time. Such vertical and horizontal soil deformations can cause significant differential movements over time compromising the integrity of the structures built on these soils. In general, the numerical results from the proposed model are in good agreement with those reported by other studies (Hamberg (1985), Vu and Fredlund (2006), Zhang and Briaud (2010) and Adem and Vanapalli (2013)).

5.2.2. Influencing Factors

A series of sensitivity analyses were carried out to study the impact of different influencing factors on expansive soil volume change response. Five parameters including three parameters for power law elastic equation (E_d, E_w and m), maximum (critical) allowable suction head at ground surface (h_{cr}) and initial suction head (h_{eq}) were considered in the sensitivity analyses.

The results obtained indicate that the changes in soil stiffness parameters have higher impact on the differential ground surface movements compared to change in h_{eq} and h_{cr}. The results also indicate that the differential ground movements are more sensitive to the decrease in E_d and m compared to increase in these parameters. The impact of E_w on the differential ground movement was found to be minimal. The sensitivity of differential ground movement to changes in h_{cr} was found to be greater for years with drier climates. This is not surprising as the probability of surface suction values approaching h_{cr} is much higher in drier conditions.

The findings of the conducted sensitivity analyses show that the numerical results are sensitive to selected soil mechanical and hydraulic parameters. Therefore, the actual ground movement in the future may be different from those obtained in this study, if any of these parameters change over the course of as a result of changing climate. In spite of this fact, the findings of this study indicate the capability of the proposed numerical model in prediction of expansive ground response to long-term climate.

5.2.3. Selection of Critical Future Climate Change Scenario

In this study, a three-staged methodology is proposed and used to select the critical future climate change scenario from a large compiled climate dataset. The climate dataset comprised of daily records for maximum and minimum temperature and precipitation from 26 GCMs and 3 SSPs proposed in CMIP6 over a 90 year period from 2011 to 2100. First, the validation approach was used to identify 4 out of 26 GCMs models that predicts the historical climate data with minimum error. Second, the expansive soil response under a sample for a single one-year climate data was analyzed to assign identify a representative climate variable that has the greatest impact on the extreme ground movements (maximum heave or shrinkage over time). Third, a statistical analysis on the projected data for the identified representative climate variable was carried out to select a future climate ensemble that can result in the most critical ground movement response to the climatic conditions. The selected future climate ensemble as well as the historical climate data was then used in the developed hydro-mechanical model to evaluate the impact of climate change on the long-term expansive soil movement patterns. The developed methodology is superior to any other methodology reported in the literature as it does not only relies on the climate change information but also takes into the consideration the actual water balance at the ground surface and associated soil deformation behavior. Therefore this methodology takes into account the effect of soil hydraulic and geotechnical properties, the physical process of water movement and soil deformation within the context of changing climate.

Based on the proposed methodology, climate data from GCM EC-Earth3-Veg for the climate change scenario SSP2-4.5 for the period 2041-2070 is selected for the numerical analysis in this study. The results of statistical analysis on the climate data indicates that 75th percentile and 90th percentile of precipitation data for the selected future climate ensemble is approximately 98% and 22% higher than the historical period. Moreover, the selected future climate ensemble includes 865 events with daily precipitation greater than 90th percentile of the historical data. Considering the dependency of soil moisture fluctuations on the intensity and frequency of precipitation events, these findings imply that climate change would adversely affect the ground differential movements in future.

5.2.4. Climate Change Impact

The selected future climate ensemble (EC-Earth3-Veg_SSP2-4.5 for the period of 2041-2070) as well as the historical climate data (1996-2010) was used in the developed hydro-mechanical model. The numerical model results for historical and future were statistically compared to evaluate the impact of climate change on the long-term expansive soil movement patterns.

In contrast to historical period, the mean and median values for future yearly ground movement are expected to be dominated by swelling behavior. For the considered future climate change scenario, the largest differential ground movement is expected to be 59 mm in 2063, which is higher than 49 mm that has been estimated for the historical period. Although the 90th and 99th

percentiles of future precipitation data are less than 20% greater than greater than the corresponding values from the historical period, the ground movement (heave) is anticipated to be considerably larger (more than 20%) than what is estimated for the historical climate.

In general, the results of the study indicate that the ground deformation response is not necessarily only correlated with the maximum daily precipitation events. The numerical results suggest that the sequence of extreme precipitation events and their concurrency especially in colder months with minimal evaporation are among the most important factors influencing the expansive ground response in the future. The frequency of subsequent precipitation events is anticipated to be higher for the critical future years i.e., 2059 and 2063 compared to the critical historical year 1998.

The results also indicate that the frequency of large ground heaving events could potentially be considerably higher for the predicted future climactic conditions. This leads to the conclusion that with changing climate the probability (and consequently the risk) of damage to the structures supported on expansive soil in Regina is expected to increase. It should be noted that the climate change impact on the risk of structural damage should be considered in conjunction with existing structural conditions and structure damage criteria.

5.3. Contributions of the Research

This study has made several contributions that would be of considerable value for both practicing engineers and researchers. Some of these contributions are as follows:

- A numerical model is developed to predict the expansive soil response to long-term climate using a single stress state (effective stress) unsaturated soil mechanics framework. This effective stress-based approach, which is first proposed by Lu et al. (2010), is used to calculate the effective stress field in the stress-strain analysis. Although since its introduction, this approach has been used to simulate several engineering applications such as slope stability assessment using local factor of safety , this is the first study to simulate expansive soil response to change in moisture content using the single stress state soil mechanics framework.

- Over last few decades, several one-dimensional methods have been proposed to simulate the expansive soil heaving/shrinkage response to changes in soil moisture. However, the numerical model that has been developed in this study can simulate the two-dimensional distribution of suction head and soil displacement with time. This model is also capable of estimating differential ground movements due to both vertical and horizontal soil deformations, which are likely to occur where asymmetric conditions govern the problem of interest.
- In recent years, the impact of climate change on expansive soils behaviour has received some attention from researchers. However, this is the first study in which a coupled hydro-mechanical numerical model has been utilized to carry out a comparison between long-term expansive ground behavior under historical and future climatic conditions.
- Moreover, this is the very first study that has compiled and assessed climate change data for the city of Regina from the latest climate modeling. The dataset comprised of 32871 daily records of precipitation, minimum and maximum temperature from 26 GCMS for 3 climate change scenarios over 90 years (from 2011 to 2100).
- This study also proposed a multi step methodology to select the critical future climate scenario. The proposed approach not only takes into consideration the climate data but also the expansive ground response to climatic variables.

- Some of the results of this study have been disseminated in the form of two peer reviewed conference proceedings, it is anticipated that other results will be disseminated in the form of two journal papers.

5.4. Recommendations for Future Research

The current study has highlighted the impact of climate change on the long-term swelling/shrinkage behavior of an expansive clay for the city of Regina. The following is a list of recommendations for future research:

- Consider other locations where the expansive clays are considered as a problematic geotechnical engineering issue;
- Develop void ratio-effective stress constitutive curves for various expansive soils based on laboratory testing data;
- Assess various mathematical equations to find a better correlation between soil stiffness and soil moisture content for different expansive soils; and
- Carry out probabilistic and risk assessment analysis to ensure the long-term safety and serviceability of the current and future geo-structures supported by expansive soils under different anticipated future climate scenarios.

Chapter 6 : References

(Chapter 1)

Adem, H.H., 2015. *Modulus of elasticity based method for estimating the vertical movement of natural unsaturated expansive soils* (Doctoral dissertation, Université d'Ottawa/University of Ottawa).

Assadollahi, H. and Nowamooz, H., 2020. Long-term analysis of the shrinkage and swelling of clayey soils in a climate change context by numerical modelling and field monitoring. *Computers and Geotechnics*, *127*, p.103763.

Bagheri, F., 2022. Effect of Climate Change on Slope Stability of Variably Saturated Embankments Using Local Factor of Safety and In-Situ Stress Finite Element Analysis, MSAc Thesis, York University.

Coduto, D.P., 2001. Foundation design. Pomona, California State Polytechnic University.

Jones Jr, D.E. and Holtz, W.G., 1973. Expansive soils-the hidden disaster. *Civil engineering*, 43(8).

Lu, N., Godt, J.W. and Wu, D.T. 2010. A closed-form equation for effective stress in unsaturated soil, *Water Resources Research*, *46*(5).

Puppala, A.J. and Cerato, A., 2009. Heave distress problems in chemically-treated sulfate-laden materials. *Geo-Strata—Geo Institute of ASCE*, 10(2), p.28.

Sun, X., 2015. The impact of climate as expressed by Thornthwaite moisture index on residential footing design on expansive soil in Australia, *Doctoral dissertation*, RMIT University.

Shi, B., Jiang, H., Liu, Z. and Fang, H.Y., 2002. Engineering geological characteristics of expansive soils in China. *Engineering Geology*, 67(1-2), pp.63-71.

(Chapter 2)

Alsherif, N.A. and McCartney, J.S., 2014. Effective stress in unsaturated silt at low degrees of saturation. *Vadose Zone Journal*, *13*(5).

Anderson, J.U., Fadul, K.E. and O'Connor, G.A., 1973. Factors affecting the coefficient of linear extensibility in Vertisols. *Soil Science Society of America Journal*, 37(2), pp.296-299.

Bishop, A.W., 1954. The use of pore-pressure coefficients in practice. *Geotechnique*, *4*(4), pp.148-152.

BIS (Bureau of Indian Standards), 1970. IS 1948-70: Indian standard classification and identification of soils for general engineering purposes. BIS, New Delhi, India.

Bishop, A.W., 1959. The principle of effective stress. *Teknisk ukeblad*, *39*, pp.859-863.

Brooks, R.H. and Corey, A.T., 1964. Hydraulic properties of porous media. Hydrology Paper No. 3. *Civil Engineering Department*, *Colorado State University*, *Fort Collins*, *CO*.

Chen, F.H. 1975. Foundations on Expansive Soils. 1st edition. Elsevier, New York.

Cui, Y.J., Nguyen, X.P., Tang, A.M. and Li, X.L., 2013. An insight into the unloading/reloading loops on the compression curve of natural stiff clays. *Applied Clay Science*, 83, pp.343-348.

Davies, O., 2011. Numerical analysis of the effects of climate change on slope stability (Doctoral dissertation, Newcastle University).

Department of the Army USA. 1983. Technical Manual TM 5-818-7. Foundations in Expansive Soils

Donaldson, G.W., 1969. The Occurrence of Problems of Heave and the Factors Affecting its Nature. In *Second international research and engineering conference on expansive clay soils* (pp. 25-36). Texas A & M Press.

Fredlund, D.G. and Morgenstern, N.R., 1977. Stress state variables for unsaturated soils. *Journal of the geotechnical engineering division*, *103*(5), pp.447-466.

Fredlund, D.G. and Rahardjo, H., 1993. *Soil mechanics for unsaturated soils*. John Wiley & Sons.

Fredlund, D.G. and Xing, A., 1994. Equations for the soil-water characteristic curve. *Canadian geotechnical journal*, *31*(4), pp.521-532.

Fredlund, D.G., Rahardjo, H. and Fredlund, M.D., 2012. *Unsaturated soil mechanics in engineering practice*. John Wiley & Sons.

Gardner, W.R., 1958. Some steady-state solutions of the unsaturated moisture flow equation with application to evaporation from a water table. *Soil science*, *85*(4), pp.228-232.

Houston, S.L., 2019. It is time to use unsaturated soil mechanics in routine geotechnical engineering practice. *Journal of Geotechnical and Geoenvironmental Engineering*, *145*(5), p.02519001.

International Building Code (IBC), 2012. Falls Church, VA, International Code Council.

Khalili, N. and Khabbaz, M.H., 1998. A unique relationship for χ for the determination of the shear strength of unsaturated soils. *Geotechnique*, *48*(5), pp.681-687.

Leong, E.C. and Rahardjo, H., 1997. Review of soil-water characteristic curve equations. *Journal of geotechnical and geoenvironmental engineering*, *123*(12), pp.1106-1117.

Lu, N. and Griffiths, D.V., 2004. Profiles of steady-state suction stress in unsaturated soils. *Journal of Geotechnical and Geoenvironmental Engineering*, *130*(10), pp.1063-1076.

Lu, N. and Likos, W.J., 2006. Suction stress characteristic curve for unsaturated soil. *Journal of geotechnical and geoenvironmental engineering*, *132*(2), pp.131-142.

Lu, N., Godt, J.W. and Wu, D.T. 2010. A closed-form equation for effective stress in unsaturated soil, *Water Resources Research*, *46*(5).

Manahiloh, K.N., Muhunthan, B. and Likos, W.J., 2016. Microstructure-based effective stress formulation for unsaturated granular soils. *International Journal of Geomechanics*, (6), p.D4016006.

Matyas, E.L. and Radhakrishna, H.S. 1968. Volume change characteristics of partially saturated soils, *Geotechnique*, *18*(4): 432-448.

Mitchell, J.K. and Soga, K., 2005. Fundamentals of soil behavior (Vol. 3, p. USA). New York: John Wiley & Sons.

Mualem, Y., 1976. A new model for predicting the hydraulic conductivity of unsaturated porous media. *Water resources research*, *12*(3), pp.513-522.

Miller, A.B., Nelson, R.W., Scott-Moncrieff, J.C., Neal, L. and Bottoms, G.D., 1992. Serial thyroid hormone concentrations in healthy euthyroid dogs, dogs with hypothyroidism, and euthyroid dogs with atopic dermatitis. *British Veterinary Journal*, 148(5), pp.451-458.

Nuth, M. and Laloui, L., 2008. Advances in modelling hysteretic water retention curve in deformable soils. *Computers and Geotechnics*, *35*(6), pp.835-844.

Patel, Anjan, 2019. Geotechnical investigations and improvement of ground conditions. Woodhead Publishing.

Peck, R.B., Hanson, W.E. and Thornburn, T.H., 1991. Foundation engineering. John Wiley & Sons.

Philip, J.R., 1986. Issues in flow and transport in heterogeneous porous media. *Transport in Porous Media*, *1*(4), pp.319-338.

Richards, L.A., 1931. Capillary conduction of liquids through porous mediums. *Physics*, *1*(5), pp.318-333.

Schafer, W.M. and Singer, M.J., 1976. A new method of measuring shrink-swell potential using soil pastes. *Soil Science Society of America Journal*, 40(5), pp.805-806.

Stavridakis, E.I., 2006. A solution to the problem of predicting the suitability of silty–clayey materials for cement-stabilization. *Geotechnical & Geological Engineering*, 24(2), pp.379-398.

Taboada, M.A. 2003. Soil shrinkage characteristics in swelling soils. Lecture given at the College on Soil Physics Trieste, 21 March 2003, Buenos Aires, Argentina.

Tran, D.T., Fredlund, D.G. and Chan, D.H., 2015. Improvements to the calculation of actual evaporation from bare soil surfaces. *Canadian Geotechnical Journal*, 53(1), pp.118-133.

Tang, A.M. and Cui, Y.J., 2009. Modelling the thermomechanical volume change behaviour of compacted expansive clays. *Géotechnique*, 59(3), pp.185-195.

Van Genuchten, M.T., 1980. A closed-form equation for predicting the hydraulic conductivity of unsaturated soils. *Soil science society of America journal*, *44*(5), pp.892-898.

Van Genuchten, M.V., Leij, F.J. and Yates, S.R., 1991. The RETC code for quantifying the hydraulic functions of unsaturated soils.

Zapata, C.E., Houston, S.L., Houston, W.N. and Dye, H., 2006. Expansion index and its relationship with other index properties. *Geotechnical Special Publication*, 147(2), p.2133.

Zhang, C. and Lu, N., 2020. Unified effective stress equation for soil. *J. Eng. Mech*, *146*(2), p.04019135.

(Chapter 3)

Adem, H.H. and Vanapalli, S.K. 2013. Constitutive modeling approach for estimating 1-D heave with respect to time for expansive soils, *International Journal of Geotechnical Engineering*, *7*(2): 199-204.

Adem, H.H. and Vanapalli, S.K. 2015. Review of methods for predicting in situ volume change movement of expansive soil over time, *Journal of Rock Mechanics and Geotechnical Engineering*, *7*(1): 73-86.

Adem, H.H., 2015. *Modulus of elasticity based method for estimating the vertical movement of natural unsaturated expansive soils* (Doctoral dissertation, Université d'Ottawa/University of Ottawa).

Alonso, E.E., Gens, A. and Josa, A. 1990. A constitutive model for partially saturated soils, *Géotechnique*, *40*(3): 405-430.

Alonso, E.E., Vaunat, J. and Gens, A. 1999. Modelling the mechanical behaviour of expansive clays, *Engineering geology*, *54*(1-2): 173-183.

Briaud, J.L., Zhang, X. and Moon, S. 2003. Shrink test–water content method for shrink and swell predictions, *Journal of geotechnical and geoenvironmental engineering*, *129*(7): 590-600.

FlexPDE, 2017. FlexPDE 6 User Manuel.

Fredlund, D.G. and Morgenstern, N.R. 1976. Constitutive relations for volume change in unsaturated soils, *Canadian Geotechnical Journal*, *13*(3): 261-276.

Fredlund, D.G. and Xing, A., 1994. Equations for the soil-water characteristic curve. *Canadian geotechnical journal*, *31*(4), pp.521-532.

Hamberg, D.J. 1985. A simplified method for predicting heave in expansive soils, M.S. thesis, Colorado State University, Fort Collins, CO.

Hu, Y., Rudaba, C. and Shahid, A., 2010, September. Behaviour of expansive soils at a water distribution pipe site. In *Proceedings of the 63rd Canadian Geotechnical Conference & 1st Joint CGS/CNC-IPA Permafrost Specially Conference (GeoCalgary)* (pp. 12-16).

Ito, M. and Hu, Y., 2011, October. Prediction of the behaviour of expansive soils. In *Proceedings, 64th Canadian Geotechnical Conference and 14th Pan-American Conference on Soil Mechanics and Geotechnical Engineering* (pp. 2-6).

Ito, M., Azam, S. and Hu, Y. 2014. A two stage model for moisture-induced deformations in expansive soils, *Environmental Systems Research*, *3*(1): 1-11.

Karunarathne, A.M.A.N., Fardipour, M., Gad, E.F., Rajeev, P., Disfani, M.M., Sivanerupan, S. and Wilson, J.L. 2018. Modelling of climate induced moisture variations and subsequent ground movements in expansive soils, *Geotechnical and Geological Engineering*, *36*(4): 2455-2477.

Khosravi, A. and McCartney, J.S. 2011. Resonant column test for unsaturated soils with suction–saturation control, *Geotechnical Testing Journal*, *34*(6): 730-739

Lloret, A. and Alonso, E.E., 1985. State surface for partially saturated soils. In *International conference on soil mechanics and foundation engineering. 11* (pp. 557-562).

Lu, N. and Kaya, M. 2014. Power law for elastic moduli of unsaturated soil, *Journal of Geotechnical and Geoenvironmental Engineering*, *140*(1): 46-56.

Lu, N., Godt, J.W. and Wu, D.T. 2010. A closed-form equation for effective stress in unsaturated soil, *Water Resources Research*, *46*(5).

Lu, N., Wayllace, A., & Formetta, G. 2016. The Slope Cube Module, *Soil Water Retention, LLC: Madison, WI, USA.*

Lytton, R.L., 1994, June. Prediction of movement in expansive clays. In *Vertical and horizontal deformations of foundations and embankments* (pp. 1827-1845). ASCE.

Mitchell, P.W., 1980. The structural analysis of footings on expansive soil. In *Expansive Soils* (pp. 438-447). ASCE.

Ng, C.W.W., Xu, J. and Yung, S.Y. 2009. Effects of wetting–drying and stress ratio on anisotropic stiffness of an unsaturated soil at very small strains, *Canadian Geotechnical Journal*, *46*(9): 1062-1076.

Oh, W.T., Vanapalli, S.K. and Puppala, A.J. 2009. Semi-empirical model for the prediction of modulus of elasticity for unsaturated soils, *Canadian Geotechnical Journal*, *46*(8): 903-914.

Overton, D.D., Chao, K.C. and Nelson, J.D., 2006, February. Time rate of heave prediction for expansive soils. In *Proceedings of the ASCE Conference GeoCongress* (Vol. 187, pp. 162-168).

Sawangsuriya, A., Edil, T.B. and Bosscher, P.J. 2009. Modulus-suction-moisture relationship for compacted soils in postcompaction state, *Journal of Geotechnical and geoenvironmental engineering*, *135*(10):1390-1403.

Šimŭnek, J., Van Genuchten, M.T., and Šejna, M. 2006. The HYDRUS software package for simulating two-and Three-Dimensional Movement of Water, Heat, and Multiple Solutes in Variably Saturated Media, Technical manual, version 1: 241.

van Genuchten, M. V., Leij, F. J., & Yates, S. R. (1991). The RETC code for quantifying the hydraulic functions of unsaturated soils.

Vanapalli, S.K. and Adem, H.H. 2013. Estimation of the 1-D heave of a natural expansive soil deposit with a light structure using the modulus of elasticity-based method, *Advances in Unsaturated soils, Edited by Caicedo, B., Murillo, C., Hoyos, L., Colmenares, JE, and Berdugo, IR, Taylor and Francis*, 101-114.

Vanapalli, S.K. and Adem, H.H., 2012, September. Estimation of the 1-D heave in expansive soils using the stress state variables approach for unsaturated soils. In *Proceedings of the 4th international conference on problematic soils, Wuhan, China* (p. 1e15).

Vu, H.Q. 2003. Uncoupled and coupled solutions of volume change problems in expansive soils, Ph.D. thesis, Department of Civil Engineering, University of Saskatchewan, Saskatoon.

Vu, H.Q. and Fredlund, D.G. 2004. The prediction of one-, two-, and three-dimensional heave in expansive soils, *Canadian Geotechnical Journal*, *41*(4): 713-737.

Vu, H.Q. and Fredlund, D.G. 2006. Challenges to modelling heave in expansive soils, *Canadian Geotechnical Journal*, *43*(12): 1249-1272.

Wray, W.K., El-Garhy, B.M. and Youssef, A.A. 2005. Three-dimensional model for moisture and volume changes prediction in expansive soils, *Journal of Geotechnical and Geoenvironmental Engineering*, *131*(3): 311-324.

Zhang, C., Hu, S. and Lu, N., 2022. Unified Elastic Modulus Characteristic Curve Equation for Variably Saturated Soils. *Journal of Geotechnical and Geoenvironmental Engineering*, *148*(1), p.04021171.

Zhang, J., Little, D.N., Hariharan, N. and Kim, Y.R., 2019. Prediction of climate specific vertical movement of pavements with expansive soils based on long-term 2D numerical simulation of rainwater infiltration. *Computers and Geotechnics*, *115*, p.103172.

Zhang, X. (2004). Consolidation theories for saturated-unsaturated soils and numerical simulation of residential buildings on expansive soils. Texas A&M University.

Zhang, X. and Briaud, J.L. 2010. Coupled water content method for shrink and swell predictions, *International Journal of Pavement Engineering*, *11*(1): 13-23.

(Chapter 4)

Assadollahi, H. and Nowamooz, H., 2020. Long-term analysis of the shrinkage and swelling of clayey soils in a climate change context by numerical modelling and field monitoring. *Computers and Geotechnics*, *127*, p.103763.

Bashir, R., Sahi, M. A., & Sharma, J. (2022). Using synthetic climate datasets for geotechnical and geoenvironmental design problems. *Canadian Geotechnical Journal*, 99(999), 1-16.

Eyring, V., Bony, S., Meehl, G.A., Senior, C.A., Stevens, B., Stouffer, R.J. and Taylor, K.E., 2016. Overview of the Coupled Model Intercomparison Project Phase 6 (CMIP6) experimental design and organization. *Geoscientific Model Development*, *9*(5), pp.1937-1958.

Environment and Climate Change Canada. 2019. Canadian Climate Normals - Climate - Environment and Climate Change Canada. Available from https://climate.weather.gc.ca/climate_normals/index_e.html. [accessed 15 June 2022]

Fredlund, D.G. and Xing, A., 1994. Equations for the soil-water characteristic curve. *Canadian geotechnical journal*, *31*(4), pp.521-532.

Harrison, A.M., Plim, J.F.M., Harrison, M., Jones, L.D. and Culshaw, M.G., 2012. The relationship between shrink–swell occurrence and climate in south-east England. *Proceedings of the Geologists' Association*, *123*(4), pp.556-575.

Karunarathne, A.M.A.N., Fardipour, M., Gad, E.F., Rajeev, P., Disfani, M.M., Sivanerupan, S. and Wilson, J.L. 2018. Modelling of climate induced moisture variations and subsequent ground movements in expansive soils, *Geotechnical and Geological Engineering*, *36*(4): 2455-2477.

Leao, S., 2014. Mapping potential risk for housing damage from ground movement due to climate change. *International Journal of Environmental Science and Development*, *5*(4), p.387.

Mitchell, J.K. and Soga, K., 2005. *Fundamentals of soil behavior* (Vol. 3, p. USA). New York: John Wiley & Sons.

Mitchell, P.W., 2013. Climate change effects on expansive soil movements. *Proceedings of the 18th ICSMGE*, pp.1159-1162.

Monteith, J.L., 1965. Evaporation and environment. In *Symposia of the society for experimental biology* (Vol. 19, pp. 205-234). Cambridge University Press (CUP) Cambridge.

Nowamooz, H., Jahangir, E. and Masrouri, F., 2013. Volume change behaviour of a swelling soil compacted at different initial states. *Engineering Geology*, *153*, pp.25-34.

Nowamooz, H., Jahangir, E., Masrouri, F. and Tisot, J.P., 2016. Effective stress in swelling soils during wetting drying cycles. *Engineering Geology*, *210*, pp.33-44.

Penman, H.L., 1948. Natural evaporation from open water, bare soil and grass. *Proceedings of the Royal Society of London. Series A. Mathematical and Physical Sciences*, *193*(1032), pp.120-145.

Pomeroy, J. W., de Boer, D., & Martz, L. W., 2005. Hydrology and water resources of Saskatchewan, *Saskatoon: Centre for Hydrology*, University of Saskatchewan.

Riahi, K., Van Vuuren, D.P., Kriegler, E., Edmonds, J., O'neill, B.C., Fujimori, S., Bauer, N., Calvin, K., Dellink, R., Fricko, O. and Lutz, W., 2017. The shared socioeconomic pathways and their energy, land use, and greenhouse gas emissions implications: an overview. *Global environmental change*, *42*, pp.153-168.

Taylor, K.E., Stouffer, R.J. and Meehl, G.A., 2012. An overview of CMIP5 and the experiment design. *Bulletin of the American meteorological Society*, *93*(4), pp.485-498.

Thornthwaite, C.W., 1948. An approach toward a rational classification of climate. *Geographical review*, *38*(1), pp.55-94.

Thornthwaite, C.W., 1948. An approach toward a rational classification of climate. *Geographical review*, 38(1), pp.55-94.

Van Vuuren, D.P., Edmonds, J., Kainuma, M., Riahi, K., Thomson, A., Hibbard, K., Hurtt, G.C., Kram, T., Krey, V., Lamarque, J.F. and Masui, T., 2011. The representative concentration pathways: an overview. *Climatic change*, *109*(1), pp.5-31.

Yoshida, R. T., Fredlund, D. G., & Hamilton, J. J., 1983. The prediction of total heave of a slab-on-grade floor on Regina clay. *Canadian Geotechnical Journal*, 20(1), 69-81.

(Chapter 5)

Adem, H.H. and Vanapalli, S.K. 2013. Constitutive modeling approach for estimating 1-D heave with respect to time for expansive soils, *International Journal of Geotechnical Engineering*, *7*(2): 199-204.

Hamberg, D.J. 1985. A simplified method for predicting heave in expansive soils, M.S. thesis, Colorado State University, Fort Collins, CO.

Lu, N., Godt, J.W. and Wu, D.T. 2010. A closed-form equation for effective stress in unsaturated soil, *Water Resources Research*, 46(5).

Vu, H.Q. and Fredlund, D.G. 2006. Challenges to modelling heave in expansive soils, *Canadian Geotechnical Journal*, *43*(12): 1249-1272.

Zhang, X. and Briaud, J.L. 2010. Coupled water content method for shrink and swell predictions, *International Journal of Pavement Engineering*, *11*(1): 13-23.